

GEOLOGICAL SURVEY OF FINLAND

**Bulletin 403**

2009



**Archaean evolution of the Tipasjärvi-Kuhmo-  
Suomussalmi Greenstone Complex, Finland**

Heikki Papunen, Tapio Halkoaho and Erkki Luukkonen

**Geological Survey of Finland, Bulletin 403**

**ARCHAEAN EVOLUTION OF THE TIPASJÄRVI-KUHMO-  
SUOMUSSALMI GREENSTONE COMPLEX, FINLAND**

by

HEIKKI PAPUNEN, TAPIO HALKOAHO and ERKKI LUUKKONEN

with 68 pages, 27 figures, 9 tables and 1 appendix CD

GEOLOGICAL SURVEY OF FINLAND  
ESPOO 2009

**Papunen, H., Halkoaho, T. & Luukkonen, E. 2009.** Archaean evolution of the Tipasjärvi-Kuhmo-Suomussalmi Greenstone Complex, Finland. *Geological Survey of Finland, Bulletin 403*, 68 pages, 27 figures, 9 tables and data CD as an appendix.

The structure of the Archaean Kuhmo greenstone belt, which forms the central portion of the Tipasjärvi-Kuhmo-Suomussalmi (TKS) greenstone complex in eastern Finland, is essentially a regional scale, northerly trending synclinorium. It was deformed and metamorphosed during several phases of deformation, youngest of which was dated as Proterozoic. Migmatized banded amphibolites, originally Fe-tholeiitic in composition, and intermediate and felsic volcanic rocks are interpreted as the oldest preserved supracrustal rock units, and are between 3100-2900 Ma in age. They are transected by and occur as enclaves within felsic and intermediate tonalite-trondhjemite-granodiorite (TTG) intrusions, which were deformed and metamorphosed during the  $D_2/M_2$  event at  $2843 \pm 18$  Ma, when the U-Pb isotope systematics of the TTG complex were homogenized. The lowermost stratigraphic unit of the TKS greenstone complex proper is composed of felsic to intermediate volcanic rocks, which have yielded zircon ages between 2810 and 2790 Ma. Tholeiitic basalts overlie this calc-alkalic felsic-mafic unit, and predate komatiitic lavas. Tholeiitic basalts commonly display pillow structures and thin interlayers of Algoma-type banded iron formations (BIF). Mafic cumulates related to the tholeiitic eruptive rocks occur as sills and interlayers, of which the Moisiovaara mafic sill has been dated to  $2790 \pm 18$  Ma. Komatiitic lavas are common in all greenstone belts, but the units are relatively thin. Lenses of olivine mesocumulates represent proximal komatiitic lava channels and display evidence of recurrent lava flow and thermal erosion. Large bodies of serpentinite in the Kellojärvi area of the Kuhmo greenstone belt and Saarikylä area in the northern part of the TKS complex were originally komatiitic layered olivine±augite cumulates that accumulated close to the volcanic centres. The uppermost komatiitic flows in the komatiitic sequence are interlayered with komatiitic basalts, which are characterized by pillowed and variolitic textures. Basalts with anomalously high Cr contents, alternating with thin komatiitic flows overlie the komatiitic basalts. In places the mafic and ultramafic rocks are overlain by a lahar-type volcanic conglomerate with fragments of the rocks of the komatiitic sequence and felsic to mafic calc-alkalic volcanic rocks. These are transitional upwards into pelitic and psammitic sedimentary rocks with intercalations of black schists, quartzites and felsic metamorphic rocks.

Although apparent evidences, such as depositional contacts are lacking, the general stratigraphic evolution and age relationships with surrounding TTG complex, as well as felsic enclaves in ultramafic volcanic rocks and contamination of the ultramafic rocks by siliceous material indicate that the greenstone belt deposited on a felsic substrate, and we argue that it formed in an intracontinental rift system.

Key words (GeoRef Thesaurus, AGI): greenstone belts, stratigraphy, metamorphic rocks, metavolcanic rocks, cumulates, geochemistry, deformation, igneous rocks, tectonics, Archean, Sotkamo, Kuhmo, Suomussalmi, Finland

*Heikki Papunen*  
*Department of Geology*  
*University of Turku*  
*FI-20014 Turku*  
*Finland*

*Tapio Halkoaho & Erkki Luukkonen*  
*Geological Survey of Finland*  
*P.O. Box 1237*  
*FI-70211 Kuopio*  
*Finland*

*E-mail: heikki.papunen@utu.fi; htpapunen@gmail.com*

ISBN 978-952-217-074-3 (paperback)  
ISBN 978-952-217-075-0 (PDF)  
ISSN 0367-522X

## CONTENTS

Introduction .....	7
Tipasjärvi-Kuhmo-Suomussalmi Greenstone Complex .....	9
Pre-greenstone TTG complex and banded amphibolites .....	9
Structure and stratigraphy of the Tipasjärvi-Kuhmo-Suomussalmi Greenstone Complex .....	10
Tipasjärvi greenstone belt .....	11
Koivumäki Formation .....	11
Vuoriniemi Formation .....	11
Kallio Formation .....	12
Kokkoniemi Formation .....	12
Kuhmo greenstone belt .....	12
Ruokojärvi Formation .....	12
Mäkisensuo Formation .....	12
Stratigraphic units of the Siivikkovaara area .....	15
Pahakangas Formation .....	15
Siivikko Formation .....	16
Kellojärvi cumulate complex .....	26
Structures and textures of cumulates .....	26
Marginal zones of the cumulate complex .....	29
Coarse-grained volcanoclastic deposits of the Ronkaperä Formation .....	32
Suomussalmi greenstone belt .....	33
Luoma and Mesa-aho Formations .....	33
Tervonen Formation .....	34
Saarikylä Formation .....	34
Huutoniemi Formation .....	35
Geochemical evolution .....	35
Analytical data .....	35
TTG complex .....	35
Felsic volcanic rocks .....	36
Pahakangas type tholeiitic basalt .....	36
Komatiites and komatiitic basalts .....	39
Komatiitic cumulates .....	41
High-Cr basalt .....	48
Felsic volcanic rocks of the Ronkaperä Formation .....	50
Discussion on the geochemical evolution .....	54
Post-greenstone mafic and felsic intrusive rocks .....	58
Proterozoic overprinting .....	59
Evolution of the greenstone belt .....	59

Conclusions .....	63
Acknowledgements .....	65
References .....	65
Appendix: Data CD .....	68

## INTRODUCTION

The Kuhmo greenstone belt (KGB) forms the central part of a 220 km long and up to 10 km wide N-S trending Archaean Tipasjärvi-Kuhmo-Suomussalmi greenstone complex in eastern Finland (Fig 1). The southern and northern parts of the complex are known as the Tipasjärvi and Suomussalmi greenstone belts, respectively. All these three belts display similar rock associations and general stratigraphical development. Therefore, it is likely that they are remnants of an originally more extensive volcanic complex, affected by subsequent erosion and tectonic disruption.

As a type section of Archaean supracrustal rock assemblage, the Kuhmo greenstone belt has been the target of regional geological mapping by the Geological Survey of Finland (Wilkman 1921, Hypönen 1973, 1976, 1978, 1983, Luukkonen 1988, 1992, 2001, Luukkonen et al. 2002, Käpyaho et al. 2006, Matisto 1958) and research programs undertaken by the universities of Oulu (Piiirainen 1988), Rennes (Martin et al. 1984) and Turku (Papunen et al. 1998). In high-strain areas, intense deformation has obliterated primary structures and textures in the supracrustal rocks, but some low-strain key areas display well-preserved structures and textures. These include the Siivikkovaara-Kellojärvi area in the Kuhmo greenstone belt, the Taivaljärvi area in the Tipasjärvi greenstone belt (Papunen et al. 1998), and the Saarikylä (Engel & Dietz 1989) and Kiananniemi areas in the Suomussalmi greenstone belt, where detailed field studies were undertaken to revise and better define the stratigraphy and evolution. This revision was combined with regional nickel sulphide exploration, and hence special emphasis was placed on the recognition and classification of flow types and the mutual relationships between the cumulate and flow facies of komatiitic rocks. The

study also revealed new insights into the overall evolution of the Kuhmo greenstone belt.

The Fennoscandian Archaean rocks in the eastern and northern parts of the shield have been divided into five provinces, the Karelian, Belomorian, Kola, Murmansk and Norrbotten (see Hölttä et al. 2008). Slabunov et al. (2006) subdivided the Karelian Province into Western Karelian, Vodlozero and Central Karelian Terranes. Both the TTG association and greenstones of the Central Karelian Terrane are mainly Neoproterozoic, 2750–2700 Ma in age, whereas the Western Karelian and Vodlozero Terranes comprise Mesoproterozoic, 3200–2800 Ma lithologies (Sorjonen-Ward & Luukkonen 2005, Slabunov et al. 2006). The Pudasjärvi block in the western part of the Western Karelian Terrane comprises the oldest rocks of Fennoscandia, the Siurua trondhjemitic orthogneiss, which yield ages of 3500 Ma (Mutanen & Huhma 2003). The Paleoproterozoic supracrustal Kainuu schist belt and related tectonic features divide the Western Karelia Terrane into eastern Kianta block and the western Pudasjärvi-Iisalmi blocks. The Tipasjärvi-Kuhmo-Suomussalmi greenstone complex locates in the Kianta block. Different authors have divergent views of the origin of the greenstone belts in the Karelian Province, for example, Puchtel et al. (1997) inferred oceanic plateau origin for the Kostomuksha, Puchtel et al. (1999) proposed island arc origin for the Sumozero-Kenozero belt and Luukkonen (1992) continental rift zone for the Tipasjärvi-Kuhmo-Suomussalmi belt. The division of the Archaean into different terranes and megablocks, as well as the diversity of the opinions on the origin of greenstone belts, reflect the complex and variable geotectonic and accretionary history of the Fennoscandian Archaean shield.

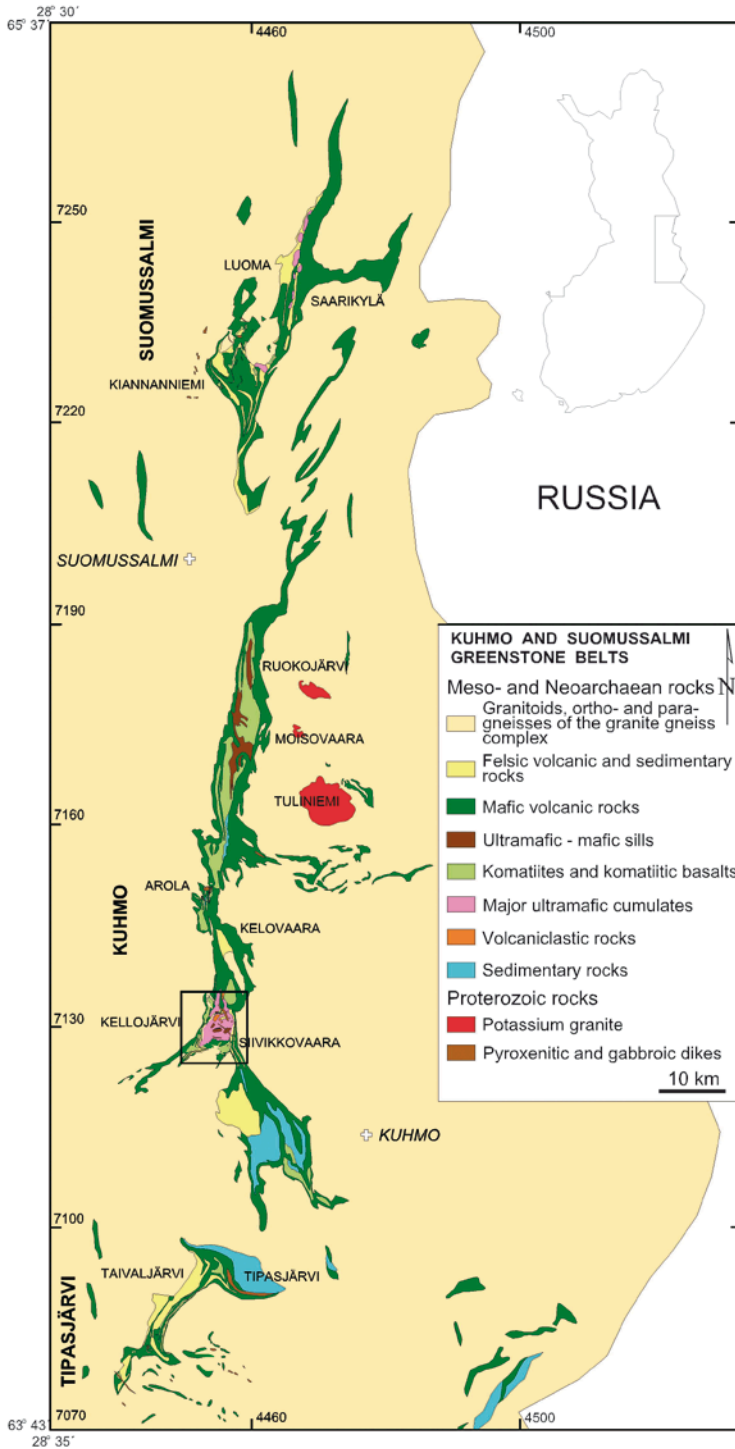


Figure 1. Tipasjärvi-Kuhmo-Suomussalmi greenstone complex in eastern Finland. Area of Kellojärvi-Siivikkovaara (Fig. 2) indicated with black line. Modified after Korsman et al. (1997).



In this study we summarise our detailed field and geochemical data on the Tipasjärvi-Kuhmo-Suomussalmi greenstone complex and discuss the

origin and evolution of the greenstone belt and present a geotectonic model.

## TIPASJÄRVI-KUHMO-SUOMUSSALMI GREENSTONE COMPLEX

Generalized lithostratigraphic sequences and chronostratigraphic interpretations of the TKS greenstone complex were published by Piirainen (1988), Luukkonen (1992), Papunen et al. (1998), Huhma et al. (1999) and Vaasjoki et al. (1999). The stratigraphic sequences vary slightly in different parts of the complex, as is typical for an area composed mainly of volcanic material. On the basis of detailed structural observations Luukkonen (1992)

combined a polyphase deformation history with the evolution of the greenstone complex. The revised stratigraphic interpretation (Table 1) and the geotectonic evolutionary model presented here are derived from the studies by Luukkonen (1992) and Papunen et al. (1998). Although the rocks described below are metamorphosed, the prefix “meta” is omitted in the text for the sake of brevity.

Table 1. Comparison of stratigraphic formations of the greenstone belts.

	Tipasjärvi Group	Kuhmo Group	Suomussalmi Group
<b>Kianta Supergroup</b>	Kokkoniemi Formation	Ronkaperä Formation	Huutoniemi Formation
	Kallio Formation	Siivikko Formation	Saarikylä Formation
	Vuoriniemi Formation	Pahakangas Formation	Tervonen Formation
	Koivumäki Formation	Mäkisensuo Formation	Mesa-aho Formation
	Basement gneiss complex	Ruokojärvi Formation	Luoma Formation
		Basement gneiss complex	Basement gneiss complex

### Pre-greenstone TTG complex and banded amphibolites

The heterogeneous tonalite-trondhjemite-granodiorite (TTG) complex is composed of banded and foliated grey gneisses, tonalites, trondhjemites and granodiorites, which were deformed during several events denoted  $D_{1-6}$  by Luukkonen (1992). The banding is composed of interlayered mafic minerals, biotite and hornblende, alternating with plagioclase, quartz and minor potassic feldspar. The grey gneisses are abundant to the east of the Kuhmo greenstone belt, whereas the bedrock to the west consists mainly of granitoids, typically granodiorite to tonalite in composition, which were intruded during various tectonic events in pre- and syn-  $D_3$  deformation as well as re-activated  $D_3$  structures (late- and post- $D_3$ ) at the time interval from 2790 to 2680 Ma (Luukkonen 1992). The eastern terrane displays a higher metamorphic grade than the west-

ern one, and according to the deep crustal seismic reflection and refraction surveys the Archaean crust is 10 km thinner east of the KGB than to the west of it (Yliniemi 1986, Kukkonen et al. 2006), although this might to some extent be the result of Proterozoic modification of the lithospheric fabric (Kontinen & Paavola 2006). The TTG granitoids are peraluminous and display low initial Sr isotope ratios (0.7023), fractionated REE patterns with HREE depletion and low Yb values.

Close to the greenstone complex the banded, folded and migmatitic TTG changes frequently to leucocratic tonalite, which is medium-grained, massive to foliated, and in places cataclastic and nebulitic. All the observed contacts of the TTG complex against the greenstone belt rocks are abrupt and are interpreted to be tectonic in nature, resulting

from  $D_3$  deformation (Luukkonen 1988, Vaasjoki et al. 1999).

The age of the TTG complex is not uniform everywhere; it was re-melted, deformed and metamorphosed under granulite/amphibolite facies condition during  $D_2/M_2$  at  $2843 \pm 18$  Ma resulting in extensive formation of migmatites.

Banded and migmatized amphibolites occur as disrupted remnants within various parts of the granitoid complex. They record the first deformation phases ( $D_{1-2}$ ) and on that basis Luukkonen (1992) regarded the banded amphibolites as the oldest unit of the Archaean sequence. Geochemical compositions of the amphibolites correspond to Fe-rich tholeiites and they probably represent an earlier extensive greenstone formation event. The age of banded amphibolites is unknown, but they are provisionally assigned an age of 3100–2900 Ma, because the rocks of the tonalite-trondhjemite-granodiorite suite (TTG) intrude them, and because they experienced the early  $D_{1-2}$  deformation. The observation is confirmed by the single crystal zircon U-Pb analyses with secondary ion mass spectrometer (SIMS) by Käpyaho et al. (2007) where the cores of zircons from mesosome of the Lylyvaara migmatite yield ages up to  $2942 \pm 6$  Ma. Detrital zircons of the Kelovaara quartzite (Fig. 1) have been dated by the U-Pb method to 3100–2996 Ma (diffusion model age; cf. Hyppönen 1983) indicating that an old felsic crust existed prior to the extensive igneous and metamorphic episode at 2830 Ma. Tentative Sm-Nd isotope determinations from

the TTG mesosome gave model ages over 3000 Ma with some of them ranging between 3900 and 3700 Ma (Luukkonen et al. 2002), but the ages are not reliable since metamorphism can cause fractionation of Sm/Nd and increase the Sm/Nd ratio leading to old  $T_{DM}$  model ages (O'Brien et al. 1993, Käpyaho et al. 2006).

The age of the Luoma Formation at Saarikylä, Suomussalmi (Fig. 1) is disputable, but the formation is here regarded as the older supracrustal unit than the Suomussalmi greenstone belt. Also the Ruokojärvi Formation (Fig. 1) at the eastern margin of the Kuhmo greenstone belt yields an age of  $3007 \pm 7$  Ma, and represents distinctly older volcanic unit than the Kuhmo greenstone belt proper. The classification is discussed later on in connection with the stratigraphy of the Kuhmo and Suomussalmi greenstone belts.

Käpyaho et al. (2006) classified the tonalites in four age groups and considered that the age obtained from Haasiavaara tonalite,  $2830 \pm 2$  Ma represents the oldest, the Huuskovaara tonalite,  $2814 \pm 3$  Ma the second plutonic phase, the age of Viitavaara tonalite,  $2785 \pm 7$  Ma represents the third generation of tonalities and the Purnu tonalite,  $2747 \pm 3$  Ma the fourth age group in the sequential growth of the Archaean crust. Granodiorites and diorites with sanukitoid geochemical characteristics intruded after tonalites and form the age group of 2740–2700 Ma, and finally leucocratic granitoids intruded in the period of 2700–2680 Ma.

## STRUCTURE AND STRATIGRAPHY OF THE TIPASJÄRVI-KUHMO-SUOMUSSALMI GREENSTONE COMPLEX

The TKS greenstone complex represents a symmetrical wide synclinorium with oldest units at the margins and the younging directions pointing to the centre of the greenstone belt complex. According to Luukkonen (1992) the greenstone belts were deformed by  $D_3$ , but the earliest regionally recognized phases of deformation,  $D_{1-2}$ , cannot be observed

inside the greenstone belts. Lithostratigraphical rock units are described below, starting with the oldest units (Table 1), for different domains within the TKS greenstone complex, after which an attempt is made to correlate stratigraphical units along the entire complex.

## Tipasjärvi greenstone belt

Felsic-dominated volcanic rocks are more abundant in the Tipasjärvi greenstone belt than elsewhere in the TKS greenstone complex, where they occur only as isolated occurrences at both the eastern and western margins of the complex. A disseminated Ag-Zn-Pb sulfide deposit is associated with felsic volcanic rocks in the Taivaljärvi area (Fig.1) and this area was studied in detail as the type sequence of felsic volcanic rocks (Taipale 1983, Papunen et al. 1989).

### *Koivumäki Formation*

The felsic to intermediate calc-alkalic volcanic rocks form the lowermost unit of the Tipasjärvi greenstone sequence and are defined as the Koivumäki Formation (Table 2). Lithologically and stratigraphically this 2790±3 Ma old unit (Vaasjoki 1999) can be correlated in the Kuhmo greenstone belt with the 2798±15 Ma old Juurikkaniemi felsic-dominated unit of the Ontojärvi area, the Mäkisen-suo Formation of the Siivikkovaara area and the 2810±48 Ma old felsic unit from the Vuosanka area. The ages are thermal ion multicollector mass spectrometer (TIMS) U-Pb ages from zircon fractions (Luukkonen 1992).

The rocks of the Koivumäki Formation are either massive quartz-porphyrries or more commonly volcanic breccias, and layered tuffs and tuffites indicating shallow water or subaerial eruption (Taipale 1983). The Taivaljärvi Ag-Zn-Pb occurrence is

located in the middle of the felsic succession where a number of quartz veins characterize the ore zone. The deposit was divided into four ore bodies with different base and precious metal ratios and the ore bodies are roughly parallel to primary stratigraphic layering. Geochemistry and mineralogy of the host rocks indicate potassic and magnesian hydrothermal alteration. An extensive quartz-kyanite rock layer is present some 100 meters stratigraphically above the mineralized zone. The felsic rocks between the deposit and the layer of quartz-kyanite rock are K-Mg altered, whereas no alteration has been found stratigraphically above the quartz-kyanite rock. The kyanite-quartz rock is interpreted as the metamorphic equivalent of an intensely leached cap-rock developed in an epithermal hydrothermal system (Papunen et al. 1989).

The basal contact of the Koivumäki Formation with the underlying TTG gneisses is not exposed in outcrop, but drilling reveals that the felsic succession is underlain by a homogeneous felsic porphyry which grades transitionally into TTG granitoid.

Higher up in the succession alternating layers of mafic and felsic tuffs (Taipale 1983) indicate that mafic eruptions occurred contemporaneously with felsic volcanism.

### *Vuoriniemi Formation*

A sulfide- and graphite-bearing cherty layer and magnetite banded iron formations mark the upper

Table 2. Stratigraphy of the Tipasjärvi greenstone belt.

Formation	Lithology	Thickness (Age)
Kokkonniemi	Mica schists / pelites, felsic volcanoclastics	(2746±8; Kontinen 2007, pers. com.)
Kallio	MgO-rich lavas: Cr basalts, komatiitic basalts, komatiites	200 m
Vuoriniemi	Tholeiitic basalts, tuff, BIF, black schists, mafic-felsic mixed metatuff	250 m
Koivumäki	Felsic tuff and pyroclastic breccias, quartz-porphyry, Ag-Zn-Pb deposit, quartz-kyanite rock ("a cap rock" of volcanic hydrothermal alteration system)	500 m (2790±3 Ma; Vaasjoki 1999)
Basement	Tonalite-trondhjemite, granodiorite, gray gneisses	(2832±3 Ma; Hyvärinen 1989) (2814±3 Ma; Käpyaho et al. 2006)

contact of the Koivumäki Formation with the overlying Vuoriniemi Formation, indicating a break in the volcanic activity at the end of the Koivumäki succession. The next phase in the greenstone belt evolution consists of eruption of voluminous pillowed tholeiitic lavas of the Vuoriniemi Formation, with interlayers of tuffs, graphite schists and sulfide facies iron formations.

#### *Kallio Formation*

Komatiitic lavas with spinifex and pillow textures in the overlying Kallio Formation are abundant in the northern part of the Tipasjärvi greenstone belt, whereas in the south they occur only as thin horizons with local small cumulate serpentinite bodies.

Komatiitic basalts of the Kallio Formation display pillow and variolitic textures and basaltic lavas with anomalously high concentrations of chromium (630–2420 ppm Cr), named Cr and high-Cr basalts by Halkoaho et al. (2000) are also present.

#### *Kokkonniemi Formation*

Mica schists and metapelites of the Kokkonniemi Formation overlie the ultramafic-mafic volcanic succession. Taipale (1983) interpreted the Kokkonniemi Formation as weathering products of the underlying volcanic rocks. The available age determination of the mica schist, (SIMS)  $2746 \pm 8$  Ma age (Kontinen 2007, pers. com.) supports the interpretation.

### **Kuhmo greenstone belt**

Mafic volcanic rocks, the most voluminous rocks of the greenstone belts, occur along both the eastern and western margins of the Kuhmo greenstone belt (KGB) with the stratigraphical younging directions revealing that the belt represents a regional scale synclinal structure. The well-preserved volcanic structures and textures within mafic rocks in the low-strain Siivikkovaara area (Figs 1, 2 and 3) enable establishment of a type section for the Kuhmo greenstone belt, which is described below in detail (e.g. Papunen 1960, Hanski 1980, Hyppönen 1983, Gruau et al. 1992). The volcanic succession defined in this low-strain area formed the basis for extrapolation into areas of high strain and polyphase deformation, and the results are compared below with the observations of the Siivikkovaara stratigraphical sequence.

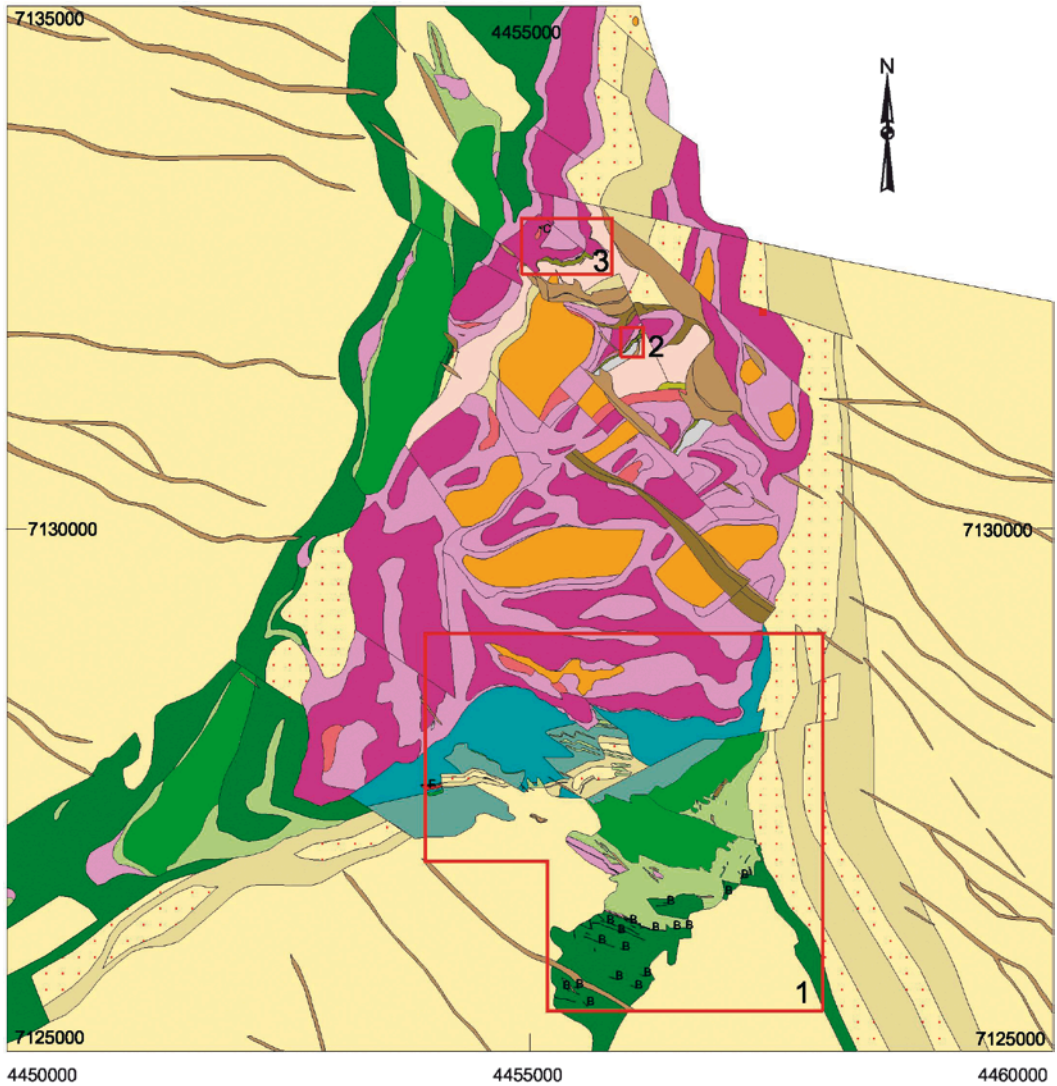
#### *Ruokojärvi Formation*

A small isolated sequence composed of felsic volcanic rocks, volcanic conglomerates, tuffs and tuffites is exposed near Lake Ruokojärvi, at the eastern margin of the northern extension of the Kuhmo greenstone belt (Fig.1). TIMS U-Pb age determinations from four zircon fractions from a

recrystallized homogeneous felsic tuff gave an age of  $3007 \pm 7$  Ma (Luukkonen et al. 2002). Although located at the margin of the KGB, the age of the Ruokojärvi felsic tuff permits correlation with the felsic volcanic rocks of the Luoma Formation in the Suomussalmi greenstone belt (Tables 3 and 5); the sequence is thus older than the TKS belt proper.

#### *Mäkisensuo Formation*

In the Siivikkovaara area a sequence of felsic to mafic volcanic rocks occur at Mäkisensuo (Fig. 3). It is, however, buried beneath surficial deposits and geochemical studies are based on samples obtained from drilling by Outokumpu Oy (Papunen et al. 1998). The rocks are intensely deformed and display low-grade Zn-Pb mineralization. The total thickness of the unit in the eastern part of Mäkisensuo is 300 m and the sequence thins westwards to 100 m. Although the Mäkisensuo felsic to mafic unit is not directly dated, and the drilling profiles do not uncover the relationship with other formations it is here tentatively correlated stratigraphically with the Juurikkaniemi and Vuosanka felsic volcanic rocks in the Kuhmo greenstone belt, and the Koivumäki Formation in the Tipasjärvi greenstone belt.



Legend

Meso- and Neoproterozoic rocks

TTG basement, granodiorite and tonalite

Reworked basement (felsic porphyries)

Greenstone belt

Mafic volcanic rocks (CA)

Felsic volcanic rocks (CA)

Tholeiitic basalt

Banded iron formation

Komatiitic flows and cumulates

Olivine adcumulate

Olivine meso-orthocumulate

Olivine-clinopyroxene cumulate

Plagioclase-augite cumulate

Margin clinopyroxenite

Chlorite schist inclusion

Komatiitic flows

Komatiitic basalt

High-Cr basalt (Cr 1300-4500 ppm)

Cr basalt (Cr 450-1300 ppm)

Volcaniclastic rocks

Phyllite

Proterozoic rocks

Wehrlitic and pyroxenitic dikes

Gabbroic dike

Figure 2. Geological outline of the Kellojärvi-Siivikkovaara area in the central part of the Kuhmo greenstone belt. Areas of detailed maps are indicated with red line: 1. Siivikkovaara-Pahakangas (Fig. 3); 2. NW of Hyttimäki at crossroads area (Fig. 11B); 3. west of Ensilä (Fig. 11A). CA = calc-alkalic (Tulenheimo 1999).

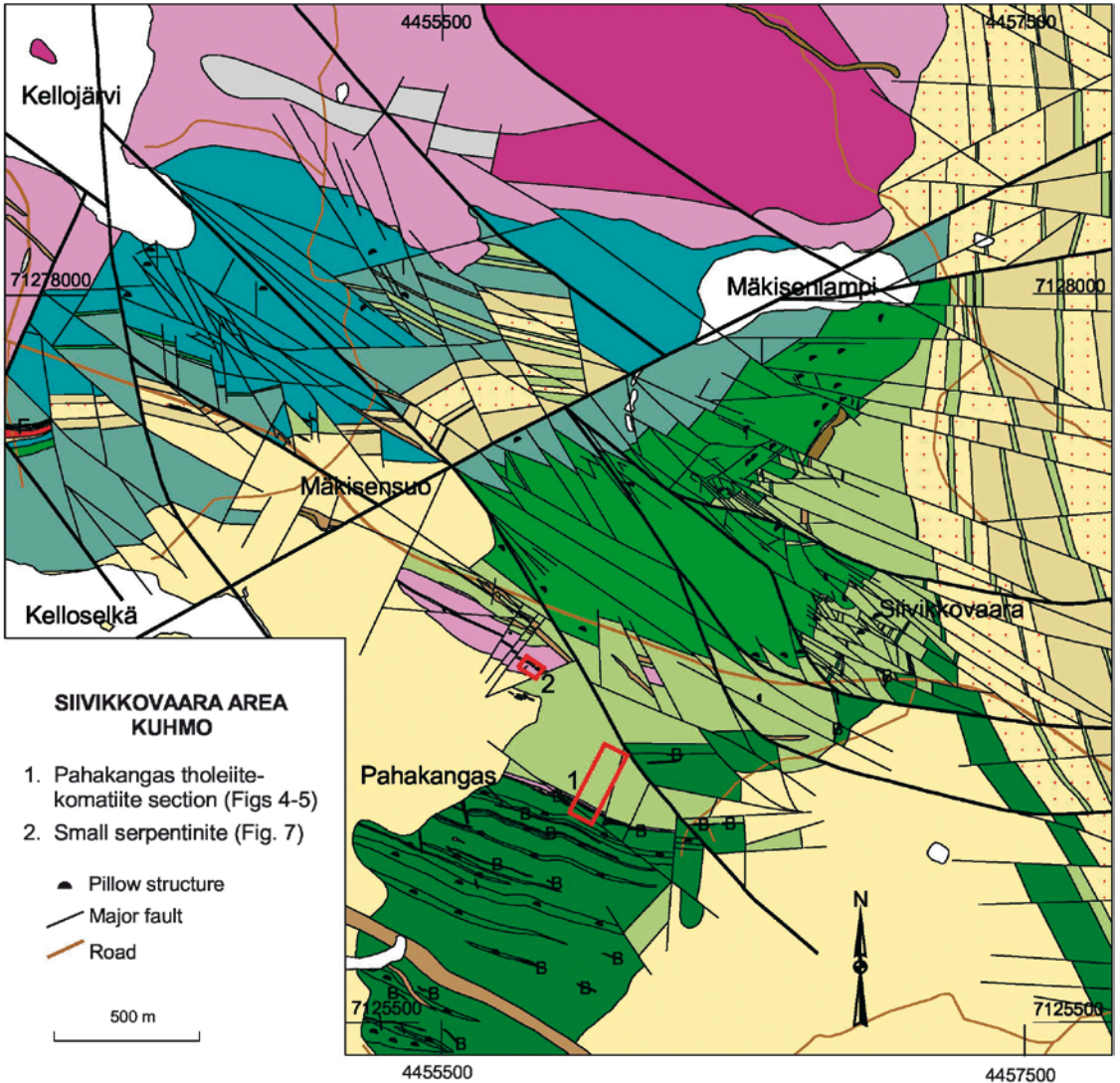


Figure 3. Geology of the Siivikkovaara-Pahakangas-Mäkisensuu volcanic succession of the Kuhmo greenstone belt. Red rectangles indicate areas of Fig. 4 (1) and Fig. 7 (2).

Table 3. Stratigraphy of the Kuhmo greenstone belt.

Formation / "Member"	Lithology	Thickness	Interpretation (Age)
Ronkaperä	Pelitic sediments and quartzites, pyroclastic intermediate-mafic volcanic rocks	300 m	Subaerial volcanism, lahar deposits (2744±34 Ma from a greywacke in Petäjaniemi; Peltonen 2007, pers. com.)
Unconformity? -----			
Siivikko/"Suo"	Cr-rich basalts, komatiitic interlayers	500 m	
Siivikko / "Mäkinen"	Komatiitic basalts, Kellojärvi cumulates of komatiitic basalts	300 m 300 m	Upper part of the Kellojärvi cumulate complex
Siivikko/"Vaara"	Komatiitic non-fractionated flows, Komatiitic fractionated flows, Komatiitic cumulates of Kellojärvi	500 m 50 m 300 m	Lower part of the Kellojärvi cumulate complex (2771±8 Ma; rim of a zircon crystal from a felsic enclave in komatiitic cumulate; Peltonen 2007, pers. com., Peltonen et al., in prep.)
Pahakangas	Tholeiitic basalts, BIF interlayers	1000 m	(2790±18 Ma from the Moisiovaara sill, which is geochemically similar to the Pahakangas tholeiitic basalts; cf. Luukkonen 1992)
Start of rifting .....			
Mäkisensuu	Bimodal calc-alkalic mafic-felsic volcanic rocks and sedimentary interlayers	300 m in W 1000 m in E	(2798±15 Ma from Juurikkaniemi, Ontojärvi, felsic volcanic rocks; cf. Hyppönen 1983. 2810±48 Ma from Vuosanka felsic volcanic rocks/hypabyssal felsic rock; cf. Hyppönen 1983).
Ruokojärvi	Felsic tuff, pyroclastic breccias and volcanic conglomerates	200 m	(3007±7 Ma; Luukkonen et al. 2002).

### Stratigraphic units of the Siivikkovaara area

The volcanic sequence in the Siivikkovaara area comprises tholeiitic basalts, thin komatiitic flows, and different types of komatiitic cumulates, komatiitic basalts and overlying Cr-rich basalts. The sequence will be described, from lowermost to uppermost, in the following paragraphs.

#### *Pahakangas Formation*

Papunen (1960) and Hanski (1980) described the tholeiitic basalts of the Pahakangas area (Fig. 3). This area experienced low-strain deformation and the lava flow layering is subvertical, trending roughly E-W, with a younging direction towards the north. Thus the Pahakangas-Siivikkovaara area

reveals a valuable cross section through the greenstone belt, which forms a basis for stratigraphic interpretation. Layers of massive and pillow basalts occur alternately. The upper contacts of the pillow textured basalts are locally covered with a thin layer of chert or banded iron formation (BIF), but the lower contacts against the massive parts of the flows are abrupt and the pillows are brecciated by the underlying injected massive lava. These features indicate that massive lower parts of the flows extruded later and inflated the pillow-textured flow tops. The pillow layers range up to 10–20 m in thickness, but the massive parts may reach thicknesses of 70 m.

The pillows display loaf shapes with an average aspect ratio of two to three. Hyaloclastite layers between the pillows are hydrothermally altered to a white massive albite-clinozoisite-quartz rock,

which also locally extends to the interior of the pillow wherever high porosity facilitated hydrothermal fluid flow.

The basalt is fine-grained and aphyric, composed of hornblende, albite and clinozoisite with local hornblende pseudomorphs after primary clinopyroxene xenocrysts. Albitic plagioclase is fine-grained and commonly displays skeletal habit (Hanski 1980). The uppermost part of the Pahakangas Formation consists of glomeroporphyritic basalts with single crystals and groups of plagioclase phenocrysts up to 1–3 cm in diameter. The glomeroporphyritic flows are amygdaloidal with quartz, epidote, carbonate and albite filling the original vesicles. Pillow cores within these flows are altered to epidote-albite-quartz rock indicating former presence of hollow or porous spaces. Amygdules are absent from the flows underlying the glomeroporphyritic flows.

The substrate of the basalt flows is not preserved. Fine-grained granodioritic/tonalitic dikes and contact breccias are common at the margins of the Pahakangas basalt.

A porphyritic felsic sill was intruded within the upper contact zone of the basalts. It is subparallel with respect to lithologic layering, more foliated than the granodioritic dikes and composed of oligoclase and quartz phenocrysts in a fine-grained felsic matrix. Major element compositions and REE spectra resemble those of the granodiorite west of Pahakangas. Tourpin (1991) dated a quartz-oligoclase porphyry dike at the Siivikkovaara hill, in the same stratigraphic level as in Pahakangas, at  $2770 \pm 30$  Ma (U-Pb dating of zircon).

In addition to basalts the Pahakangas Formation includes Algoma-type banded iron formation (BIF) and associated hornblende-garnet-biotite rocks (Papunen 1960). The BIF is composed of alternating quartz, grünerite and magnetite (martite) bands. The BIF layers overlie the pillow basalts, and massive, non-pillow basalt overlies the BIF layers. Intense hydrothermal alteration characterizes the pillow basalt below BIF, and locally the pillows display zoned propylitic alteration. The BIF layer follows the surface topography of the pillow basalt and varies in thickness from a few cm to tens of metres. The BIF layers are at thickest in the central part of the

Pahakangas basalt area and thins laterally towards the margins of the basalt area. Disseminated sulfides are common in the BIF, and sulfides are also found within the altered basalt below BIF.

Combined pillow and massive tholeiitic basalt flows range up to 90 metres in thickness. In the other parts of the greenstone belts, the tholeiitic basalt units are not as thick as at Pahakangas, and BIF interlayers are rare. The Pahakangas Formation is capped by a thick BIF, indicating a considerable hiatus in volcanic activity before eruption of the overlying Siivikko Formation (Table 3). The uppermost BIF layer is sulfide-rich and can be classified as an oxide-sulfide-facies iron formation.

At Moisiovaara, in the northern part of the Kuhmo greenstone belt, a pegmatoid-textured tholeiitic mafic sill, geochemically similar to the Pahakangas tholeiitic basalt, has been mapped. It is dated by the U-Pb zircon method to  $2790 \pm 18$  Ma, which is interpreted as the time of crystallization of the mafic sill (Luukkonen 1992), and hence coeval with the Pahakangas tholeiites.

### *Siivikko Formation*

*Komatiitic Vaara Member.* A 1–2 m thick tremolite rock forms the lowermost layer of the komatiitic Vaara Member, which overlies the thick sulfidic BIF of the Pahakangas Formation. Figures 4 and 5 depict the stratigraphic column of the first sixteen komatiitic flows and Table 4 gives selected assays of their chemical compositions. Locally a 3–4 m thick dike of porphyritic felsic quartz-oligoclase rock, similar to the felsic sill mentioned above at the top of tholeiitic basalt sequence, is present between tremolite rock and the overlying 20 m thick olivine ortho-mesocumulate, which represents the B-layer of the first fractionated komatiite flow (the komatiite terminology applied here is from Hill et al. 1990). Upwards, a thin layer of aligned hopper olivines (B1-layer) follows the olivine ortho-mesocumulate (B2), then a 4 m thick (A-) layer of platy olivine spinifex (Fig. 6A) and 2 m thick layer of random spinifex. Locally a 3 m thick pyroxene spinifex layer with stringy beef and random pyroxene textures overlies the platy spinifex layer.



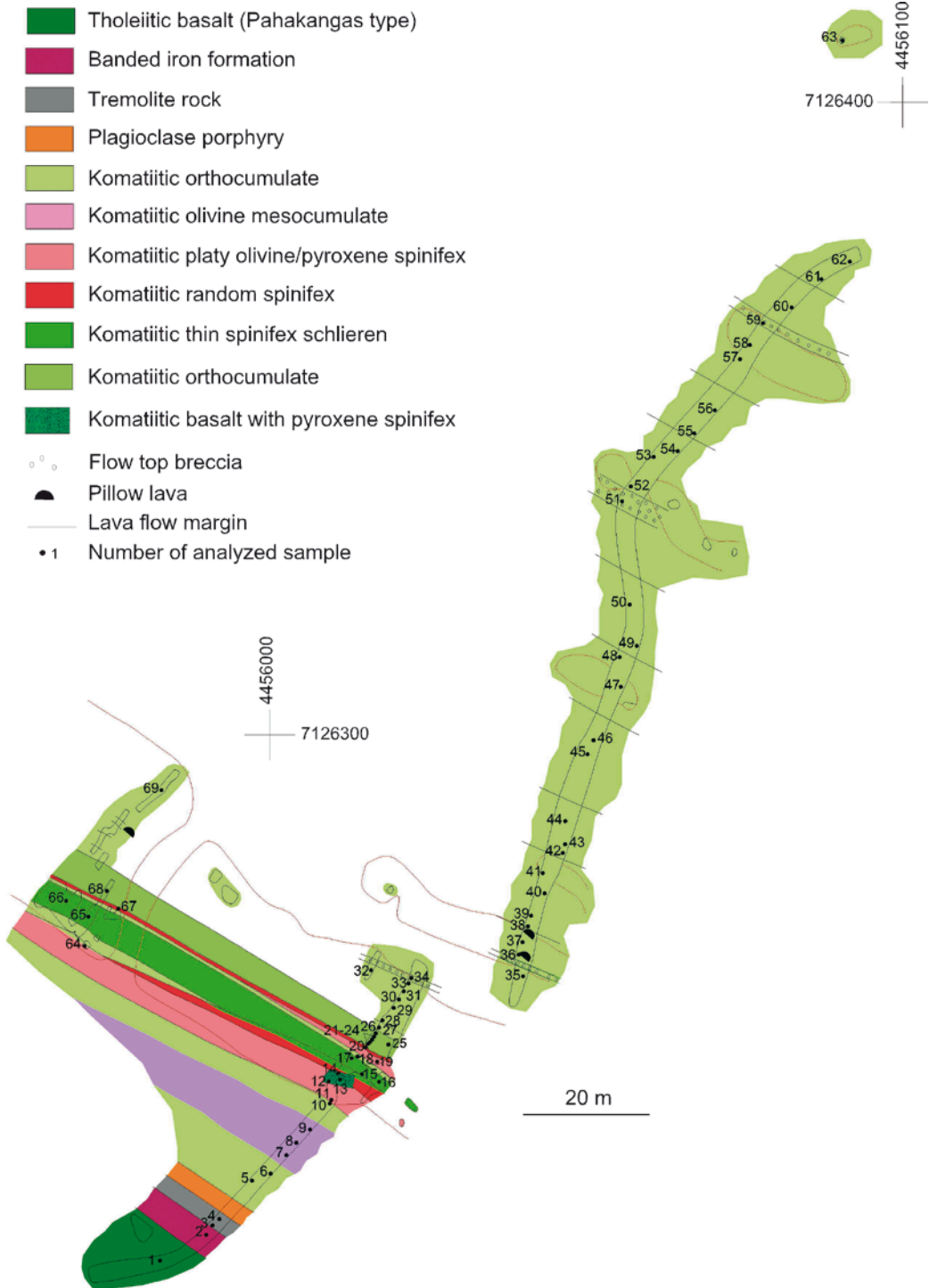


Figure 4. Detailed map of outcrops depicts the tholeiite-komatiite succession at Pahakangas area. The numbers refer to analyses presented in full in Papunen et al. (1998) and in the Appendix data-CD; selected analyses are presented in Table 4 to exemplify the chemical compositions.

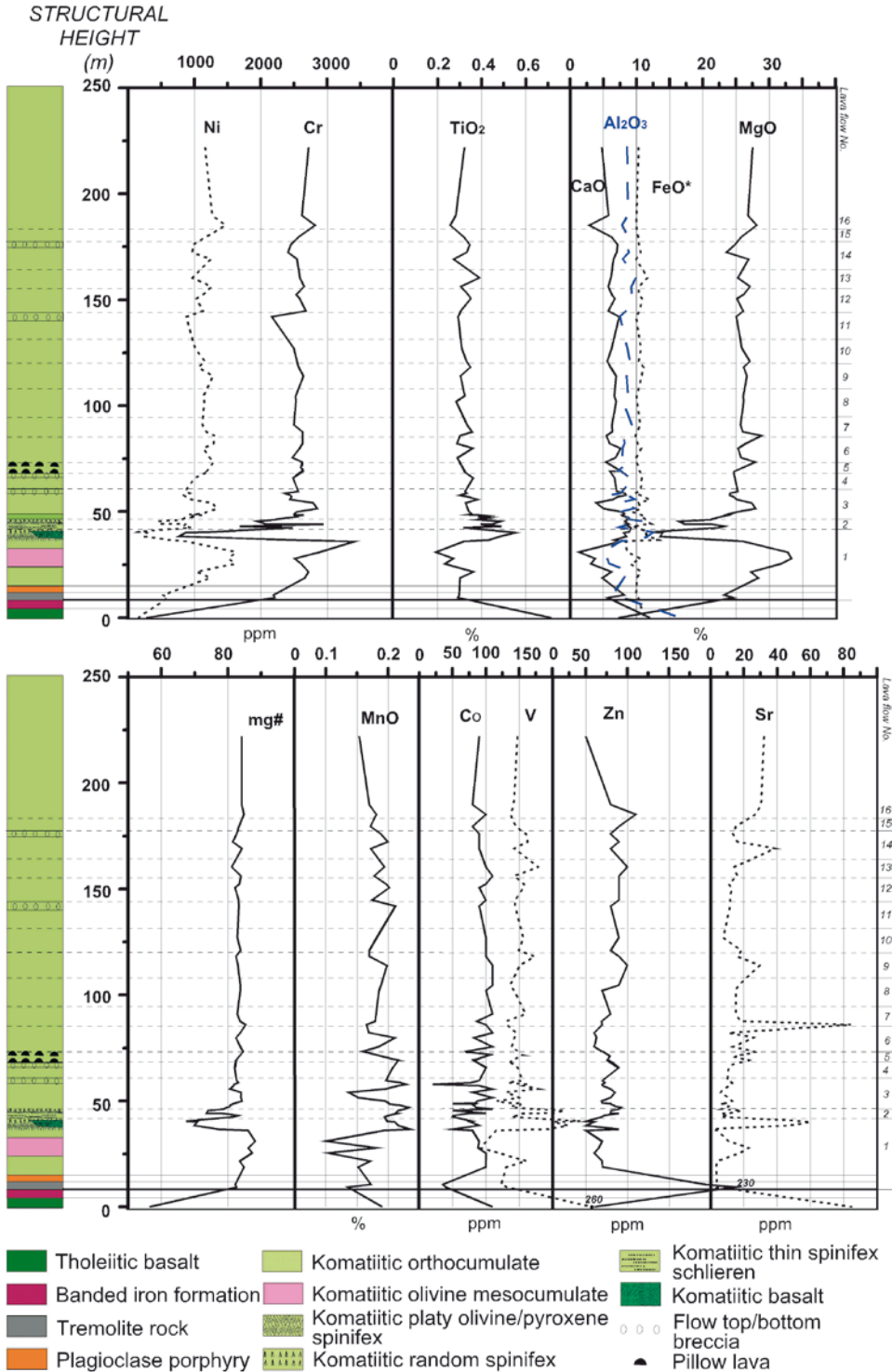


Figure 5. Geochemistry of the tholeiite-komatiite succession depicted in Fig. 4, Pahakangas area. The analyses are presented in Papunen et al. (1998) and in the Appendix data-CD.

Table 4. Selected analyses of the rock types described in Figures 4 and 5 of the Pahakangas area (normalized to volatile-free). The numbers refer to Figure 4 (n.d. = not determined; mg# = 100\*(MgO/40.32)/[(MgO/40.32)+0.9\*(FeO/71.85)]. FeO\* = total Fe as FeO. Stratigraphic height was measured from tholeiitic basalt upwards).

Nr. in Fig 4		1	2*	3	4*	5*	9*	10	14
Sample ID		6TOH 93		8TOH 93				17TOH 93	21TOH 93
Rock		Thol	BIF	Contact	Contact	Olivine	Olivine	Komat.	Komat.
type		basalt	BIF	hybr. flow	hybr. flow	orthocum	mesocum.	flow	basalt
Stratigr. level m		0.0	7.8	9.4	10.7	18.8	31.0	36.0	40.5
SiO <sub>2</sub>	%	50.22	n.d.	50.85	51.40	47.72	51.59	49.21	50.77
TiO <sub>2</sub>	%	0.71	n.d.	0.29	0.30	0.30	0.19	0.32	0.53
Al <sub>2</sub> O <sub>3</sub>	%	16.50	n.d.	7.75	6.41	8.09	4.90	7.60	12.15
FeO*	%	11.14	n.d.	10.31	9.96	10.09	8.63	8.35	11.63
MnO	%	0.19	n.d.	0.14	0.17	0.15	0.10	0.19	0.20
MgO	%	7.29	n.d.	24.63	23.18	28.39	32.85	26.16	12.15
CaO	%	12.06	n.d.	5.67	8.17	4.83	1.30	7.61	8.93
Na <sub>2</sub> O	%	1.56	n.d.	<0.01	0.06	<0.01	<0.01	0.02	3.33
K <sub>2</sub> O	%	0.228	n.d.	0.015	0.011	0.007	0.008	0.008	0.114
Cr <sub>2</sub> O <sub>3</sub>	%	0.04	n.d.	0.32	0.32	0.39	0.42	0.50	0.18
P <sub>2</sub> O <sub>5</sub>	%	0.07	n.d.	0.03	0.01	0.03	0.01	0.02	0.03
mg#		56.45		82.55	82.17	84.78	88.29	86.11	67.41
Al <sub>2</sub> O <sub>3</sub> /TiO <sub>2</sub>		23.09		26.56	21.37	26.97	25.79	23.87	23.08
Ni	ppm	150	n.d	600	522	1240	1620	890	150
Co	ppm	110	5	40	35	100	90	80	80
Cu	ppm	250	27	30	11	40	<10	10	80
Zn	ppm	60	n.d.	230	194	70	70	50	50
S	ppm	1080	70	0	150	280	600	0	70
V	ppm	260	n.d.	132	123	131	101	115	242
Sr	ppm	85	2	3	4	3	11	4	55
Cr	ppm	272	n.d.	2210	2191	2668	2887	3414	1245
As	ppm	50	58	320	440	104	1350	110	10
Ba	ppm	9	7	90	52	6	12	27	27
Rb	ppm	1.37	0.40	0.46	0.40	0.40	0.40	1.37	2.74
Y	ppm	18.0	5.0	8.6	12.5	7.4	1.5	6.0	13.0
Zr	ppm	30	6	23	37	11	6	7	22
Pb	ppm	<5	10	12	14	10	8	10	<5
Li	ppm	n.d	1	5	4	2	2	n.d.	n.d.
Sc	ppm	n.d	<2	20	20	18	14	n.d.	n.d.
Ga	ppm	n.d	1	9	8	8	6	n.d.	n.d.
Nb	ppm	6.0	0.5	1.0	1.0	1.0	1.0	8.0	5.0
W	ppm	10	1	17	<1	17	2	<1	<1
La	ppm	n.d.	1	0.9	0.7	0.7	0.8	n.d.	n.d.
Ce	ppm	n.d.	2.1	2.2	1.7	2.1	1.2	n.d.	n.d.
Pr	ppm	n.d.	0.4	0.4	0.4	0.4	0.2	n.d.	n.d.
Nd	ppm	n.d.	1.8	1.6	2.3	1.9	1.1	n.d.	n.d.
Sm	ppm	n.d.	0.5	0.7	1.1	0.7	0.3	n.d.	n.d.
Eu	ppm	n.d.	0.3	0.2	0.3	0.2	0.1	n.d.	n.d.
Gd	ppm	n.d.	0.8	1.3	1.9	1.2	0.5	n.d.	n.d.
Tb	ppm	n.d.	0.1	0.2	0.3	0.2	0.1	n.d.	n.d.
Dy	ppm	n.d.	0.9	1.5	2.1	1.4	0.3	n.d.	n.d.
Ho	ppm	n.d.	0.2	0.3	0.4	0.3	0.1	n.d.	n.d.
Er	ppm	n.d.	0.5	0.9	1.3	0.9	0.2	n.d.	n.d.
Tm	ppm	n.d.	0.1	0.1	0.2	0.1	<0.1	n.d.	n.d.
Yb	ppm	n.d.	0.5	0.9	1.2	0.9	0.2	n.d.	n.d.
Lu	ppm	n.d.	0.1	0.1	0.2	0.1	<0.1	n.d.	n.d.

\* = analysis presented in Papunen et al. 1998

Table 4. Continued.

Nr. in Fig 4		16*	19*	24*	29	35	36*	47	48
Sample ID		38TOH 93		43TOH 93		62TOH 93		88TOH 93	
Rock		Komat.	Komat.	Komat.	Komat.	Komat.	Komat.	Komat.	Komat.
type		flow	spinifex	flow	flow	flow	flow	flow	flow
Stratigr. level m		43.1	45.5	48.5	54.1	65.8	69.2	114.0	118.2
SiO <sub>2</sub>	%	49.31	49.71	47.83	49.83	46.68	48.64	45.98	47.84
TiO <sub>2</sub>	%	0.49	0.49	0.39	0.33	0.36	0.32	0.30	0.32
Al <sub>2</sub> O <sub>3</sub>	%	7.96	10.90	8.47	7.50	9.51	7.18	8.53	8.76
FeO*	%	9.37	11.41	10.82	10.38	10.81	10.48	10.80	10.27
MnO	%	0.20	0.22	0.20	0.14	0.21	0.22	0.20	0.17
MgO	%	23.36	16.39	23.93	27.39	24.85	24.85	26.70	25.81
CaO	%	8.83	8.22	7.76	3.91	6.70	7.67	6.97	6.23
Na <sub>2</sub> O	%	0.20	2.29	0.18	0.10	0.21	0.23	0.10	0.19
K <sub>2</sub> O	%	0.011	0.060	0.011	0.000	0.285	0.011	0.005	0.015
Cr <sub>2</sub> O <sub>3</sub>	%	0.25	0.28	0.39	0.41	0.36	0.39	0.39	0.37
P <sub>2</sub> O <sub>5</sub>	%	0.02	0.02	0.02	0.02	0.03	0.01	0.03	0.02
mg#		83.15	73.99	81.40	83.93	81.99	82.43	83.04	83.27
Al <sub>2</sub> O <sub>3</sub> /TiO <sub>2</sub>		16.27	22.24	21.72	22.90	26.27	22.44	28.06	27.49
Ni	ppm	836	450	1117	1273	1000	1188	1280	1170
Co	ppm	51	50	84	80	100	81	110	80
Cu	ppm	2	<10	83	17	10	19	70	50
Zn	ppm	72	80	80	85	90	76	100	90
S	ppm	50	1260	1510	280	0	420	390	0
V	ppm	147	218	152	131	148	136	151	145
Sr	ppm	9	19	10	6	11	24	30	15
Cr	ppm	1682	1943	2650	2787	2484	2641	2648	2573
As	ppm	68	n.d.	n.d.	n.d.	10	n.d.	10	10
Ba	ppm	1	n.d.	n.d.	3	45	n.d.	36	27
Rb	ppm	0.20	n.d.	n.d.	0.04	6.40	n.d.	1.37	2.29
Y	ppm	7.2	n.d.	n.d.	8.0	11.0	n.d.	7.0	6.0
Zr	ppm	25	n.d.	n.d.	15	7	n.d.	7	7
Pb	ppm	8	n.d.	n.d.	9	<5	n.d.	<5	10
Li	ppm	10	n.d.	n.d.	n.d.	n.d.	n.d.	n.d.	n.d.
Sc	ppm	24	n.d.	n.d.	n.d.	n.d.	n.d.	n.d.	n.d.
Ga	ppm	9	n.d.	n.d.	9	n.d.	n.d.	n.d.	n.d.
Nb	ppm	1.5	n.d.	n.d.	0.1	5.0	n.d.	7.0	3.0
W	ppm	<1	n.d.	n.d.	<1	<1	n.d.	<1	10
La	ppm	0.4	n.d.	n.d.	0.7	n.d.	n.d.	n.d.	n.d.
Ce	ppm	1.5	n.d.	n.d.	1.6	n.d.	n.d.	n.d.	n.d.
Pr	ppm	0.3	n.d.	n.d.	0.5	n.d.	n.d.	n.d.	n.d.
Nd	ppm	1.6	n.d.	n.d.	2.5	n.d.	n.d.	n.d.	n.d.
Sm	ppm	0.7	n.d.	n.d.	1.0	n.d.	n.d.	n.d.	n.d.
Eu	ppm	0.2	n.d.	n.d.	0.3	n.d.	n.d.	n.d.	n.d.
Gd	ppm	1	n.d.	n.d.	1.3	n.d.	n.d.	n.d.	n.d.
Tb	ppm	0.2	n.d.	n.d.	0.3	n.d.	n.d.	n.d.	n.d.
Dy	ppm	1.3	n.d.	n.d.	1.9	n.d.	n.d.	n.d.	n.d.
Ho	ppm	0.3	n.d.	n.d.	0.4	n.d.	n.d.	n.d.	n.d.
Er	ppm	0.9	n.d.	n.d.	1.1	n.d.	n.d.	n.d.	n.d.
Tm	ppm	0.1	n.d.	n.d.	0.2	n.d.	n.d.	n.d.	n.d.
Yb	ppm	0.9	n.d.	n.d.	1.3	n.d.	n.d.	n.d.	n.d.
Lu	ppm	0.1	n.d.	n.d.	0.2	n.d.	n.d.	n.d.	n.d.

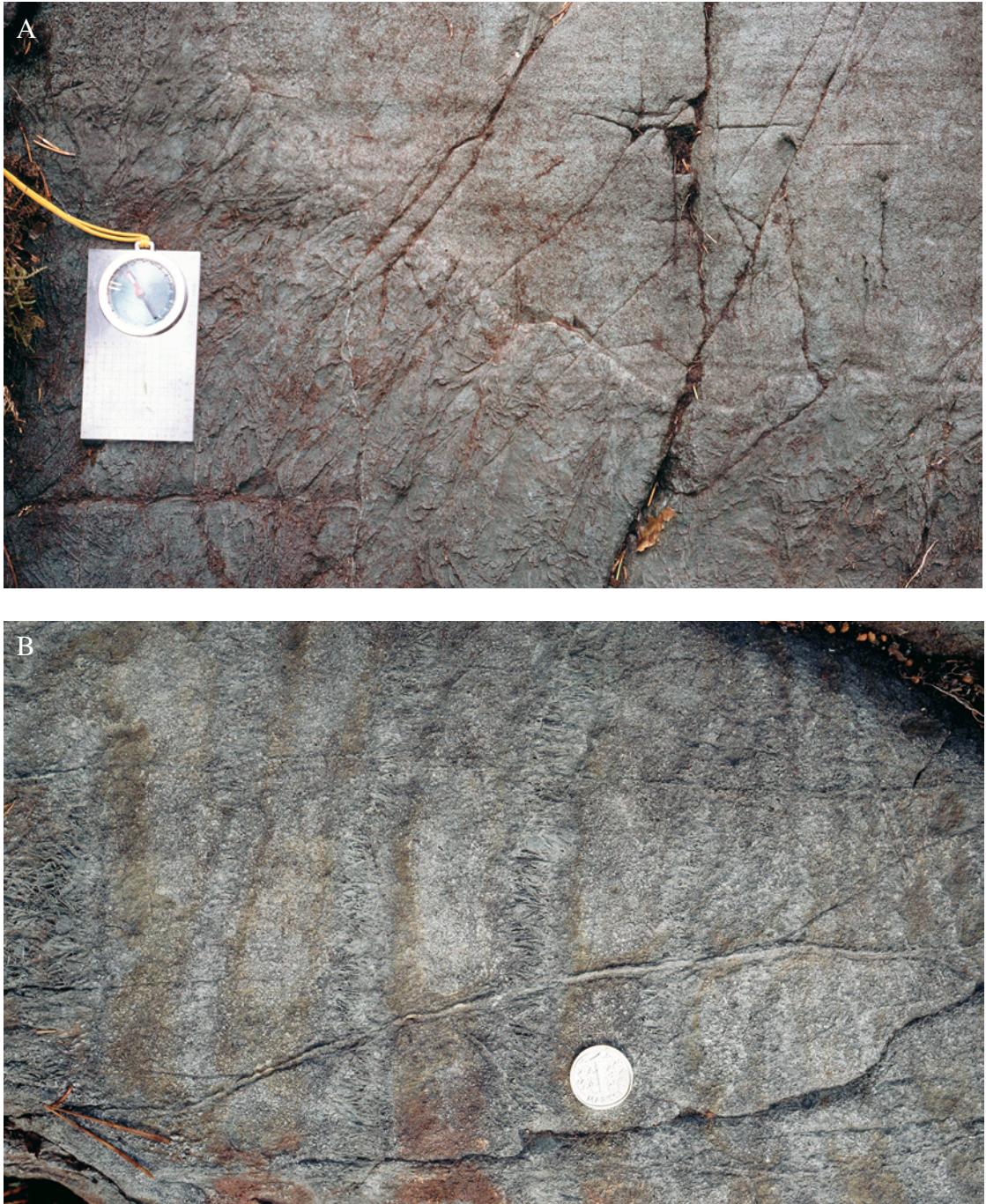


Figure 6. A. Random spinifex flow-top zone of the underlying komatiitic flow was thermally eroded and left the long sheeted spinifex at the contact against overlying orthocumulate of the next flow, Pahakangas (4455970/7126265). The length of the compass is 12.5 centimetres. B. Thin spinifex “dikes” (vertical in photo) in komatiitic orthocumulate (4455970/7126270). The diameter of the coin is 2.5 centimetres. C. Komatiitic flow bottom/top breccia, Siivikkovaara (4456705/7126625). D. Foliated ( $D_2$ ) komatiitic dike (left) cutting the banded amphibolite ( $D_{1,2}$ ) in Vuosanka (4456920/7144730). The length of the scale is 15 centimetres. Figs A-C: photos T. Halkoaho, Fig. D: photo E. Luukkonen.



Figure 6. Continued.

The 2–3 m thick olivine orthocumulate (B) layer of the second flow contains up to 60 spinifex-textured dikes, 2–10 cm thick, subparallel to layering (Fig. 6B). The spinifex crystals are parallel to each other, extending across the dike, and a thin random spinifex seam borders both contacts. The second flow locally eroded the A zone of the underlying first flow, so that the flow top breccia and random spinifex layer are missing (Fig. 6A). The third flow is 2 m thick and contains a 0.5 m cumulate layer, a one metre thick platy spinifex layer and 0.5 m thick random spinifex at the flow top.

The next flows above the third fractionated flow are non-fractionated, locally pillow-structured and brecciated at the top (Fig. 6C), but without spinifex textures. The next flow (fourth in order) displays a massive orthocumulate layer 3 m thick, overlain by a 9 m thick orthocumulate with polyhedral jointing and a one metre thick flow top breccia. The 10 m thick fifth flow consists totally of polyhedral jointed orthocumulates and again a metre of flow top breccia. The sixth flow is 4 m thick and contains pillow-like structures at the basal and uppermost parts of the flow and the central part is polyhedrally jointed. Above it, there are at least 11 flows of polyhedral-jointed orthocumulates with local flow top breccias ranging in thickness from 11 to 15 metres.

Despite the well-preserved textures, the minerals of the flows are now entirely metamorphic. The main minerals are serpentine, talc and magnesite in the cumulate layers and tremolite, chlorite, albite and carbonate in the spinifex layers. The degree of talc-carbonate alteration varies and it can be followed by magnetic susceptibility surveys of the outcrops. Intensely altered samples are non-magnetic.

15–30 cm wide komatiitic dikes transects the  $D_{1-2}$  deformed banded amphibolite in the Vuosanka area (Fig. 6D). The dikes clearly indicate that the ultramafic volcanism extruded through pre-existing deformed supracrustal formations.

“*Small serpentinite body*” of the Pahakangas area. A lens-shaped ultramafic metacumulate (horizontal dimensions 650 m x 120 m) occurs 600 m northeast from the well-studied Pahakangas profile (Fig. 3). The lens is clearly discernible as a magnetic anomaly, divided into two equal parts by a 10 m

wide zone of low magnetic intensity that runs parallel to the layering. This zone is a layer of chlorite-tremolite rock and differs in composition from the main mass of serpentinite and talc-carbonate rock. The zone includes felsic fragments of granodioritic composition and up to 1.5 metres in diameter (Fig. 7). The core of a single zircon crystal from the enclave yields an age of  $2798 \pm 7$  Ma and the rim  $2771 \pm 8$  Ma (Peltonen 2007, pers. com., Peltonen et al., in prep.). The age of the core correlates with the age of the Juurikkaniemi felsic volcanic rock (Table 3) and also with the age of the Viitavaara tonalite ( $2785 \pm 7$  Ma, Käpyaho et al. 2006). We consider that the felsic enclaves were carried away from the felsic substrate of the komatiitic flow and were heated and recrystallized with the flowing lava. The age of the rim relates to the heating effect of the komatiitic eruption.

The serpentinite/talc-magnesite rock was originally an olivine mesocumulate. Primary minerals have been totally altered to antigorite, talc and magnesite, but the mesocumulate texture is still evident.

The overlying 130 m thick sequence of komatiitic flows is thinner than the 500 m thick flow sequence in the Pahakangas area. The serpentinite body could therefore be at a higher stratigraphic level than the fractionated flows and the associated B-zone serpentinites in Pahakangas. However, the exact stratigraphic position of the serpentinite body is not well established since the sequence is intensely faulted and the basal contact of serpentinite/komatiite is here intruded by a porphyritic granodiorite.

*Komatiitic basalts of the Mäkinen Member.* The bedrock at the Siivikkovaara hill, 800–1300 m northeast of the Pahakangas area (Fig. 3), is intensely faulted and composed of tens of small tectonic blocks, resulting in a complex chessboard-like map pattern. Besides massive non-fractionated komatiitic lava flows, fractionated flows with olivine  $\pm$  pyroxene spinifex A-layers, flow-top breccias, pillow-structures and coarse-fragmented breccias have also been observed. Interlayers of komatiitic basalts with stringy beef pyroxene spinifex A-layers are common at the upper stratigraphic part of the komatiitic lava sequence indicating contemporane-

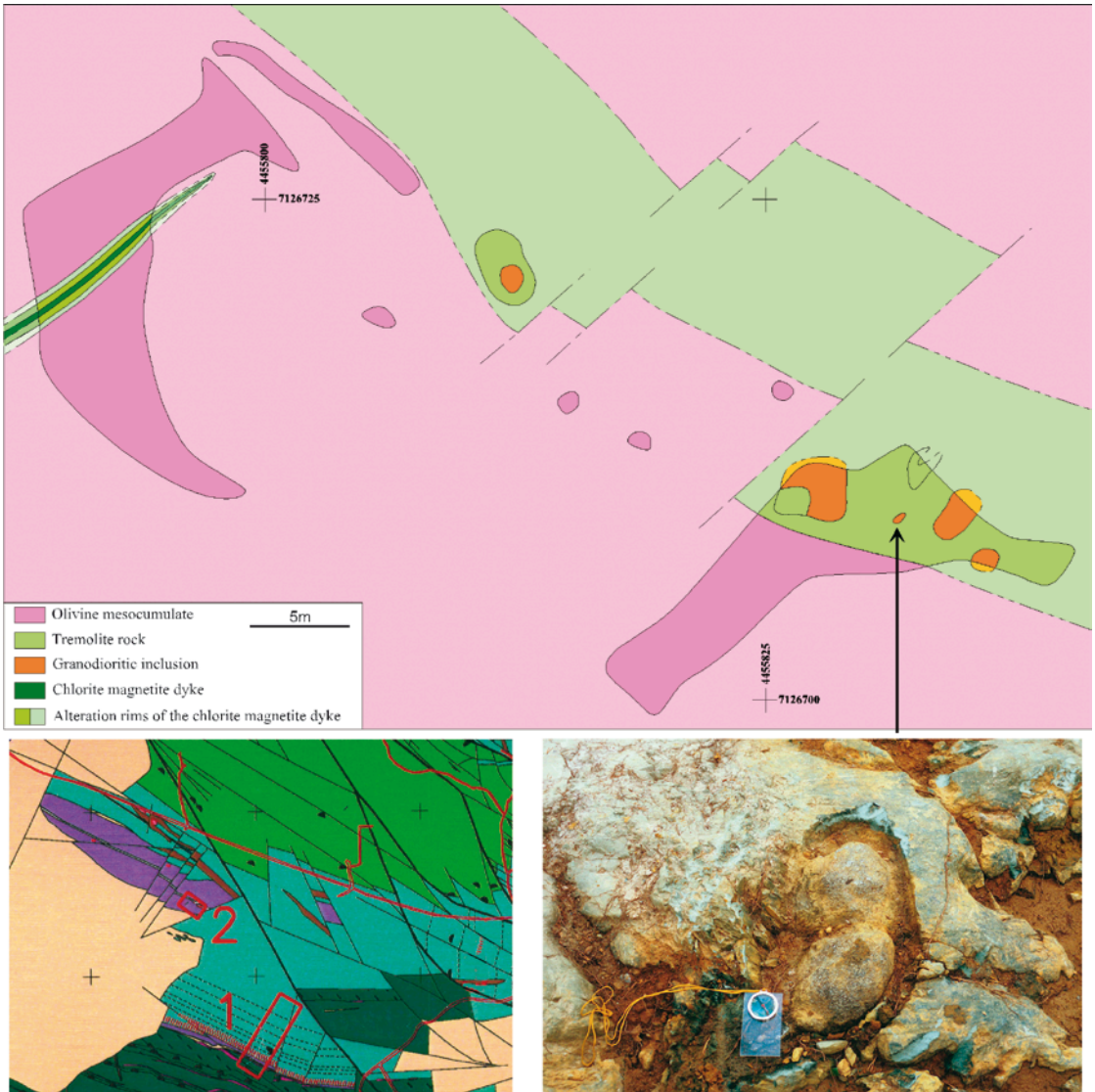


Figure 7. Detailed sketch of the small serpentinite body with felsic fragments. Darker colour indicates outcrop. The location map is a part of Fig. 3; the sketch area is marked with 2; the analysed section of Pahakangas komatiites with 1. The length of the compass in photo (4455832/7126709) is 12.5 centimetres. Photo T. Halkoaho.

ous eruptions of komatiitic basalt and komatiite lava flows. Upwards the volcanic stratigraphic succession passes into non-fractionated flows of komatiitic basalt that display well-preserved pillow structures with variolitic textures (Fig. 8A).

*Cr basalts of the Suo Member.* In the Mäkisensuo area the Suo Member of the Siivikko Formation

overlies the stratigraphically lowermost calc-alkalic felsic to mafic Mäkisensuo Formation. The Suo Member starts with a 250 m thick layer of basalt that is anomalously Cr-rich (1300–2800 ppm Cr), which was designated as high-Cr basalt by Halkoaho et al. (2000). This high-Cr basalt unit also includes three 10–30 m thick komatiitic interlayers indicating



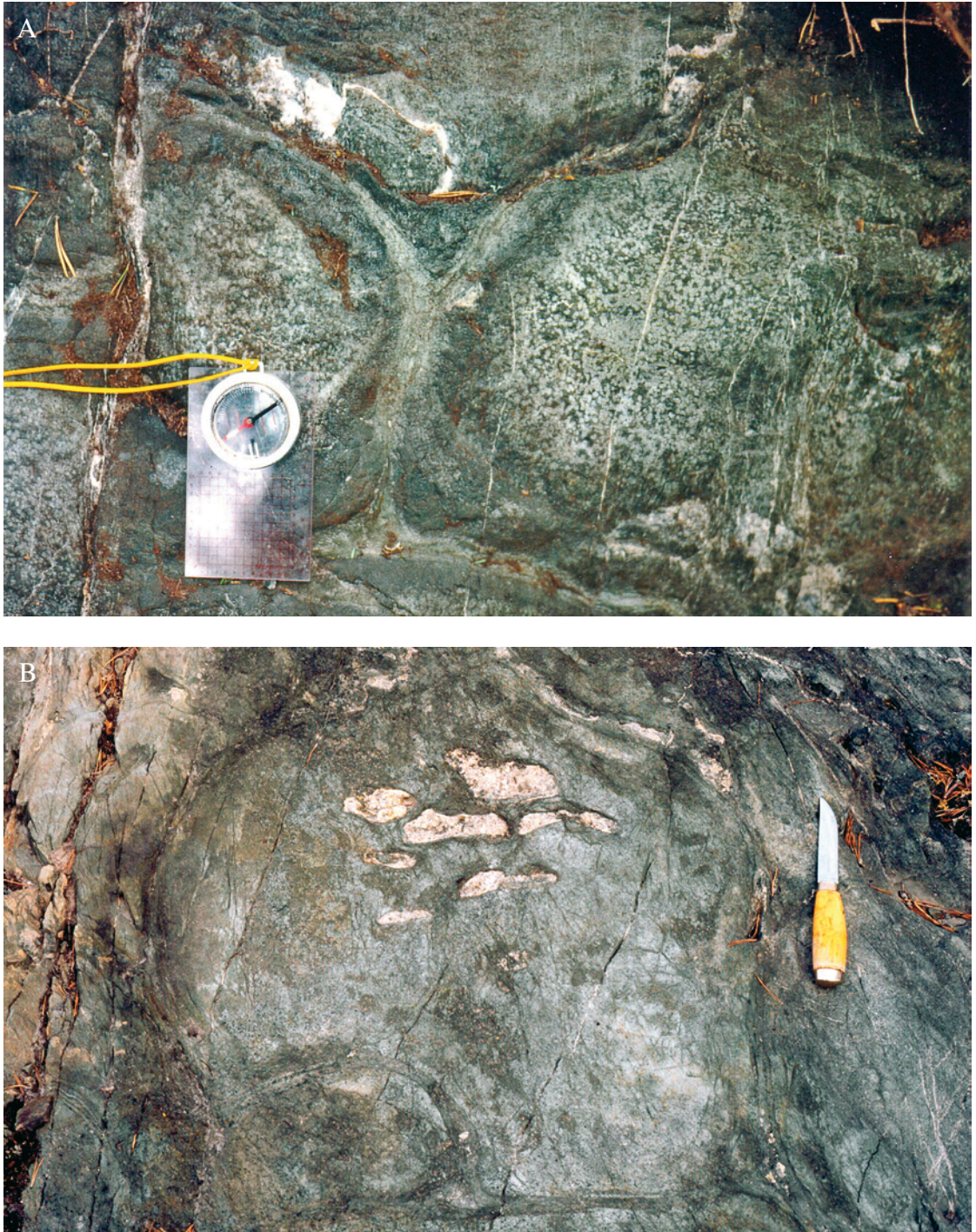


Figure 8. A. Variolitic pillow lava of komatiitic basalt, near the farmhouse of Viitaja (4455985/7126835). The length of the compass is 12.5 centimetres. B. Pillow lava structure in the high-Cr basalt, Mäkisensuu area (4455365/7128000). Some pillows contain drainage cavities (white inclusions) filled with quartz, and epidote±carbonate. The length of the knife is about 20 centimetres. Photos T. Halkoaho.

that the komatiitic volcanism was contemporaneous with the high-Cr basalt. The high-Cr basalt displays well preserved pillow structures with central cavities filled with quartz (Fig. 8B). Xenolithic inclusions of komatiitic basalt have also been observed within the high-Cr basalt.

Mafic lava known as “Cr basalt” occurs stratigraphically above the high-Cr basalt unit. The Cr basalt is distinguished from high-Cr basalts by lower Cr tenors (500–1300 ppm) and is separated from the underlying sequence by a 6 m thick layer of tremolite-biotite/chlorite rock (12.5 wt. % MgO, 3800 ppm Cr), which contains a weak sulfide dissemination. The sequence of pillow and massive Cr basalt lava flows attains a total thickness of 250 m.

### **Kellojärvi cumulate complex**

The Kellojärvi ultramafic cumulate complex covers an area of 24 km<sup>2</sup>. On the basis of interpretation of magnetic surveys, it is 3–5 km thick, layered, folded and faulted and the magnetic image conveys the impression of tectonic imbrication of several bodies with different orientations in a low-strain area. The maximum dimension in an E-W direction is up to 4 km and the western branch extends about 6 km northwards and southwest along the greenstone belt (Fig. 2).

The complex is composed of serpentinites and talc-magnesite rocks, although primary igneous textures are still preserved indicating that the rocks were originally ultramafic cumulates (Fig. 9). The rocks were olivine ad- and mesocumulates with minor olivine orthocumulate, olivine-clinopyroxene adcumulates and clinopyroxene adcumulates (clinopyroxenites). The classification of olivine cumulates as ad-, meso- and orthocumulates is based both textures and geochemical estimation of the olivine to intercumulus melt ratio.

Only a few grains of primary olivine have been detected; most of the preserved olivine is metamorphic. Based on the whole-rock geochemistry, the primary cumulus olivines ranged in composition from Fo<sub>89</sub> to Fo<sub>83</sub> (Tulenheimo 1999), indicating some variation in primary melt composition.

Anorthositic inclusions up to a few metres wide have been encountered in the area northwest of the farmhouse Ensilä (see Figs 11A and 25). The inclusions display sharp contacts, shearing and intense alteration.

A heterogeneous sequence composed of gabbro, pyroxenite and anorthosite with peridotite interlayers occurs at Niittyjoki in the central part of the ultramafic complex. During years 2002–2004 Geological Survey of Finland drilled some holes into a geophysical magnetic low in the central part of the ultramafic complex at Niittyjoki and intersected a non-outcropping heterogeneous layered gabbro-pyroxene-peridotite sequence (Halkoaho & Niskanen 2004). Due to tectonic disturbances, it was not possible to connect the different layers from one hole to another. These rocks are enriched in LREE compared to common ultramafic members of the Kellojärvi complex and they display microtextures, such as chromitite seams and intercumulus phlogopite/chlorite, which indicate that the sequence represents felsic contamination of the komatiitic melt.

Two single zircon crystals of the Niittyjoki intermediate “hybrid” rock were dated (SIMS) at 2798±8 and 2752±5 Ma (Peltonen 2007, pers. com.). A zircon fraction from the pyroxenite-gabbro-anorthosite body at Niittylahti was dated by the U-Pb (TIMS) method at 2757±6 Ma and a single zircon crystal with SIMS at 2798±4 Ma (Luukkonen et al. 2002, Peltonen 2007, pers. com.). The Niittylahti body contains enclaves of ultramafic olivine cumulates, which indicate that the gabbro sequence transects the Kellojärvi cumulate complex. We consider that the gabbros are younger than the komatiite cumulate, and represent about 2757–2752 Ma old mafic intrusive phase, which was contaminated during ascent by older felsic crustal and greenstone belt materials.

### *Structures and textures of cumulates*

Layering is a characteristic feature of the cumulate complex. Visible rhythmic layering is common in olivine cumulates at the margins of the complex. It is due to the variation of the proportions of olivine

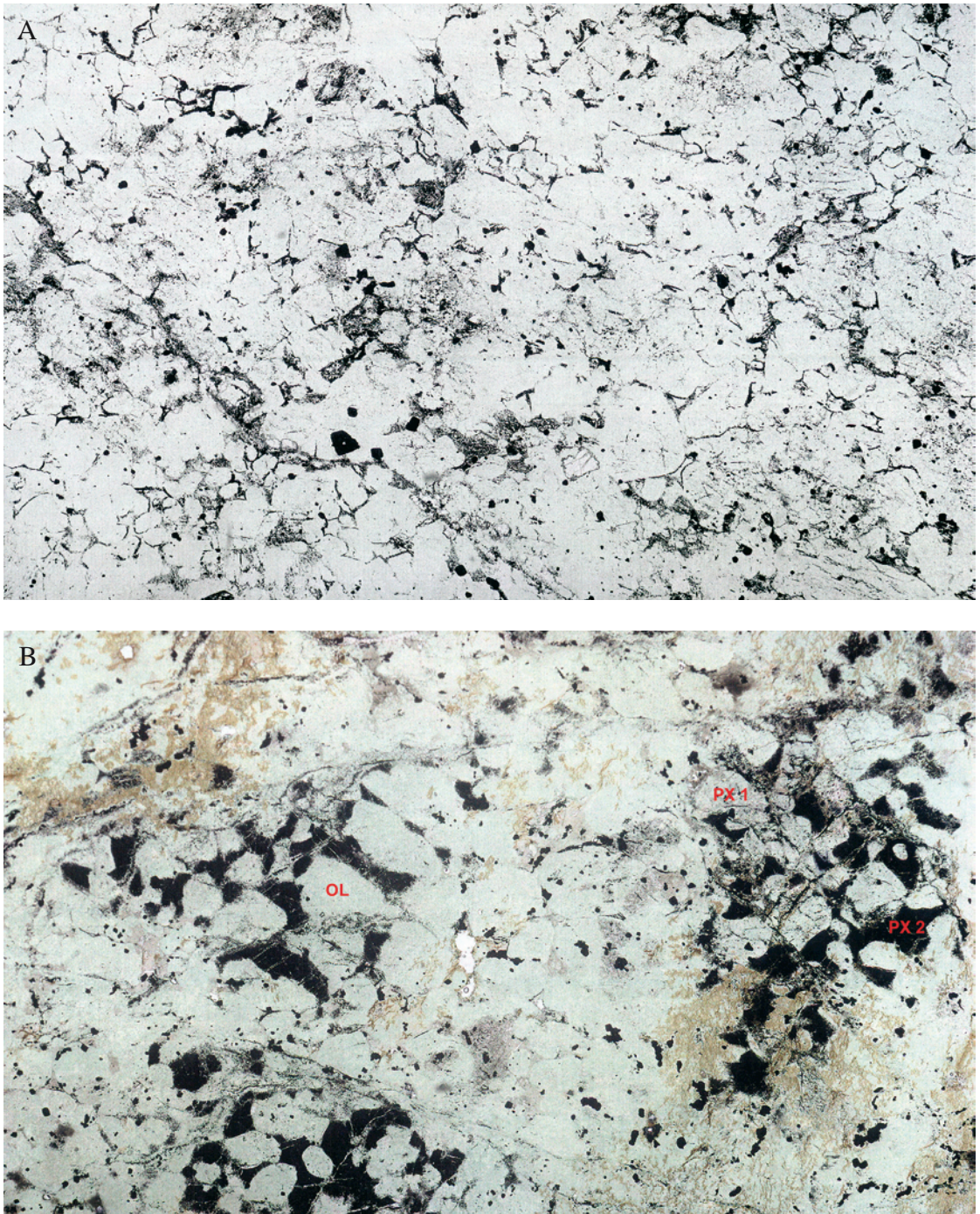


Figure 9. Thin section images (transparent light without polarizers) of the Kellojärvi serpentinite: A. olivine adcumulate (266-TOH-93, 4457265/7129720); B. olivine orthocumulate with pseudomorphs of olivine (OL), low-Fe pyroxene (PX 1) and black augite (PX 2) oikocrysts (258-TOH-93, 4454420/7129910) and the Proterozoic wehrlitic dike (see Fig. 25); C. poikilitic olivine orthocumulate with intercumulus augite oikocrysts; OL = pseudomorph of olivine, PX = pseudomorph of augite (272-TOH-93, 4455400/7130750). Field of view in all photos is 40 mm. Photos H. Papunen.

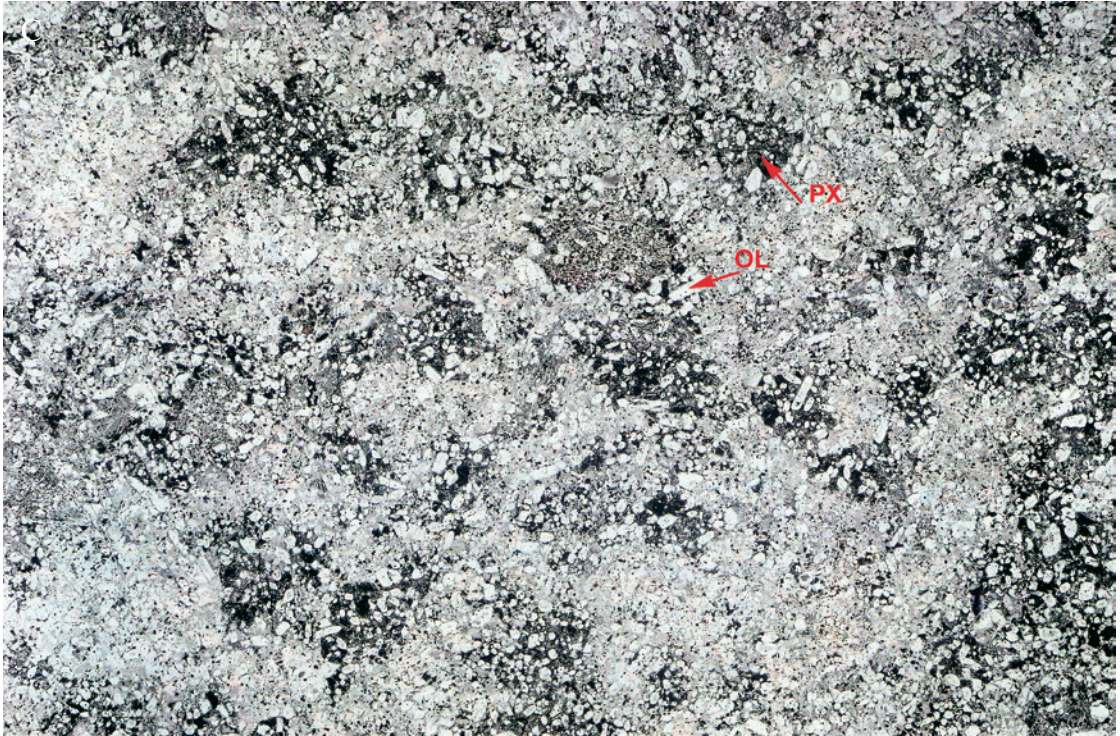


Figure 9. Continued.

and clinopyroxene cumulus crystals. In Näätäniemi, the layering consists of 2–5 cm thick pyroxenitic layers in olivine-clinopyroxene adcumulate. 10–20 cm fragments of clinopyroxenite disturb the planar layering, and the layers locally display slumping, erosional and cross bedding structures. The layering is also tectonically faulted and brecciated (Fig.10).

Fine-grained magnetite and ilmenite in chlorite-tremolite pseudomorphs of clinopyroxene reveals

that the pyroxene precursor was iron-rich (Fig. 9B). Locally, colorless non-pigmented tremolite-actinolite grains form pseudomorphs after a Ca-bearing pyroxene, which originally contained less iron and more magnesium than the pigmented pyroxene. Black-pigmented pseudomorphs of large clinopyroxene oikocrysts characterize massive olivine meso- and orthocumulates. The oikocrysts have preserved the habits of enclosed former olivine cumulus crystals (Figs 9B and C).



Figure 10. Pyroxenite fragment in layered ultramafic cumulate, Näätäniemi (4453110/7128020). Length of the knife is 6 cm. Photo H. Papunen.

### *Marginal zones of the cumulate complex*

Three well-outcropped localities at the marginal zone of the cumulate complex were mapped in detail (Tulenheimo 1999). The marginal zone against the felsic wall rock consists of green, massive amphibole rock, which represents former clinopyroxenite (Fig. 11B). It contains xenoliths of wall rock that are contorted due to partial melting. The width of the clinopyroxenite contact zone varies from 20 to 50 metres.

Upwards in the stratigraphy, the contact of metapyroxenite against massive to oikocrystic olivine ortho/mesocumulate is sharp, with embayments indicating thermal erosion.

A thin (<10 m) layer of orthopyroxenite, white on weathered surfaces, with dark clinopyroxene oikoc-

rysts, occurs locally between the clinopyroxenite and olivine cumulate. It commonly displays sharp contacts against both clinopyroxenite and olivine cumulate, but in places the orthopyroxenite changes gradually to clinopyroxenite. In the area west of Ensilä, the contact pyroxenite is coarse-grained and pegmatoidal, with large crystals of pyroxene.

A raft (1.5 x 5 m) of chlorite-amphibole-magnetite rock occurs within olivine cumulate a few tens of metres from the marginal zone pyroxenite. Another similar, ten metres wide inclusion was found about 100 metres away from the contact zone. The inclusions contain crystals of diopside up to 3 cm in size (see Fig. 12). The geochemistry of the rafts indicates that they could be derived from of the Pahakangas-type volcanic complex.

West of Ensilä, the cumulate complex is in contact

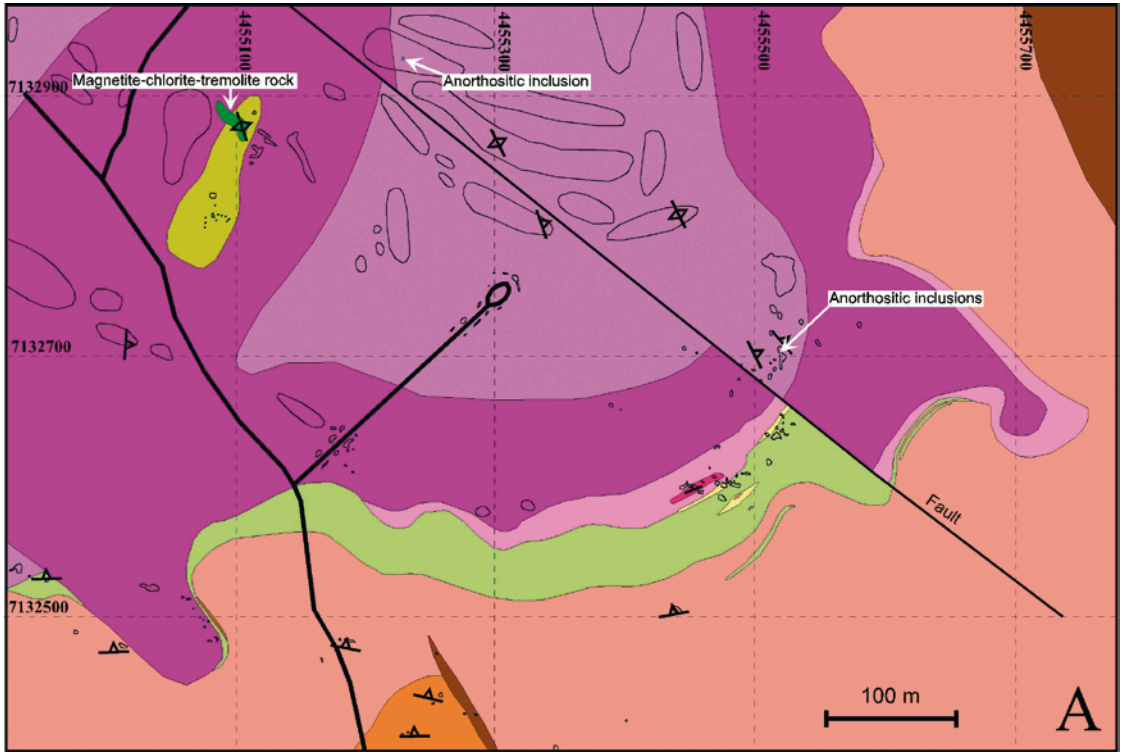
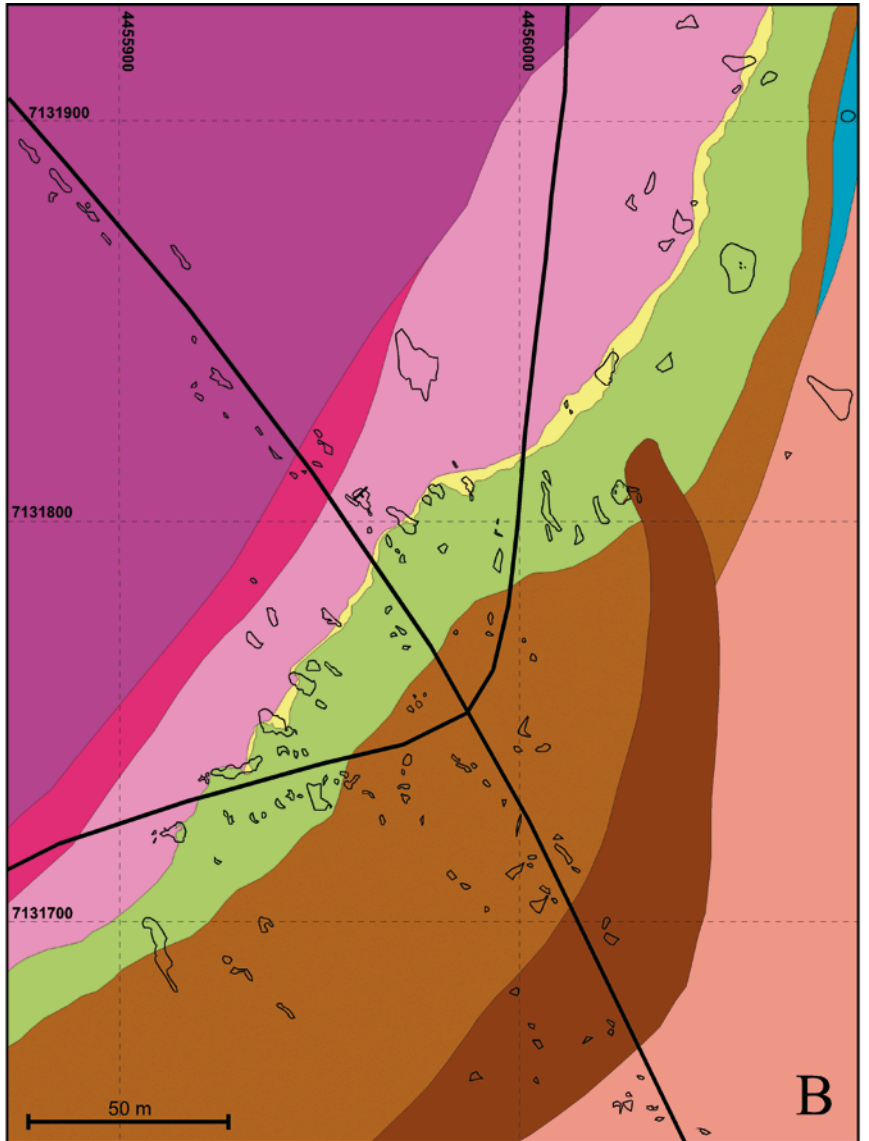


Figure 11. Detailed maps depict the contact zone of the cumulate complex west of Ensilä (A) and NW of Hyttimäki at the crossroads area (B) (Tulenheimo 1999). Legend see Fig. 11B.

with felsic oligoclase-quartz-phyrlic sheared and schistose rock that contains rare small fragments of biotite-rich gneiss (Fig. 11A). The age relations of the marginal clinopyroxenite and felsic rock were only observed in drill core, where the felsic rock intrudes the marginal pyroxenite as dikes. The felsic oligoclase-quartz porphyry is similar in

composition and appearance to the felsic porphyry dikes that occur between the Pahakangas Formation tholeiites and komatiites in the Siivikkovaara area. According to Luukkonen et al. (2002) the minimum U/Pb age of zircon separated from the felsic rock is 2780 Ma.



**Basement**

■ Tonalitic basement, plagioclase porphyry

**Marginal zone of the Kellojärvi ultramafic complex**

- Anorthosite (plagioclase adcumulate)
- Gabbro (plagioclase augite adcumulate)
- Clinopyroxenite (augite adcumulate)
- Websterite (poikilitic orthopyroxene orthocumulate with intercumulus augite)
- Wehrlite (poikilitic olivine orthocumulate with intercumulus augite)
- Wehrlite (olivine augite adcumulate)

**Layered sequence of the Kellojärvi ultramafic complex**

- Dunite (olivine ad-mesocumulate with intercumulus augite)
- Wehrlite (olivine mesocumulate with intercumulus augite)
- Clinopyroxenite (augite adcumulate)

**Other rocks**

- Volcaniclastics
- Proterozoic mafic dike

- ↗ Layering
- ↘ Foliation
- Outcrop
- Road

Figure 11. Continued.

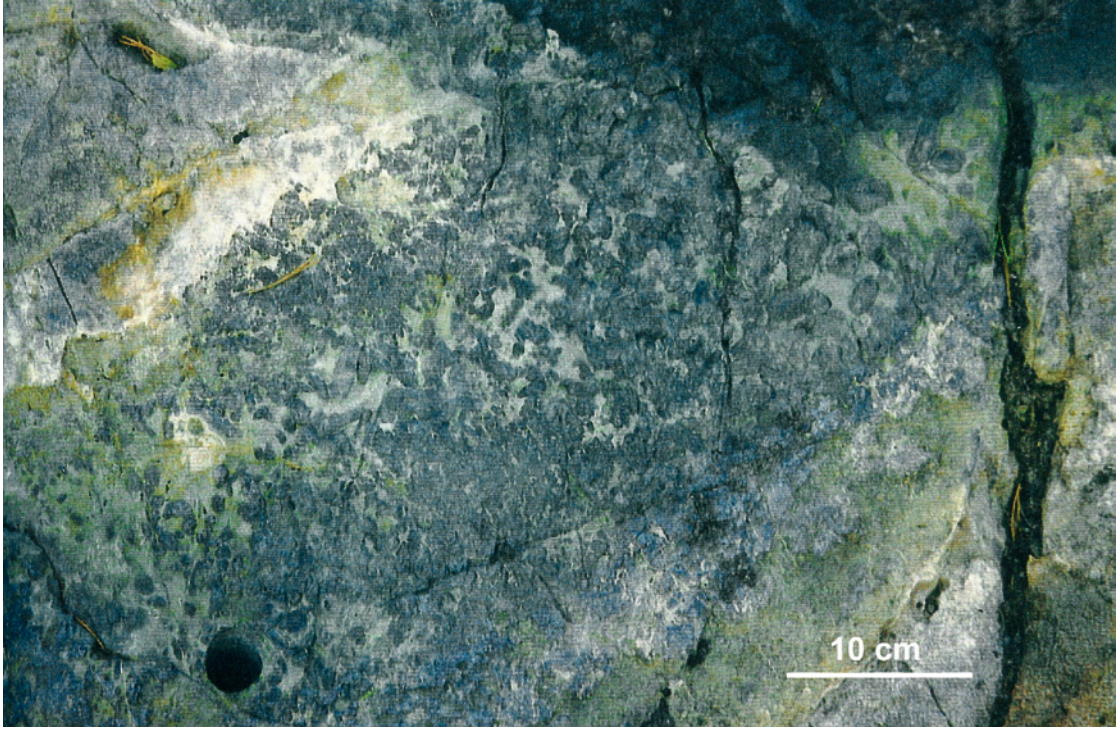


Figure 12. A raft of chlorite-amphibole rock containing large pseudomorphs of clinopyroxene crystals in the central part of the raft (4455795/7131925) at the crossroads area NW from the Hyttimäki farm (see Fig. 25). Photo H. Papunen.

### **Coarse-grained volcanoclastic deposits of the Ronkaperä Formation**

Volcanoclastic rocks ranging from fine-grained tuffs to conglomerates occur in several localities around the Ronkaperä bay (see Fig. 25), and as small isolated occurrences within the central and northern part of the Kellojärvi ultramafic complex. Most of the outcrops are volcanic conglomerates with clasts and matrix consisting entirely of volcanic material (Fig. 13). Stratigraphic contact relationships with the other stratigraphic units are not seen in outcrop, but because there are a few clasts of high-Cr basalt and komatiitic basalt in the conglomerate, the unit is interpreted to occur stratigraphically at the top of mafic-ultramafic volcanic succession. Most of the fragments are either dacitic or andesitic calc-

alkalic volcanic rocks, which are either massive or locally amygdaloidal and porphyritic in texture. TTG gneiss fragments have not been found. Mafic tuffaceous layers display well preserved graded and cross bedding. However, the conglomerates are mainly massive, without bedding, and are clast to matrix supported. Nieminen (1998) interpreted the sequence mostly as lahar type volcanoclastics.

At Hietaperä, to the south of the Siivikkovaara area, quartzites occur at the top of the entire volcanic-sedimentary succession. In some other areas, the upper sedimentary sequence is composed of sulfidic sediments, mica schists, greywackes (2744±34 Ma greywacke from Petäjaniemi, Kuhmo, Peltonen 2007, pers. com.), conglomerates and phyllites, which are derived from greenstone materials and TTG.





Figure 13. Poorly sorted volcanic conglomerate of the Ronkaperä Formation (4455390/7131990) NW from the Hyttimäki farm (see Fig. 25). The length of the scale is 15 centimetres. Photo E. Luukkonen.

### Suomussalmi greenstone belt

The northern part of the TKS greenstone complex, the Suomussalmi greenstone belt (SGB), extends 60 km in a north-south direction from Kiannanniemi to Saarikylä, where it bifurcates into N-trending and E-trending branches (Fig. 1). The metamorphic grade of the eastern branch is upper amphibolite facies, which is higher than the middle to low-amphibolite facies assemblages of the greenstone belt proper. Structure of the greenstone belt is complicated due to polyphase folding and faulting, which make the stratigraphic study of the greenstone evolution more difficult than in Kuhmo and Tipasjärvi belts. The following interpretations (Table 5) are based on well-outcropped sections and related age determinations.

#### *Luoma and Mesa-aho Formations*

A sequence of bimodal, mainly pyroclastic calc-alkalic volcanic rocks of felsic to mafic composition occur at the western margin of the Suomussalmi greenstone belt at Saarikylä and Kiannanniemi (Fig. 1). Piirainen (1988) named this sequence in Saarikylä the Luoma Group (= Luoma Formation in this text), and considered it to be the oldest supracrustal unit of the TKS greenstone sequence. Vaasjoki et al. (1999) reported a U-Pb TIMS age of  $2966 \pm 9$  Ma from zircons from a felsic-intermediate tuffite, and proposed that the ages of the Luoma Formation differ considerably from the ages of the greenstone belt proper. New age determinations made on single

Table 5. Stratigraphy of the Suomussalmi greenstone belt.

Formation	Lithology	Thickness (Age)
Huutoniemi	Mica schists /pelites, felsic-intermediate tuffs, pyroclastic breccias, volcanic conglomerates, black schists	200 m (2774±8 Ma; Luukkonen et al. 2002)
Saarikylä	Komatiitic olivine ad-, meso- and orthocumulates, olivine-pyroxene cumulates of komatiitic basalts, Cr basalts, local felsic volcanoclastic units	500 m
Tervonen	Tholeiitic basalts with BIF interlayers, tuffs, mafic sill	400 m
Mesa-aho	Felsic-intermediate tuff/tuffite, hyababysal dikes	100-200 m; (2818±15 Ma; Luukkonen et al. 2002)
Luoma	Felsic-intermediate-mafic tuff/tuffite, lava, with quartz porphyry dikes, banded amphibolites	500 m; (2943±20 Ma; Luukkonen et al. 2002)

zircon grains with SIMS method yield ages of 2959 ±12 Ma and 2825±27 Ma for the zircons of this Luoma felsic-intermediate tuffite. Additionally, zircons from the Luoma felsic volcanic rock gave the age of 2943±20 Ma, and the monazite of the Luoma quartz porphyry dike, the age 2942±3 Ma (Luukkonen et al. 2002). These ages clearly indicate that volcanic rocks of the Luoma Formation are older than the ordinary TKS greenstone complex and they probably belong to the same supracrustal formation and age group as the pre-greenstone banded tholeiitic amphibolites mentioned above (see also Table 9). Engel and Dietz (1989) documented an unconformity between the Luoma Formation and the other rocks of the greenstone belt proper. Furthermore, quartz porphyry dikes that cut the Luoma volcanic rocks at Mesa-aho, also dated by single zircon SIMS method, gave an age 2818 ±15 Ma. This age correlates well with initial phase observed elsewhere for the evolution of the TKS greenstone complex (Luukkonen et al. 2002). We here agree with the interpretation by Vaasjoki (1999) and consider that the Luoma Formation represents the older greenstone belt correlative with pre-greenstone banded amphibolites, and name the initial felsic formation of the Suomussalmi greenstone complex the Mesa-aho Formation (Table 5). The extent of the Mesa-aho Formation needs further consideration in the field surveys and datings since the lithologic differences between the Luoma and Mesa-aho rocks are not evident.

#### *Tervonen Formation*

Major part of the Kiannaniemi-Saarikylä sequence comprises tholeiitic basalts with locally well-preserved pillow textures. In Kiannaniemi the sequence overlying basalts was studied with diamond drillings due to nickel deposits of Hietaharju and Peura-aho. Here the basalts are overlain by felsic volcanic rocks and graphitic black schists and these, in turn, by cumulates of komatiites and komatiitic basalts. We name the basalt unit the Tervonen Formation and combine the sequence starting with felsic and ultramafic rocks to the Saarikylä Formation.

#### *Saarikylä Formation*

A layer of felsic porphyry with associated graphitic schist occurs between the tholeiitic and komatiitic basalt units in the Kiannaniemi area. Disseminated and massive Ni-Cu sulfide deposits are located in the cumulates of the komatiitic basalts (Kurki & Papunen 1985, Luukkonen et al. 2002). Similarly, a felsic volcanoclastic unit is sporadically present at the Saarikylä area between komatiites and komatiitic basalts (Luukkonen et al. 2002).

Locally the rocks of Mesa-aho and Tervonen Formations may be absent, in which case komatiitic lavas and cumulates are the basal greenstone unit. At Saarikylä, for example, where the Luoma volcanic rocks are exposed on the western margin of

the greenstone belt, the SGB sequence begins with komatiitic lavas and cumulates, which directly overlie the Luoma Formation rocks. The 1–10 m thick units of komatiitic lavas are chlorite-amphibole schists with no preserved primary structures. The serpentinized cumulates are the metamorphic equivalents of olivine mesocumulates and adcumulates with minor amounts of orthocumulates. They form lenticular bodies up to 15 km long and 500 m wide and display weak compositional layering. Two of them, the Vaara and Kauniinlampi units, contain disseminated Ni sulfide mineralization (Luukkonen et al. 2002). Although the mineralogy is metamorphic, primary cumulus textures, including pseudomorphs of hopper olivines are locally preserved. The next stratigraphic unit above the komatiites comprises komatiitic pillow basalts and Cr basalts (Halkoaho et al. 2000).

The eastern, Tormua branch of greenstone is composed of banded amphibolites, uraltite porphyries/gabbros and small isolated areas of felsic to

intermediate volcanic rocks. Dating of single zircon crystals from the Tormua uraltite gabbro gave an age of  $2866 \pm 4$  Ma (Peltonen 2007, pers. com.), which combines it to pre-greenstone plutonic succession, or the zircons were inherited from there.

#### *Huutoniemi Formation*

The uppermost stratigraphic unit of the Suomussalmi sequence consists of felsic to intermediate volcanic rocks, volcanoclastic sedimentary rocks, phyllites and graphite-sulfide-bearing black schists. This sequence was studied at Huutoniemi, east of Kiannanniemi, where the felsic rock sequence was intersected with diamond drillings. We also include the felsic to intermediate, recrystallized volcanic rocks at Kilpasuo, northeastern part of the Tormua branch, to this formation. SIMS dating of zircons yielded an age of  $2774 \pm 8$  Ma for the Kilpasuo felsic rocks (Luukkonen et al. 2002).

## Geochemical evolution

### Analytical data

A number of geochemical analyses have been published in earlier studies of the region (Taipale 1983, Martin et al. 1983, Luukkonen, 1988, 2001, Papunen et al. 1989, Engel & Dietz 1989), but a large volume of new analyses were made during the study of komatiite volcanology during the 1990's, since the classification of komatiites was not possible without geochemical information. Major elements were assayed from fused samples and trace elements from pressed powder samples by the XRF method at the CSIRO laboratories, Western Australia. Certain trace elements were assayed with ICP-MS and ICP-OES by Genalysis Laboratory Services Pty. Ltd., Western Australia. Additional XRF analyses were done from pressed powder samples at the Outokumpu Oyj Geoanalytical laboratory, Outokumpu. Analytical data are stored in a Microsoft Excel file together with corresponding field and petrographic data, and is included in the appendix of this paper as a CD-ROM. For the comparison of

different rock types a number of elemental x-y and ternary diagrams were prepared, but due to large number of geochemical data the primary analyses were stored in the appendix and only the calculated averages, mean values and ranges of concentrations of elements in different rock types were presented in tables. The spider diagrams depicting the distribution of elements in the rocks and presented in the next pages were constructed with a Minpet 2.02 program (Minpet Geological Software Inc.) using the normalizing values for average chondrites and primitive mantle from Sun and McDonough (1989) and for continental crust from Taylor and McClenan (1985).

### TTG complex

The geochemistry of the TTG complex is here briefly described for the purpose of comparison with the rocks of the greenstone belt. In this study a number of felsic intrusive rocks were analysed along the margins of the TKS greenstone belt and

more data was obtained from the works of Martin et al. (1983), Luukkonen (1988, 2001), Käpyaho (2006) and Käpyaho et al. (2006, 2007). The pre-greenstone grey gneisses are inhomogeneous due to migmatization, but mesosomes (Martin et al. 1983, Martin 1987, Luukkonen 2001, Käpyaho 2006, Käpyaho et al. 2006, 2007) display rather constant compositions, characterized by high Na/K values, negative  $Nb_N$  anomalies, low  $[Nb/La]_N$  ratios and high  $[Zr/Ti]_N$  values, while major element abundances are close to average tonalite in composition (Table 6 and Fig. 14). The  $V/(Ti/1000)$  ratio ranges from 20 to 50 and granodiorites yield the highest values round 50.

### Felsic volcanic rocks

Taipale (1983) studied the felsic volcanic rocks of the Tipasjärvi area, and Papunen et al. (1989) presented representative analyses of volcanic rocks around the Taivaljärvi Ag-Zn-Pb occurrence (Table 6). The stratigraphically lowermost felsic volcanic rocks and massive felsic porphyries are rhyodacites and dacites, which higher up in the stratigraphy become more intermediate in composition. Figure 15 depicts the spider diagrams of felsic volcanic rocks.

The trace element distribution of the felsic volcanic rocks is very similar to that of tonalitic paleosomes, where the characteristic features are negative  $Nb_N$  anomalies and  $[Nb/La]_N$  ratios are below mantle values, whereas the  $[Zr/Ti]_N$  ratios are  $>1$ , ranging up to 10 in rhyolites (Table 6). The  $V/(Ti/1000)$  ratio is close to 50, clearly higher than in mafic and ultramafic volcanic rocks described below. The concentrations of compatible elements (Cr, Ni) are lower in felsic rocks than in average tonalite. Also the REE distribution patterns of intermediate volcanic rocks are similar to those of tonalitic grey gneisses, with a slightly U-shaped HREE distribution pattern (cf. Martin et al. 1983). The fractionation of REE indicated by  $[La/Yb]_N$  ratio (20) is in intermediate volcanic rocks very close to that of granodiorite, whereas the grey gneisses display somewhat higher fractionation ( $[La/Yb]_N = 100$ ). Characteristic of felsic volcanic rocks is a negative

$Eu_N$  anomaly, whereas the intermediate volcanic rocks display a slight positive  $Eu_N$  anomaly.

The Saarijärvi and Luoma felsic volcanic rocks of the Suomussalmi greenstone complex (Engel & Dietz 1989; Table 6) display the characteristic features mentioned above for Taivaljärvi, although the depletion of compatible elements is not as prominent as in the Taivaljärvi felsic rocks, and the values of the Suomussalmi felsic rocks correspond to those of average continental crust. The  $[Cr/Ni]_N$  ratios of Suomussalmi volcanic rocks are  $>1$ , compared to values  $<1$  for the Taivaljärvi rocks. The negative  $Nb_N$  anomaly is very prominent in the Saarijärvi felsic volcanic rocks and the  $Nb_N$  is about  $0.1 * La_N$ , which has been used as reference material (Puchtel et al. 1997, 1999). The REE pattern of the Saarijärvi felsic rocks is almost identical with the Taivaljärvi felsic rocks although the Eu anomaly is absent at Saarijärvi (Figs 15 and 16).

### Pahakangas type tholeiitic basalt

The geochemistry of the Pahakangas type mafic volcanic rocks (Table 4) indicates basaltic to basaltic-andesite compositions, and in the Jensen diagram (Fig. 20) the analyses plot in the high magnesium tholeiite (=HMT) and calc-alkalic (=CA) fields. In the trace element diagram the mantle normalized  $[Nb/La]_N$  is slightly below 1, but the value is  $>1$  if normalized with average continental crust.  $[Zr/Ti]_N$  values are  $<1$  (0.4) and the  $V/(Ti/1000)$  ratios range from 15 to 20, on average 17 (Fig. 17). The high variance of LIL elements may partly derive from hydrothermal alteration, which cannot be avoided in the samples of pillow lavas. The chondrite normalized REE distribution pattern (Fig. 18B) does not indicate fractionation, but the concentrations are 5–6 times higher than the mantle values. A similar enrichment factor is observed for the average LIL and HFS elements, but the compatible elements, Cr and Ni, are clearly depleted. A slight positive Eu anomaly is evident in some samples and correlates with the presence of plagioclase phenocrysts. Compared to MORB the rocks display slight enrichment of LIL and depletion of HFS elements.

Table 6. Geochemistry of felsic volcanic rocks: selected assays of Pahakangas and Mäkisensuo felsic rocks (normalized to volatile-free) and average chemical compositions of Suomussalmi, Tipasjärvi and Ronkaperä felsic volcanic rocks (n.d. = not detected; - not determined). mg# see Table 4.

Rock type		Mäkisensuo andesite	Mäkisensuo andesite	Mäkisensuo andesite	Pahakangas granodiorite	Pahak. felsic porphyry	Pahak. felsic porphyry	Luoma felsic volcanic rock
Sample		SII-17 190.3	SII-16 85.2	SII-16 101.75	166-TOH-93	5-1-JSK-93	4-HP-92	average
SiO <sub>2</sub>	wt.%	58.21	60.25	62.21	66.80	68.94	72.39	73.34
TiO <sub>2</sub>	wt.%	0.69	0.58	0.69	0.53	0.48	0.44	0.56
Al <sub>2</sub> O <sub>3</sub>	wt.%	15.52	15.14	15.53	16.40	15.10	14.07	12.38
FeO	wt.%	7.86	6.32	5.80	4.20	4.23	3.87	3.27
MnO	wt.%	0.15	0.11	0.10	0.06	0.08	0.03	0.06
MgO	wt.%	5.11	6.25	4.82	2.71	1.73	1.84	1.56
CaO	wt.%	8.15	5.64	6.45	2.21	2.47	0.37	2.37
Na <sub>2</sub> O	wt.%	3.52	4.47	3.89	5.98	6.45	6.89	2.41
K <sub>2</sub> O	wt.%	0.70	1.12	0.41	0.98	0.41	0.03	2.21
P <sub>2</sub> O <sub>5</sub>	wt.%	0.08	0.12	0.11	0.14	0.12	0.08	0.07
Total		100.00	100.00	100.00	100.00	100.00	100.00	98.23
mg#		56.28	66.19	62.20	56.09	44.74	48.49	48.58
Cr	ppm	442	267	303	61	66	17	230
Ni	ppm	200	180	120	40	30	10	56
Co	ppm	40	20	110	10	–	93	20
V	ppm	238	123	190	84	50	39	74
Cu	ppm	60	60	40	10	–	17	26
Pb	ppm	150	20	10	10	10	14	26
Zn	ppm	250	60	40	40	30	36	52
Bi	ppm	10	10	10	–	–	–	3
S	ppm	20400	–	–	141	916	131	n.d.
Rb	ppm	26	29	18	34	20	–	52
Cs	ppm	30	10	10	20	10	–	–
Ba	ppm	206	251	134	288	144	41	772
Sr	ppm	123	139	87	116	193	66	146
Nb	ppm	16	19	20	8	10	2	17
Zr	ppm	44	89	67	112	216	144	122
Y	ppm	16	6	14	13	21	17	19
Nb/Y	ppm	1.00	3.17	1.43	0.62	0.48	0.12	0.89
Th	ppm	–	–	–	–	–	–	7
U	ppm	1	8	6	4	8	–	1
La	ppm	20	20	20	n.d.	n.d.	n.d.	32
Ce	ppm	20	40	30	n.d.	n.d.	n.d.	46
Cl	ppm	40	70	60	60	70	–	102
Nd	ppm	–	–	–	–	–	–	–
Sm	ppm	–	–	–	–	–	–	–
Eu	ppm	–	–	–	–	–	–	–
Tb	ppm	–	–	–	–	–	–	–
Yb	ppm	–	–	–	–	–	–	–
Lu	ppm	–	–	–	–	–	–	–

Table 6. Continued.

Rock type		Saarijärvi felsic volcanic rock	Taivaljärvi in-term. volcanic rock	Taivaljärvi Na felsic volcanic rock	Taivaljärvi K felsic volcanic rock	Ronkaperä andesite	Ronkaperä dacite
Sample		average	average	average	average	average	average
SiO <sub>2</sub>	wt.%	81.44	66.10	70.35	78.40	58.47	68.98
TiO <sub>2</sub>	wt.%	0.14	0.43	0.55	0.14	0.91	0.45
Al <sub>2</sub> O <sub>3</sub>	wt.%	9.16	15.80	15.47	11.00	15.43	15.58
FeO	wt.%	1.50	3.91	2.93	0.77	8.00	3.61
MnO	wt.%	0.04	0.11	0.07	0.05	0.19	0.06
MgO	wt.%	1.22	1.50	0.91	0.57	4.22	1.49
CaO	wt.%	0.53	3.34	1.88	1.09	6.96	2.74
Na <sub>2</sub> O	wt.%	1.33	3.30	3.38	0.06	3.76	5.05
K <sub>2</sub> O	wt.%	2.51	2.48	2.21	4.11	1.05	1.54
P <sub>2</sub> O <sub>5</sub>	wt.%	0.03	0.12	0.12	0.12	0.10	0.08
<b>Total</b>		97.90	97.09	97.87	96.31	99.08	99.58
<b>mg#</b>		61.69	43.17	38.10	59.29	51.08	45.02
Cr	ppm	66	8	10	n.d.	295	15
Ni	ppm	29	9	13	5	106	15
Co	ppm	10	10	8	2	28	6
V	ppm	27	66	43	5	162	34
Cu	ppm	11	36	17	5	32	10
Pb	ppm	11	28	14	33	24	11
Zn	ppm	38	100	80	197	108	20
Bi	ppm	–	1.9	0.4	0.2	–	–
S	ppm	n.d.	n.d.	n.d.	n.d.	457	10
Rb	ppm	56	100	78	167	36	43
Cs	ppm	2	8	4.1	1.2	–	–
Ba	ppm	428	480	373	490	259	257
Sr	ppm	75	230	137	7	237	162
Nb	ppm	3	7	12	20	3	6
Zr	ppm	82	70	173	123	108	186
Y	ppm	7	10	30	33	24	20
Nb/Y	ppm	0.43	0.70	0.39	0.61	0.11	0.31
Th	ppm	11	2.1	6.7	13.0	–	–
U	ppm	3	0.5	1.8	3.6	–	–
La	ppm	28	14.0	30.4	31.9	11	24
Ce	ppm	48	27.0	52.8	65.0	25	44
Cl	ppm	80	–	8.3	0.0	29	25
Nd	ppm	–	10.0	22.0	26.0	–	–
Sm	ppm	–	2.2	4.4	5.8	–	–
Eu	ppm	–	0.8	0.6	0.5	–	–
Tb	ppm	–	0.3	0.7	0.8	–	–
Yb	ppm	–	0.6	2.0	2.9	–	–
Lu	ppm	–	0.1	0.4	0.5	–	–

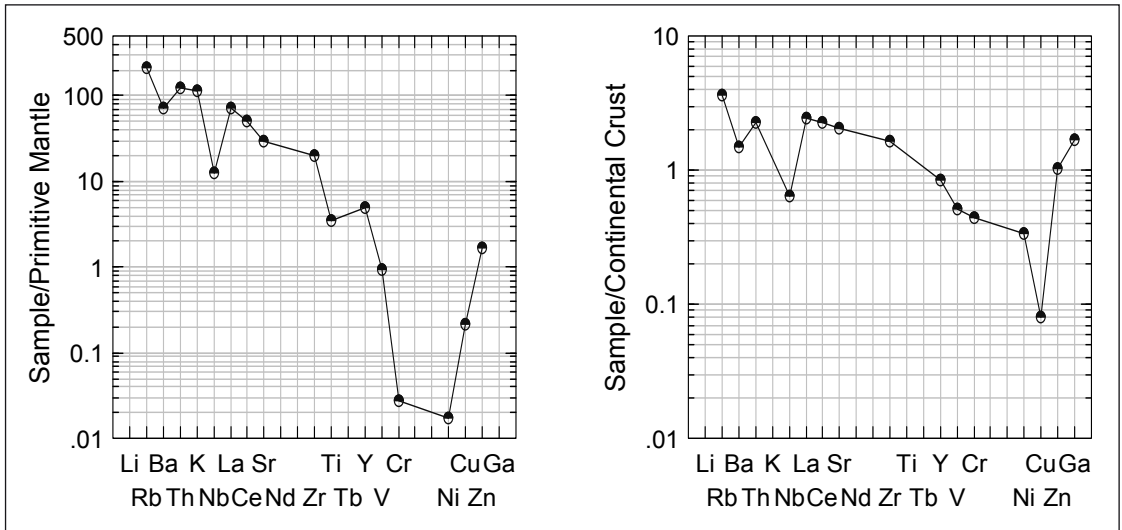


Figure 14. Average compositions of tonalitic mesosome (Luukkonen 2001) normalized with primitive mantle and continental crust.

### Komatiites and komatiitic basalts

Komatiitic lavas, both A-layers of fractionated flows and non-fractionated flows contain on average 23 wt. % MgO, although random values up to 26 % MgO are seen in the diagrams (see Figs 5 and 20, Tables 5 and 7). The cumulus B-layers of fractionated flows are not included in these diagrams, but are presented separately with all the other cumulates. However, the accumulation of minor olivine may shift the value of MgO content upwards, and the existence of small amounts of olivine cannot be quantified in the metamorphic mineral assemblage. The komatiites are of Al non-depleted type with  $Al_2O_3/TiO_2$  values commonly exceeding 20. The same value applies to the komatiitic basalts, as well as for basalts stratigraphically overlying the komatiitic basalts. Distribution of Cr and Ni correlates with MgO, but a few anomalously high Cr values also exist, some of which correspond to the anomalous Cr basalts (see Halkoaho et al. 2000). In addition the observed accumulation of chromite in some komatiitic flows may also increase the Cr content.

Mantle normalized trace element diagrams (Fig. 21) display  $[Nb/La]_N$  values  $<1$  for komatiitic basalts and  $>1$  for komatiites. Another distinctive feature between the komatiitic basalts and komatiites is the negative Sr anomaly in komatiites and positive value in komatiitic basalts. A conspicuous feature is the very low  $Zr_N$  value, and the anomaly is more negative for komatiitic basalts than for komatiites. Ti concentrations are higher in komatiitic basalts than in komatiites, resulting in a higher  $[Ti/Zr]_N$  value for komatiitic basalts than for komatiites. An interesting feature is the wide distribution of Cu tenors, which partly correlates with Ni values and may indicate that a random factor (reaction with substrate sulfides) depleted chalcophile elements in some lava flows. The REE distribution pattern indicates slight HREE enrichment in komatiitic lavas, whereas komatiitic basalts are non-fractionated.

A sequence of sheeted komatiite flows studied in the Pahakangas area display high variance of elemental concentrations in the lowermost fractionated flows, where the mesocumulate B-layers are the most magnesian rock types (Fig. 5, Table 4). Upwards the sequence turns to non-fractionated flows,

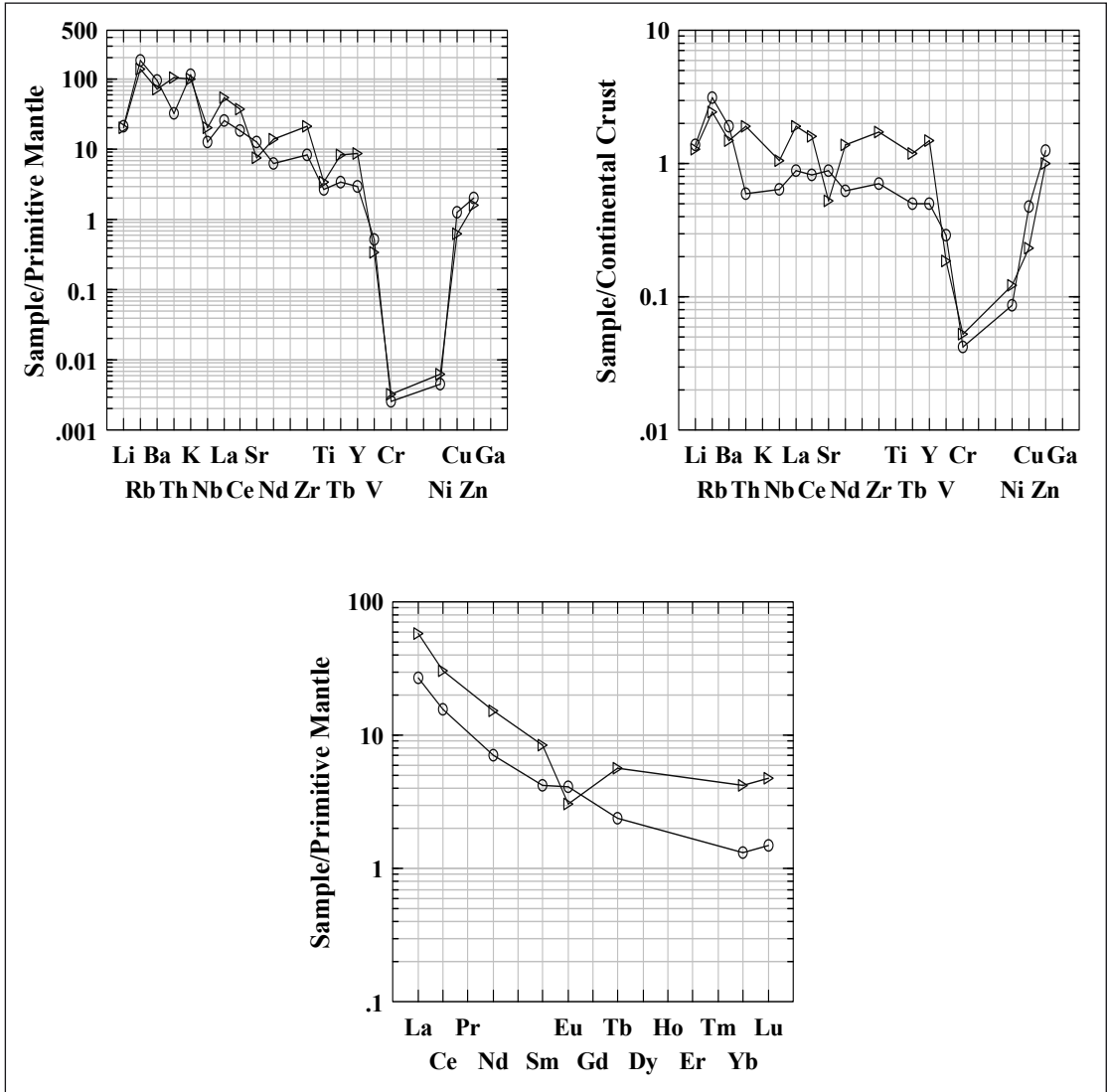


Figure 15. Spider diagrams of average felsic volcanic rocks ( $\Delta$ ) and the overlying intermediate volcanic rocks (O) of the Taivaljärvi area (data from Papunen et al. 1989).

where flow top breccias indicate flow boundaries. The compositions of the non-fractionated upper flows are very constant, except that the concentration of Cr increases slightly from 2500 ppm to 2700 ppm upwards in the sequence, and in flows 5–16 the average Sr content is slightly higher than in

flows 1–4. The highest content of zinc in the flow sequence, 230 ppm, is in the metapyroxenite located at the contact against the underlying BIF just below the first fractionated flow (Fig. 5).

Compared to upper non-fractionated flows, the A-layer of the first komatiitic flow is depleted in



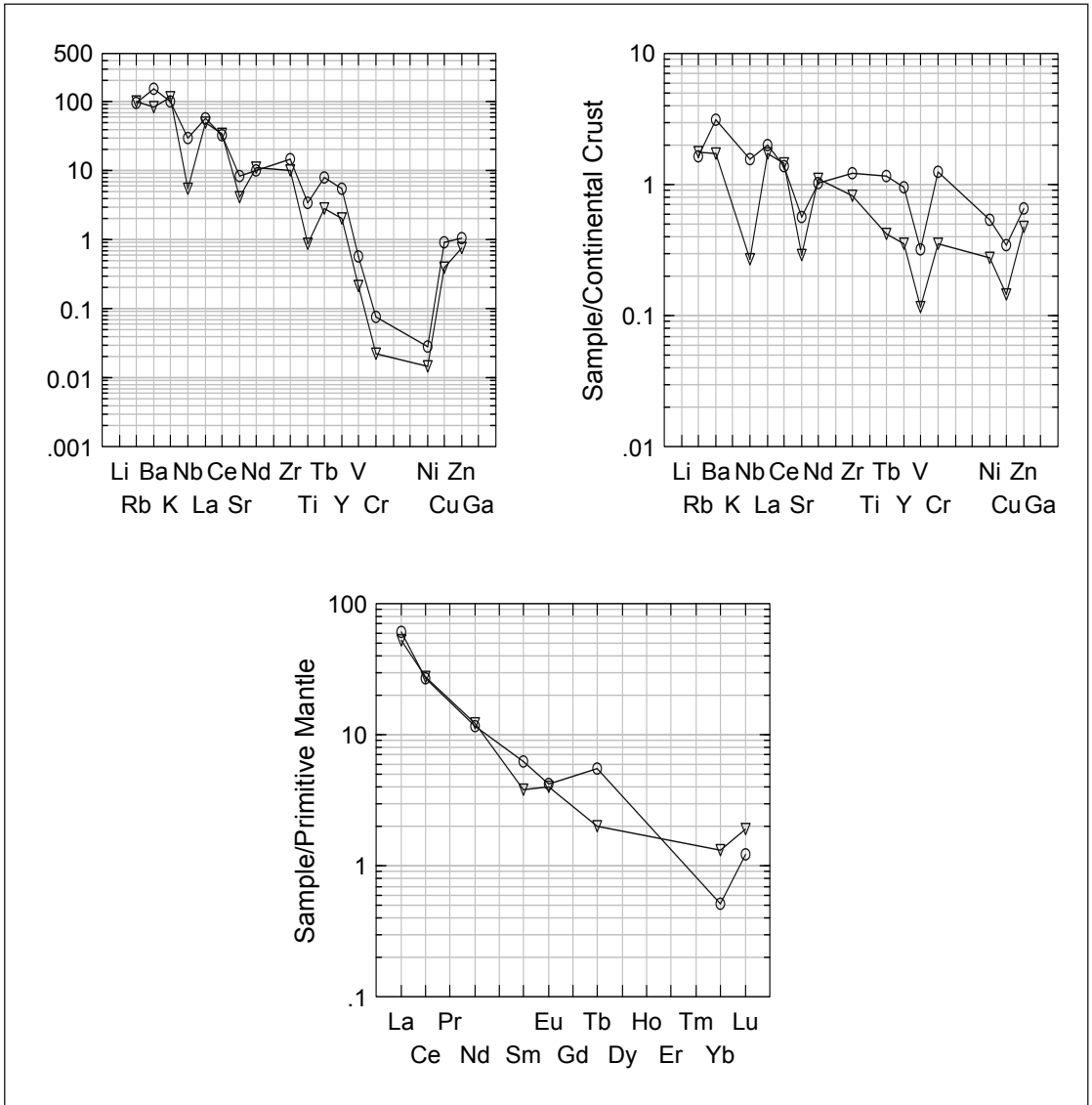


Figure 16. Comparison of trace element abundances between Luoma and Saarijärvi felsic volcanic rocks. Luoma Formation = O, Saarijärvi felsic volcanic rocks =  $\nabla$  (data from Engel & Dietz 1989).

Ni and Cr and slightly enriched in Zn and Sr. The cumulate B-layer of the same flow displays normal values of Ni and Cr. On the mantle-normalized spidergram the A-layer of the first flow also displays LREE enrichment whereas the higher flows are depleted in LREE, which is typical for komatiites (Fig. 18E).

### Komatiitic cumulates

The Kellojärvi cumulate complex is composed of olivine ad-, meso- and orthocumulates. In practice, the cumulates were divided by  $Al_2O_3$  content using the limits <1 wt.%  $Al_2O_3$  for adcumulates and 5 wt.%  $Al_2O_3$  between meso- and orthocumulates (Table 8).

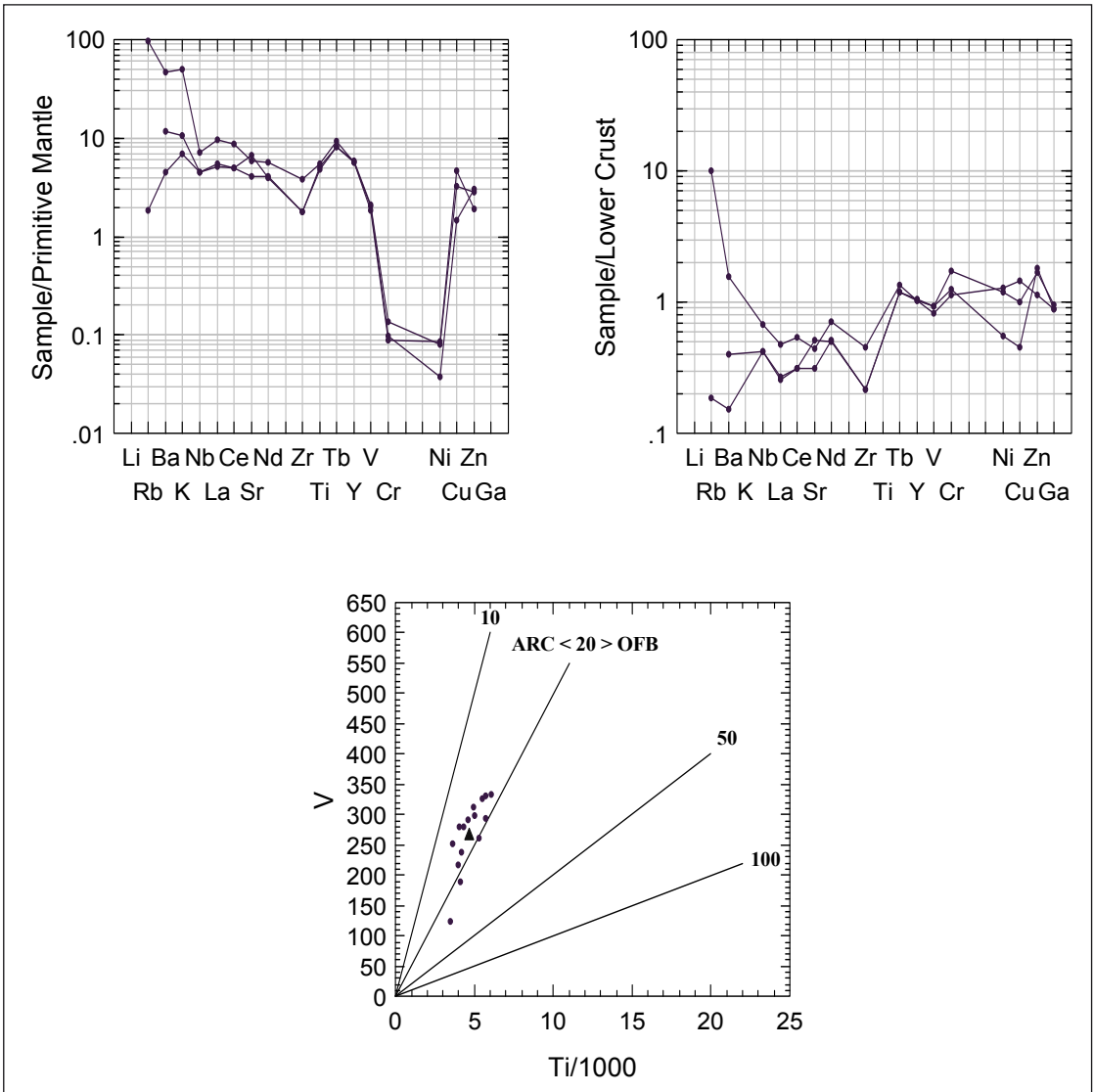


Figure 17. Trace element spidergrams and V vs. Ti/1000 plot of the Pahakangas type tholeiitic basalts. ARC = rocks of volcanic arc, OFB = ocean-floor basalts. Small triangle indicates calculated average V/Ti value of analysed samples.

Although the cumulates are totally serpentinized and locally carbonated to talc-magnesite/dolomite-magnetite rocks, primary textures are still in many cases preserved and the observed cumulus/intercumulus ratios prove the geochemical division to be correct. On the Jensen cation plot the Kellojärvi cumulates form a Mg-rich extension to the corresponding array

of komatiitic lavas and komatiitic basalts (Figs 20 and 22). Volatile-free MgO contents range from 28 wt.% in orthocumulates to 52 wt.% in adcumulates. In orthocumulates, TiO<sub>2</sub> displays a dual division: the high Ti-group ranges from 0.2 to 0.35 wt.% TiO<sub>2</sub> and the low Ti-group from 0.08 to 0.18 wt.%, and the same difference can also be observed in

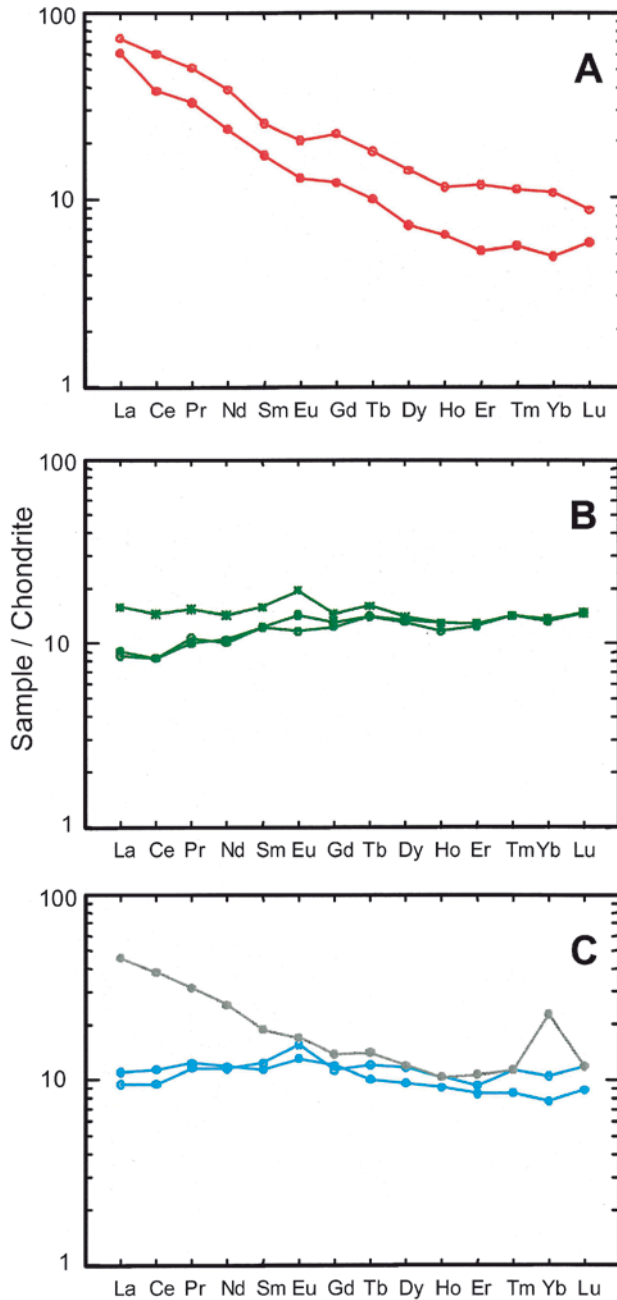


Figure 18. REE distribution diagrams of the Pahakangas-Kellojärvi rocks: A. granodiorite (o 167-TOH-93) and tonalite (169-TOH-93); B. Tholeiitic basalt (Pahakangas); C. Calc-alkalic mafic (blue: Sii-4/102.90, Sii-13/87.95) and felsic (grey: Sii-4/74.80) volcanic rocks; D. Uppermost BIF of the Pahakangas sequence (grey) and metapyroxenite (red) between komatiites and BIF; E. Fractionated komatiite lava flows: cumulate of lowermost fractionated flow (red o: Sii-8/98.05), mesocumulate (red dot: 16-TOH-93), orthocumulate (green: 12-TOH-93), random spinifex (green star: Sii-8/115.70); F. Komatiite lava flows 2-11 of the Pahakangas sequence; G. Komatiitic basalts (o 174-TOH-93, 129-TOH-94); H. Cr basalt (green: Sii-15/130.0) and high-Cr basalts (red: o Sii-15/39.0, 57-TOH-94), blue is komatiitic basalt flow between Cr basalts (195-TOH-93); I. Ultramafic cumulates of the Kellojärvi complex: olivine adcumulate (red), olivine mesocumulate (green) and augite adcumulate (grey). Normalized average chondrite from Sun and McDonough (1989). Analyses presented in the Appendix data-CD.

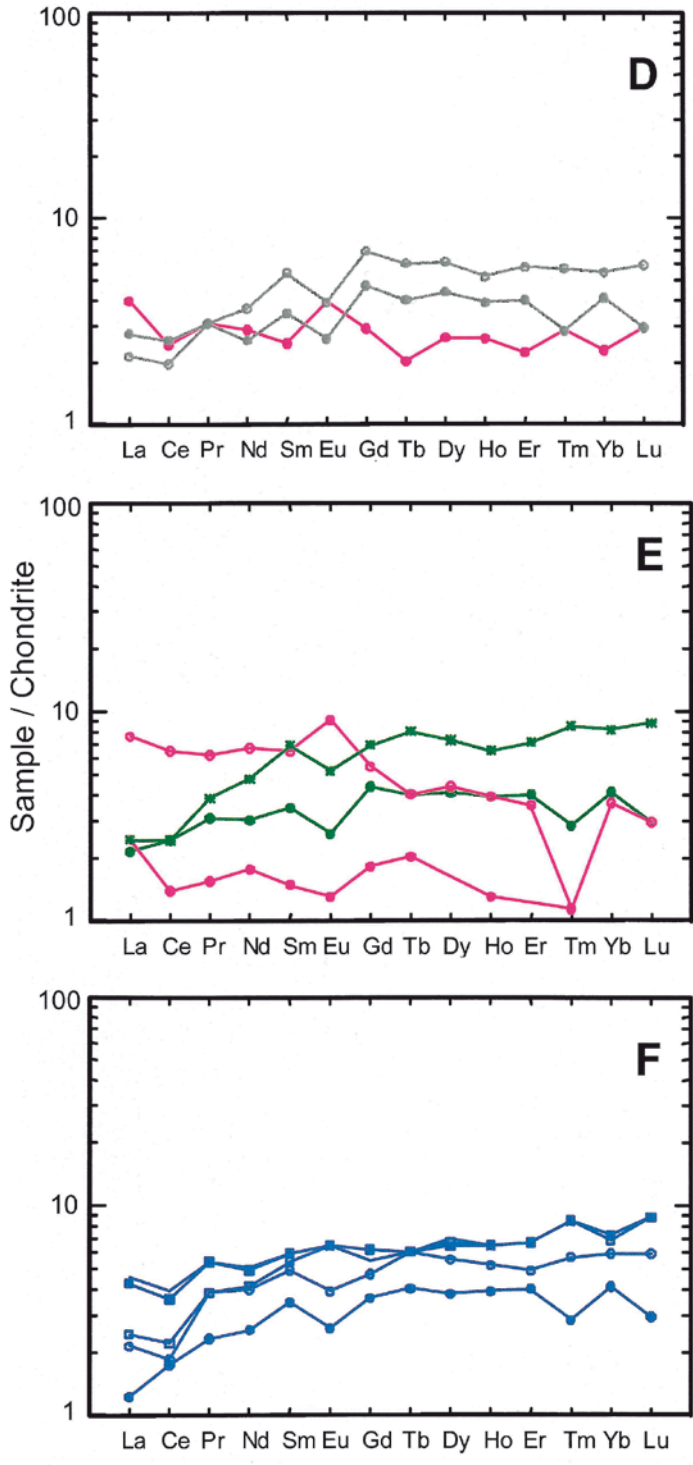


Figure 18. Continued.

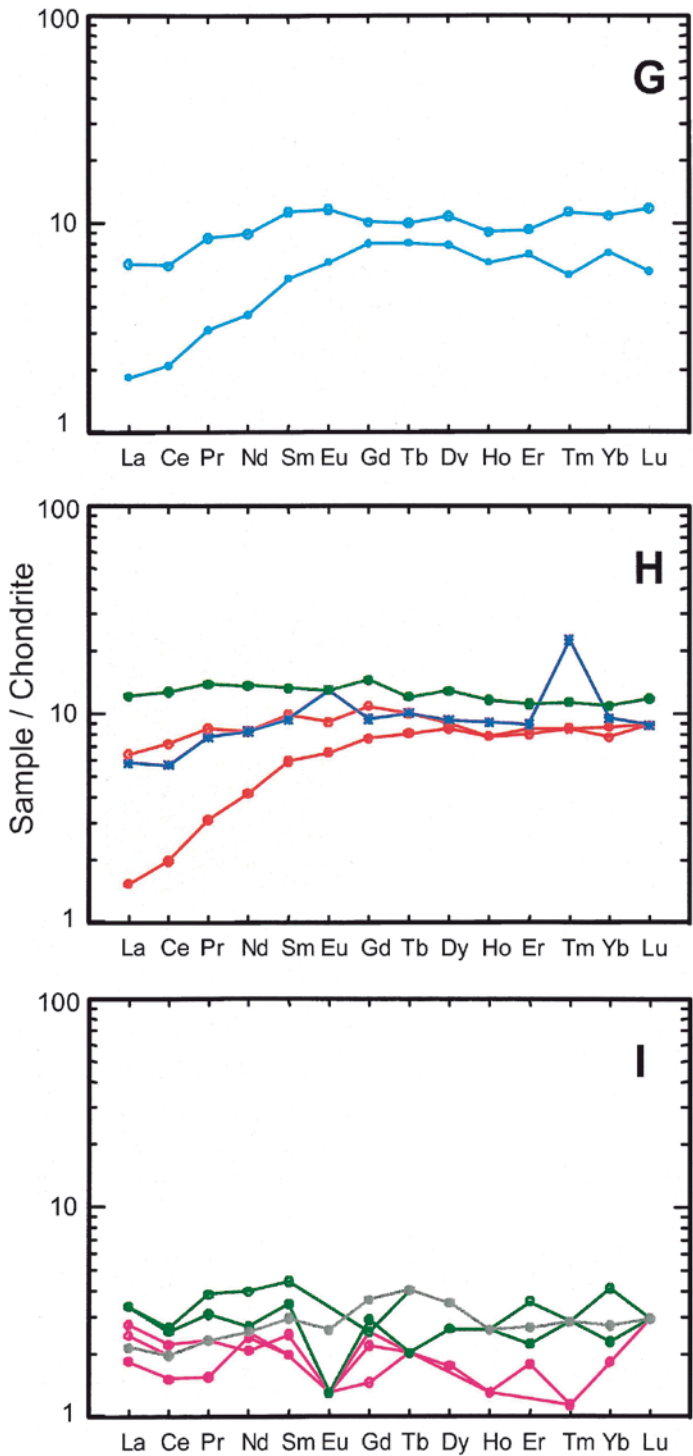


Figure 18. Continued.

Table 7. Average chemical compositions of mafic and ultramafic volcanic rocks of the Kuhmo greenstone belt. mg# see Table 4.

number	tholeiitic basalt			Cr basalt			high-Cr basalt			komatiitic basalt			komatiitic ultramafic flows		
	average	median	number	average	median	number	average	median	number	average	median	number	average	median	number
SiO <sub>2</sub>	wt.%	51.22	51.28	49.61	51.23	54.52	54.47	47.14	47.85	43.85	44.00	43.85	43.85	44.00	43.85
TiO <sub>2</sub>	wt.%	0.84	0.84	0.58	0.59	0.58	0.60	0.55	0.54	0.35	0.32	0.35	0.35	0.32	0.35
Al <sub>2</sub> O <sub>3</sub>	wt.%	15.63	15.53	13.29	13.75	13.10	13.36	11.54	11.85	7.64	7.71	11.54	11.54	7.71	11.54
FeO	wt.%	11.30	11.40	16.01	13.96	10.92	9.65	11.15	10.85	10.18	9.93	11.15	11.15	9.93	10.18
MnO	wt.%	0.20	0.20	0.62	0.47	0.29	0.24	0.23	0.21	0.18	0.18	0.23	0.23	0.18	0.18
MgO	wt.%	7.61	7.78	6.74	6.44	7.31	7.25	12.42	12.30	22.51	22.90	12.42	12.42	22.90	22.51
CaO	wt.%	9.89	10.06	11.03	10.68	10.29	9.68	9.67	9.61	6.79	6.90	9.67	9.67	6.90	6.79
Na <sub>2</sub> O	wt.%	2.83	2.71	1.60	1.55	2.37	2.38	1.83	1.63	0.23	0.13	1.83	1.83	0.13	0.23
K <sub>2</sub> O	wt.%	0.29	0.22	0.31	0.22	0.22	0.20	0.15	0.12	0.03	0.01	0.15	0.15	0.01	0.03
Cr <sub>2</sub> O <sub>3</sub>	wt.%	0.04	0.04	0.13	0.14	0.34	0.31	0.19	0.16	0.36	0.37	0.34	0.34	0.37	0.36
P <sub>2</sub> O <sub>5</sub>	wt.%	0.07	0.07	0.05	0.05	0.06	0.05	0.05	0.04	0.03	0.02	0.05	0.05	0.02	0.03
OxSum	wt.%	98.80	100.00	99.67	100.00	99.22	99.99	94.91	95.70	92.16	92.64	94.91	94.91	92.64	92.16
Ni	ppm	135	137	1161	590	595	535	431	345	1077	1050	431	431	1050	1077
Co	ppm	80	70	63	60	109	95	98	90	110	100	98	98	100	110
Cu	ppm	80	70	94	70	67	35	64	30	157	17	64	64	17	157
Zn	ppm	109	96	156	90	96	90	128	90	89	80	128	128	80	89
S	ppm	836	160	10139	3860	1371	160	383	0	870	10	383	383	10	870
Cr	ppm	303	303	920	972	2334	2114	1319	1074	2462	2508	1319	1319	2508	2462
As	ppm	16	10	12	10	16	10	11	10	48	10	11	11	10	48
Ba	ppm	71	54	80	54	71	63	48	45	23	18	48	48	18	23
Cl	ppm	123	120	126	80	117	90	97	80	49	40	97	97	40	49
Rb	ppm	12	9	11	8	8	6	7	6	3	2	7	7	2	3
Sr	ppm	98	95	87	79	82	84	71	68	18	13	82	82	13	18
V	ppm	293	285	243	241	255	258	231	231	154	150	231	231	150	154
Y	ppm	15	15	15	15	12	12	10	10	7	7	10	10	7	7
Zr	ppm	35	30	22	22	17	15	18	15	11	7	17	17	7	11
La	ppm	11	10	12	10	10	10	12	10	9	10	10	10	10	9
Ce	ppm	20	20	16	20	16	20	16	20	14	10	16	16	10	14
Pb	ppm	16	10	9	10	15	10	13	10	8	9	15	13	10	8
mg#		56.77	56.81	47.62	47.96	57.44	57.15	68.72	68.71	81.10	81.79	68.72	68.72	81.79	81.10

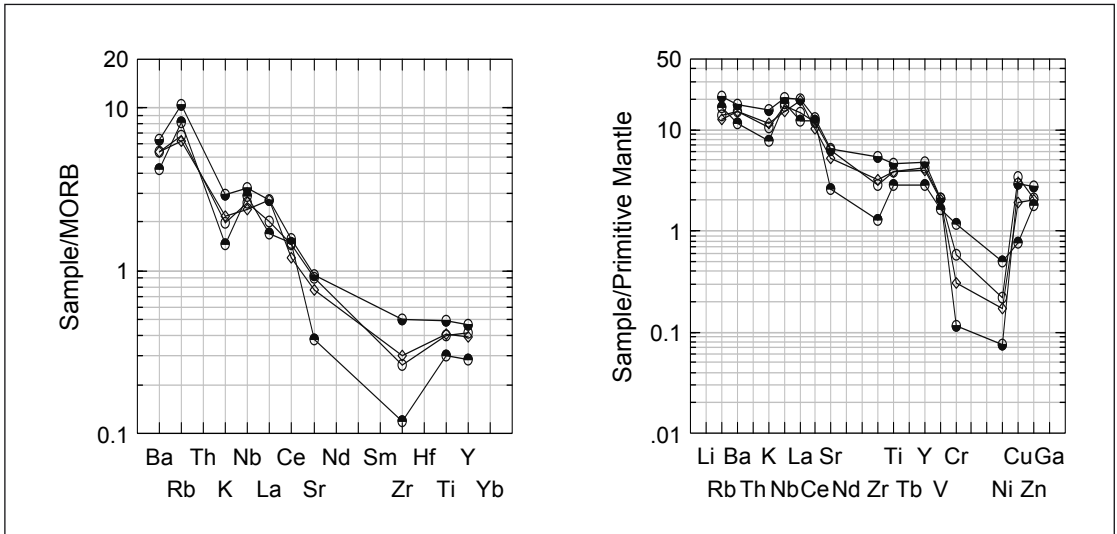


Figure 19. Comparison of trace elements of different basalt types in spider diagrams. Symbols: Cr basalt (O), high-Cr basalt (⊖ upper part black); normal tholeiitic basalt (◇); tholeiitic basalts with low Cr contents (⊖ lower part black). Analyses presented in the Appendix data-CD.

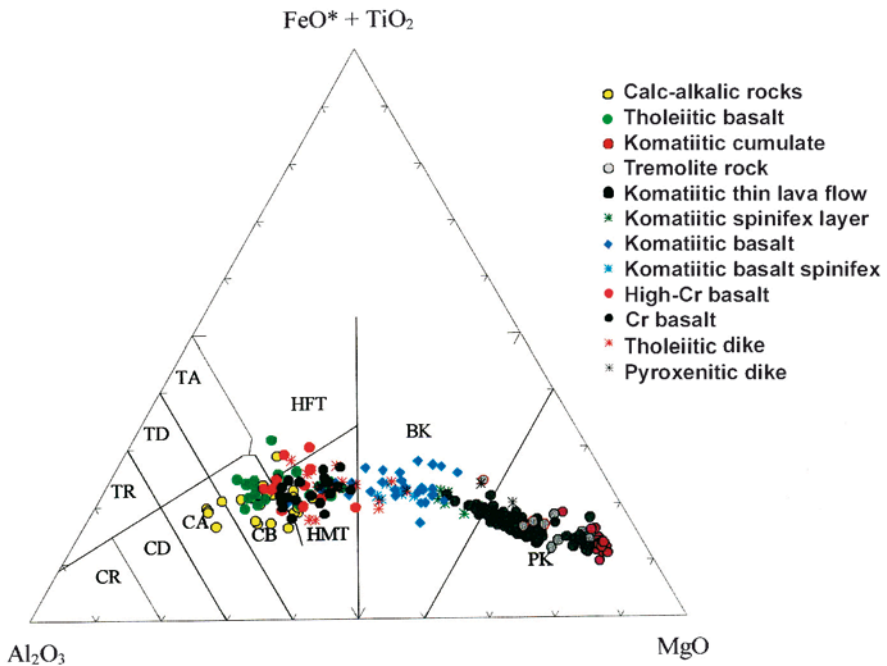


Figure 20. Volcanic rocks of the Kellojärvi area in Jensen cation diagram and x-y diagrams. Calc-alkalic rocks of the Mäkisensuo Formation and Proterozoic dike rocks are also included (Tulenheimo 1999). PK = peridotitic komatiite, BK = basaltic komatiite, HMT = high Mg tholeiite, HFT = high Fe tholeiite, CB = calc-alkalic basalt, CA = calc-alkalic andesite, CD = calc-alkalic dacite, CR = calc-alkalic rhyolite, TA = tholeiitic andesite, TD = tholeiitic dacite and TR = tholeiitic rhyolite.

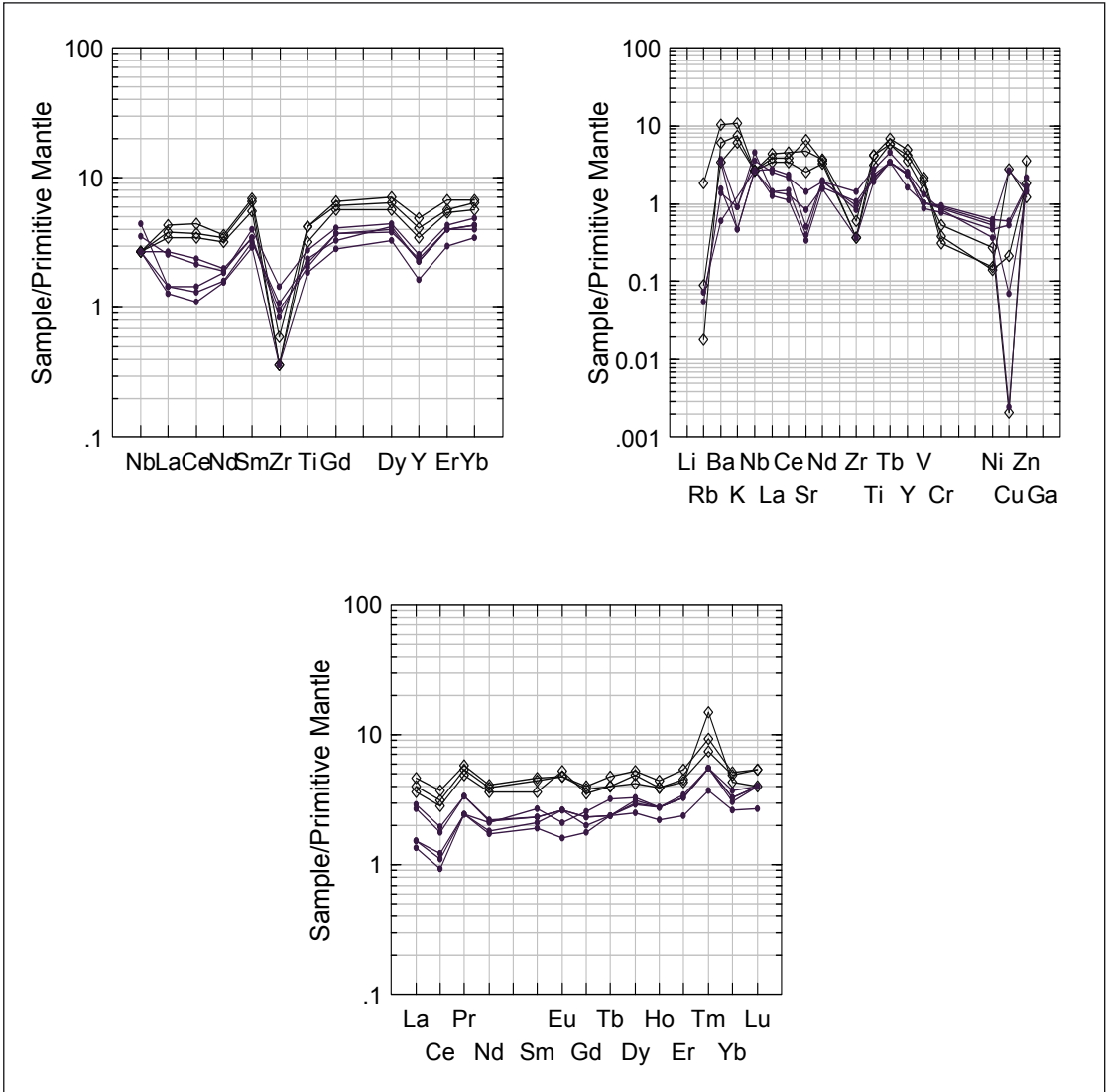


Figure 21. Trace element spidergrams of komatiitic (dot) and komatiitic basaltic lavas (diamond  $\diamond$ ).

the  $\text{Al}_2\text{O}_3$  contents (Fig. 23). It is noteworthy that a similar variation in  $\text{TiO}_2$  content can also be seen between komatiitic basalts and komatiitic lavas. Cumulates of the Proterozoic dike rocks deviate clearly from komatiites and komatiitic basalts in their  $\text{TiO}_2$  contents and in  $\text{Al}_2\text{O}_3/\text{TiO}_2$  ratios. Flat chondrite normalized REE distributions characterize the komatiitic cumulates (Fig. 18I).

### High-Cr basalt

MgO contents of this basalt type range from 4.29 to 10.13 wt. %,  $\text{Cr}_2\text{O}_3$  from 0.20 to 0.66 wt.% and Ni content 170–1680 ppm (Table 7). It is noteworthy that  $\text{Cr}_2\text{O}_3$  of high-Cr basalt is higher than in the komatiitic basalt, which contains 0.19 wt.%  $\text{Cr}_2\text{O}_3$  on average. The komatiitic interflow within



Table 8. Average chemical compositions of cumulate rocks of the Kellojärvi area, Kuhmo. Paleoproterozoic dike rocks are also included for comparison. mg# see Table 4.

		adcumulate	meso-cumulate	ortho-cumulate	contact clinopyroxenite	contact orthopyroxenite	komatiitic gabbro	Proteroz. pyroxenite dike	Proteroz. gabbro dike
number of samples		50	75	79	4	6	8	33	20
<b>SiO<sub>2</sub></b>	wt.%	43.04	44.28	47.31	52.12	51.63	51.08	46.73	48.97
<b>TiO<sub>2</sub></b>	wt.%	0.06	0.12	0.26	0.27	0.21	0.32	1.01	1.32
<b>Al<sub>2</sub>O<sub>3</sub></b>	wt.%	1.41	2.60	4.62	4.64	4.99	14.92	7.25	14.50
<b>FeO*</b>	wt.%	10.29	10.92	9.75	8.51	7.68	7.68	14.05	12.75
<b>MnO</b>	wt.%	0.16	0.18	0.20	0.25	0.17	0.17	0.32	0.34
<b>MgO</b>	wt.%	44.05	40.10	29.78	20.72	24.64	11.14	17.69	6.53
<b>CaO</b>	wt.%	0.07	0.94	7.34	12.63	9.93	11.92	11.69	12.14
<b>Na<sub>2</sub>O</b>	wt.%	0.01	n.d.	0.05	0.26	0.07	1.68	0.58	2.41
<b>K<sub>2</sub>O</b>	wt.%	n.d.	n.d.	0.03	0.09	0.17	0.94	0.30	0.88
<b>P<sub>2</sub>O<sub>5</sub></b>	wt.%	0.01	0.01	0.02	0.02	0.01	0.03	0.09	0.13
<b>Cr<sub>2</sub>O<sub>3</sub></b>	wt.%	0.54	0.54	0.455	0.43	0.44	0.08	0.23	0.02
<b>NiO</b>	wt.%	0.36	0.31	0.185	0.05	0.06	0.03	0.07	0.01
<b>Ox sum*</b>	wt.%	85.46	87.66	91.57	96.50	95.61	97.45	96.32	96.84
<b>mg#</b>		88.4	86.7	84.2	82.7	86.2	73.7	70.5	50.7
<b>Cr</b>	ppm	3159	3222	2852	2877	2884	559	1538	132
<b>Ni</b>	ppm	2395	2117	1314	360	418	255	587	107
<b>Co</b>	ppm	124	96	74	125	132	37	96	59
<b>Sc</b>	ppm	–	9.53	18.5	n.d.	n.d.	47	n.d.	n.d.
<b>V</b>	ppm	33	54	107	150	100	144	204	318
<b>Cu</b>	ppm	6	19	36	16	365	29	84	89
<b>Pb</b>	ppm	8	14	14	28	10	47	145	63
<b>Zn</b>	ppm	75	97	93	178	72	158	274	211
<b>S</b>	ppm	115	174	300	21	729	40	242	446
<b>Rb</b>	ppm	0.4	0.9	2.0	3.7	9.6	40	12	32
<b>Cs</b>	ppm	1.0	0.8	3.0	–	6.7	8.9	5.6	14.1
<b>Ba</b>	ppm	6	10	18	25	106	209	93	408
<b>Sr</b>	ppm	0.6	2.7	7.7	11	10	259	47	167
<b>Ga</b>	ppm	2.3	3.7	5.2	2.8	3.8	7.4	5.2	2.8
<b>Ta</b>	ppm	0.5	0.8	1.4	5.0	3.3	3.3	3.8	5.9
<b>Nb</b>	ppm	1.6	1.6	3.1	7.7	6.6	5.5	9.0	18.0
<b>Zr</b>	ppm	3.1	6.8	14.5	6.0	7.8	20.9	62.7	88.9
<b>Y</b>	ppm	2.4	4.0	6.7	8.3	3.7	8.4	12.5	18.7
<b>U</b>	ppm	0.8	0.6	1.3	2.8	3.0	3.6	2.3	5.0
<b>La</b>	ppm	2.7	4.5	8.3	6.8	4.4	16.5	11.3	19.5
<b>Ce</b>	ppm	4.0	5.8	9.3	11.8	10.2	10.0	24.7	35.1
<b>Cl</b>	ppm	357	64	33	21	19	98	122	286

the high-Cr basalt contains 0.44 wt.% Cr<sub>2</sub>O<sub>3</sub> and both rock types display Al<sub>2</sub>O<sub>3</sub>/TiO<sub>2</sub> values between 19 and 24. In order to study the correlation of Cr contents between other trace elements the analyses

of basalts were classified into four groups on the basis of their Cr contents. The results are depicted as spidergrams in Figure 19. Basalts with average tholeiitic compositions and those with anomalously

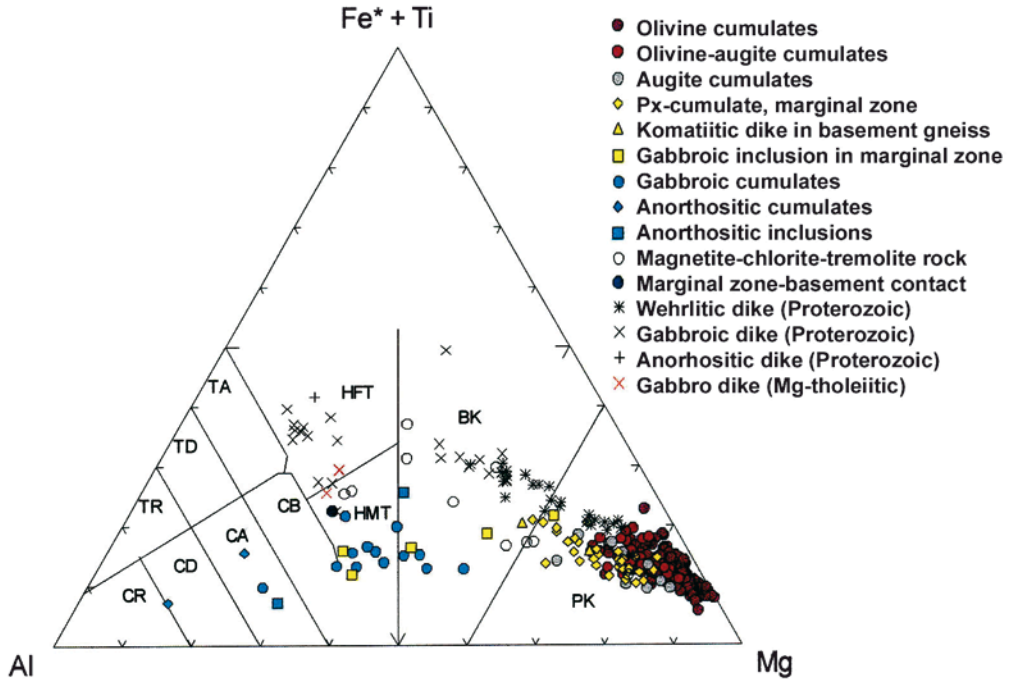


Figure 22. Kellojärvi ultramafic cumulates and fractionated mafic members in the Jensen cation diagram. The Proterozoic dikes are also included (Tulenheimo 1999). PK = peridotitic komatiite, BK = basaltic komatiite, HMT = high Mg tholeiite, HFT = high Fe tholeiite, CB = calc-alkalic basalt, CA = calc-alkalic andesite, CD = calc-alkalic dacite, CR = calc-alkalic rhyolite, TA = tholeiitic andesite, TD = tholeiitic dacite and TR = tholeiitic rhyolite.

low Cr contents display lower concentrations of Ni and higher concentrations of Ti, Y, Zr and Sr than the Cr-rich basalts. REE distribution patterns of high-Cr basalts are almost identical with those of komatiites (Fig. 18F and H), but a slightly negative Eu anomaly characterizes the high-Cr basalts.

### Felsic volcanic rocks of the Ronkaperä Formation

The lahar type volcanoclastic deposits of the Ronkaperä Formation include a suite of volcanic rocks ranging in composition from rhyolites to dacites, andesites and basalts (Table 6). The trace

element spidergrams (Nieminen 1998) indicate prominent negative  $Nb_N$  anomalies normalized both with the values of primitive mantle and average continental crust. The mantle normalized  $[Zr/Ti]_N$  values are  $>1$ . The concentrations of compatible elements vary according to rock type, but are an order of magnitude higher than the corresponding values of the Taivaljärvi felsic rocks. Accordingly, the negative  $Nb_N$  anomaly is more prominent in Ronkaperä than in the Taivaljärvi rocks. Some fragments of the basaltic rocks display high concentrations of Cr, and they were interpreted as clasts of underlying high-Cr basalts (Fig. 24).

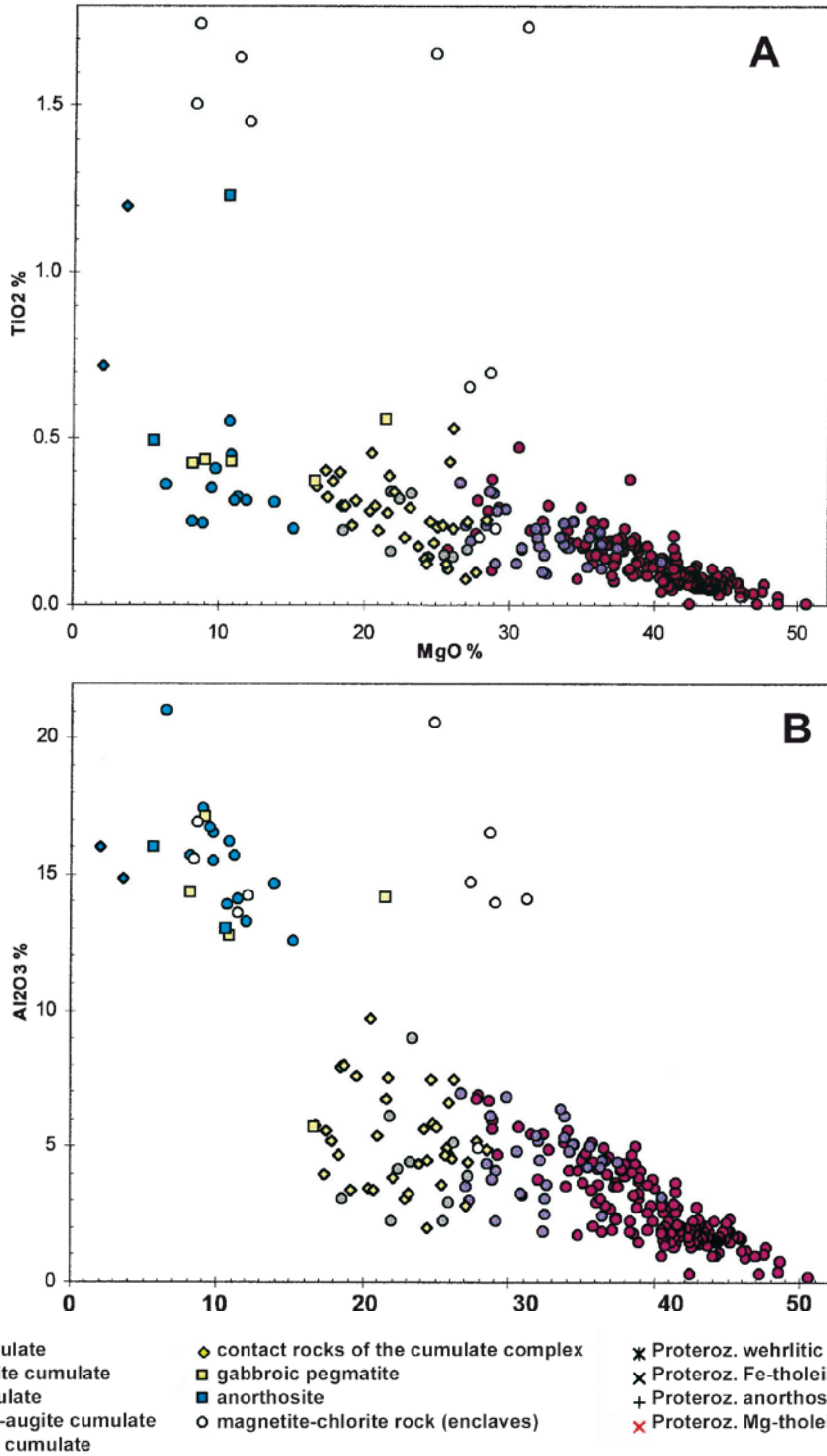
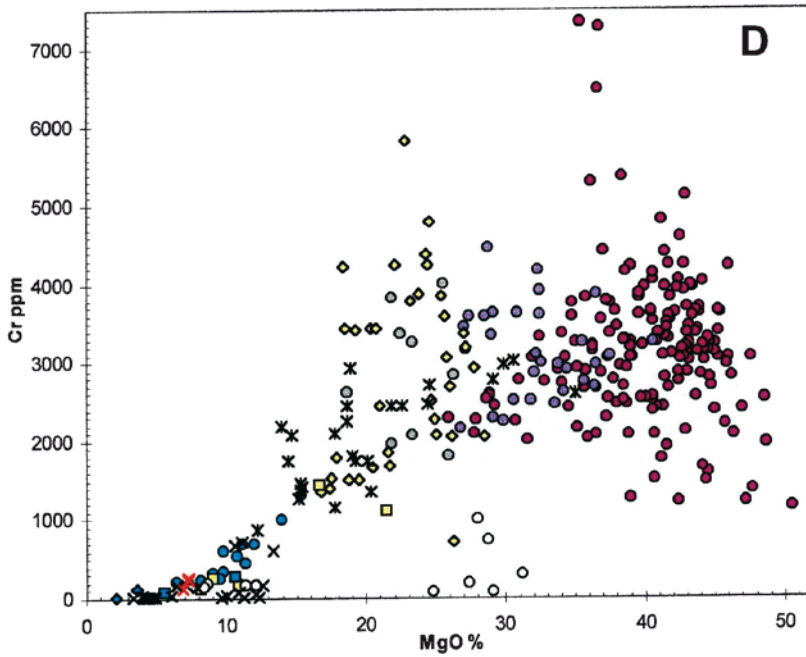
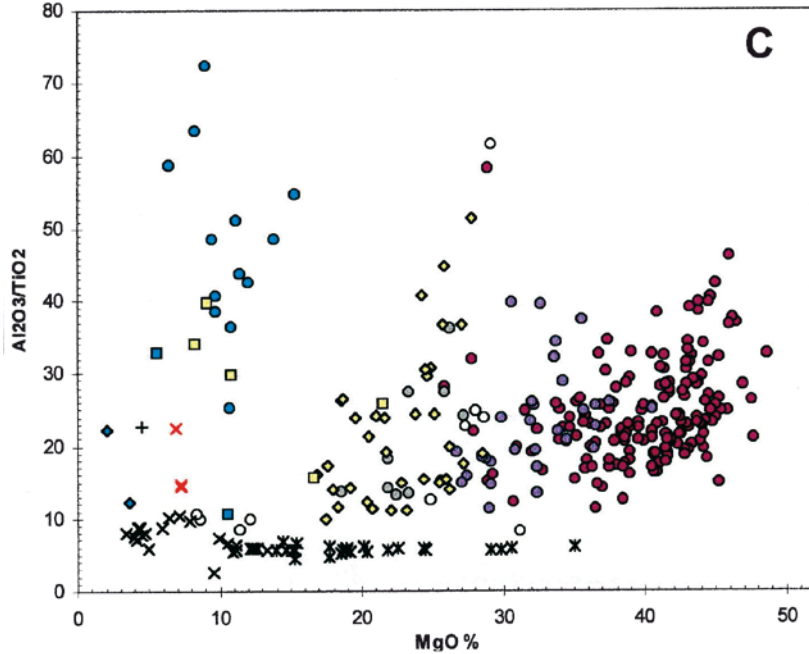
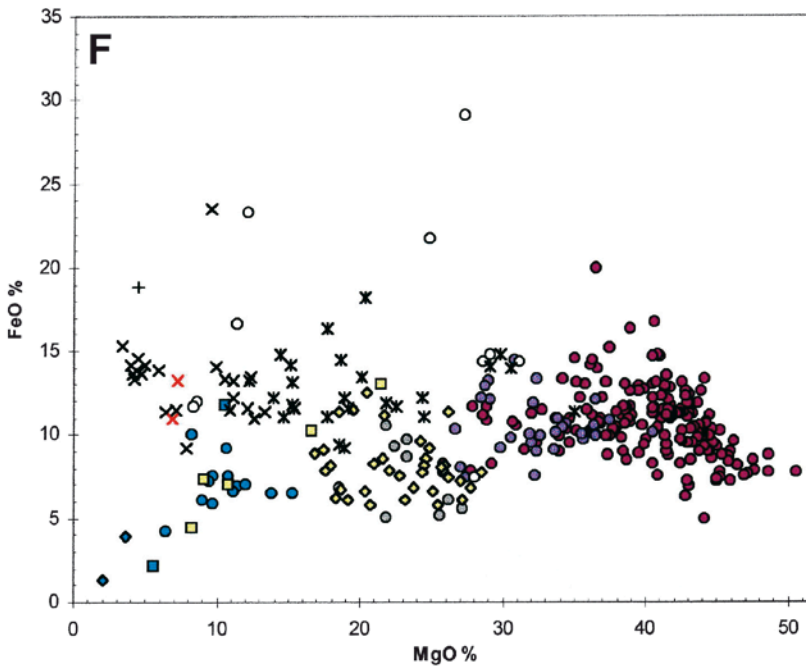
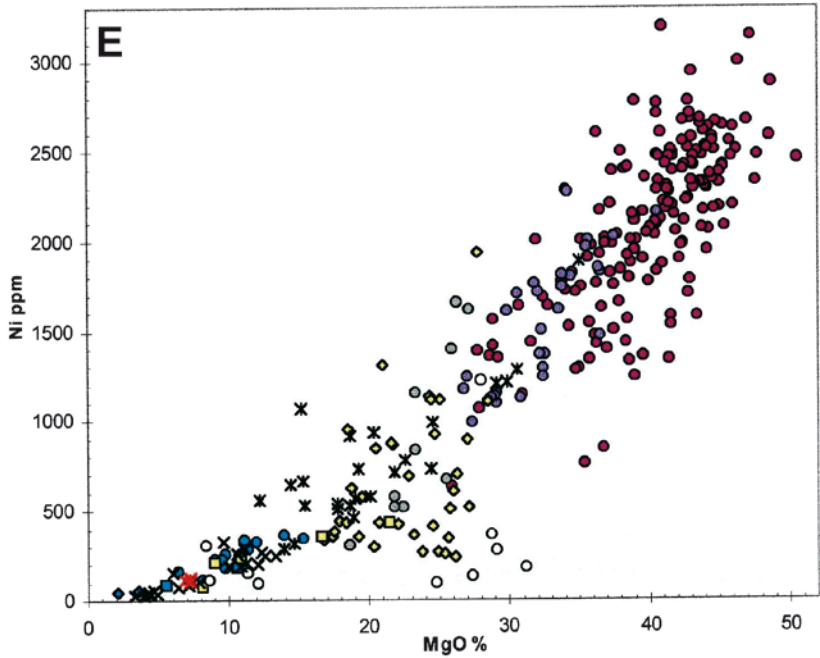


Figure 23. X-y diagrams depict MgO contents *versus* other elements of cumulates of the Kellojärvi komatiitic cumulate complex and Proterozoic dike rocks (Tulenheimo 1999).



- olivine cumulate
- olivine-augite cumulate
- augite cumulate
- plagioclase-augite cumulate
- plagioclase cumulate
- ◆ contact rocks of the cumulate complex
- gabbroic pegmatite
- anorthosite
- magnetite-chlorite rock (enclaves)
- × Proteroz. wehrlitic pyroxenite dike
- × Proteroz. Fe-tholeiitic gabbro dike
- × Proteroz. anorthositic dike
- × Proteroz. Mg-tholeiitic gabbro dike
- + Proteroz. anorthositic dike

Figure 23. Continued.



- |                               |   |                                       |
|-------------------------------|---|---------------------------------------|
| ● olivine cumulate            | ◆ contact rocks of the cumulate complex | ✱ Proteroz. wehrlitic pyroxenite dike |
| ● olivine-augite cumulate     | ■ gabbroic pegmatite                    | ✱ Proteroz. Fe-tholeiitic gabbro dike |
| ○ augite cumulate             | ■ anorthosite                           | + Proteroz. anorthositic dike         |
| ● plagioclase-augite cumulate | ○ magnetite-chlorite rock (enclaves)    | ✱ Proteroz. Mg-tholeiitic gabbro dike |
| ◆ plagioclase cumulate        |   |                                       |

Figure 23. Continued.

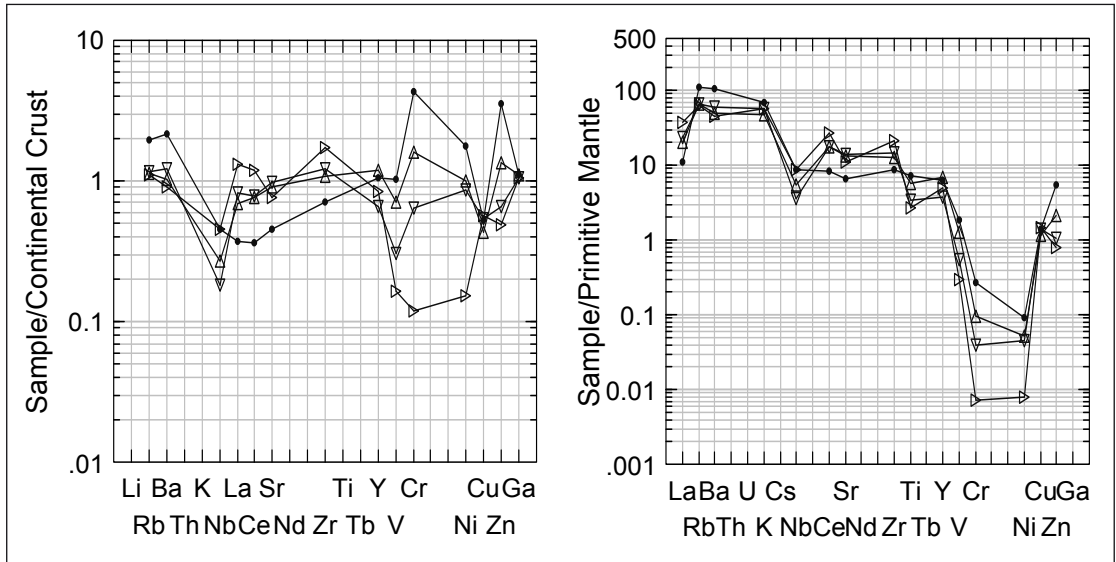


Figure 24. Average trace element compositions of the Ronkaperä Formation rhyolites ( $\triangleright$ ), dacites ( $\nabla$ ), andesites ( $\triangle$ ) and mafic volcanic rocks ( $\bullet$ ).

### Discussion on the geochemical evolution

The geochemistry of the TTG complex displays a signature similar to subduction-related magmas, although the Nb depletion is more prominent than the value for the average continental crust calculated by Taylor and McLennan (1985). The trace elements of the felsic and intermediate volcanic rocks of the Taivaljärvi area display arc magma signatures, and in this respect they are similar to the surrounding grey gneisses of the TTG complex. The distinctive geochemistry of the felsic volcanic rocks may be the result of partial melting of the TTG complex. Negative  $Eu_N$  anomalies in felsic rocks and positive anomalies in the overlying intermediate volcanic rocks prove that plagioclase was left as a residual phase in the initial batch melting of TTG, to form anorthositic cumulates. Based on the data presented by James and Hamilton (1969), low-pressure melting leaves An-rich plagioclase in residue. The process is related to that proposed for the genesis of Lofoten anorthosites by Green et al.

(1972). The intermediate rocks of Taivaljärvi were derived via subaqueous partial melting from this plagioclase-enriched residual material.  $[Nb/La]_N$  values well below those of primitive mantle and  $[Zr/Ti]_N$  ratios above the mantle value characterize both felsic volcanic rocks and the TTG rocks.

In case the greenstone belt volcanism is the result of thermal mantle plume, a zone refinement (Harris 1957, McBirney 1987) is the probable process that affects the composition of a melt formed at advanced heat front. In this process the melt migrates with the heat front and concentrates trace incompatible elements, also such as Zn, Pb and Ag, which are abundant in the Koivumäki and Mäkisensuo Formations. Incipient melting at the mantle-crust boundary and participation of mantle in the melt generation is reflected in the main element ratios, from which an example is the high Mg-number in the Tipasjärvi and Mäkisensuo felsic rocks. The compatible elements Cr and Ni retain in the mantle,

if olivine and spinel are present in the residual phases and will be depleted in the melt like in the Tipasjärvi felsic rocks. Instead, the compatible elements may partition in the melt (Mäkisensuo felsic rocks), which is generated with evolved mantle material (MORB), where olivine and spinel phases are missing. Zone refinement process explains the mentioned characteristic geochemical features of the TKS felsic rocks.

Banded chert layers above the initial felsic-intermediate volcanic phase in the stratigraphy of the Taivaljärvi area indicate a break in volcanism. The overlying Pahakangas-type basaltic-andesitic volcanism displays a primitive non-fractionated distribution of REE, although the concentrations are 4–6 times higher than those in the mantle. Distinct depletion of compatible elements, Cr and Ni, indicates that olivine-spinel residue was left in the mantle in the basaltic melt generation. High and variable concentrations of LIL elements may be the result of hydrothermal alteration of submarine pillow lavas, but they could also be concentrated in the basaltic melt fraction if the mantle was undepleted. The  $[\text{Nb/La}]_N$  ratio is close to the mantle value and this indicates that crustal contamination is minimal.

Komatiites are the only volcanic rocks in the area that display  $[\text{Nb/La}]_N$  ratios  $>1$ . Puchtel et al. (1997) observed the same feature in the komatiites of the Kostamuksha greenstone belt, NW Russia, and on the basis of extensive reference material, they suggested that it indicates an oceanic plateau origin for the lavas. However, in komatiitic basalt, the  $[\text{Nb/La}]_N$  ratios are below the corresponding mantle values, and the distribution diagram resembles that of Vetryny belt basalts or Kambalda komatiites, which were formed during intra-cratonic rifting (Puchtel et al. 1999, Barnes et al. 2004).

Some authors (see Leshner & Keays 2001) consider that trace elements, such as REE and HFSE (Th, Zr, Nb), are immobile during hydrothermal metasomatic alteration in the ocean floor, but opposite views have also been presented concerning the effect of carbonate alteration (Tourpin 1991, Gruau et al. 1992, Lahaye et al. 1995), especially in cases where a significant glass phase was present in

the primary lava. Another mechanism for changing lava composition is magmatic assimilation, which can take place along melt conduits during ascent or between lava and the substrate. Thermal erosion and assimilation of the substrate was demonstrated as a likely process in turbulently flowing hot komatiitic lavas (Huppert & Sparks 1985, Frost & Groves 1989).

If the deviating trace element ratios of komatiites and komatiitic basalts are the result of magmatic assimilation, the assimilated materials must have been quite different, having a high  $[\text{Nb/La}]_N$  ratio in the case of komatiites and a low ratio for komatiitic basalt. Surrounding Archaean TTG gneisses display low  $[\text{Nb/La}]_N$ , and slightly enriched LREE ratios similar to the corresponding values of komatiitic basalt. These features of komatiitic basalt can reflect assimilation of felsic Archaean crustal material. However, the Zr concentrations of TTG gneisses are relatively high, and the low  $\text{Zr}_N$  values of komatiitic basalts are thus inconsistent with TTG assimilation. In komatiites, the values of  $[\text{Nb/La}]_N$  ratios are  $>1$  and in this respect they resemble the Kostamuksha komatiites (Puchtel et al. 1997). A negative  $\text{Zr}_N$  anomaly and  $[\text{Zr/Ti}]_N < 1$ , as well as  $[\text{Nb/La}]_N < 1$ , characterize the Pahakangas type basalt, and these values resemble komatiitic basalt. This may reflect a similar source, whereas komatiites originate from the LREE-depleted and Nb-enriched environment. However, more trace elements and isotope assays will be needed to solve this issue.

Depleted Ni and Cr values and slightly enriched Zn and Sr as well as enrichment of LREE in the mantle-normalized spidergram of the first komatiite flow could all be explained as a consequence of contamination as the komatiitic lava assimilated felsic to intermediate substrate material. The Pahakangas type basalt or BIF as a contaminant cannot explain the REE pattern, because both have flat chondrite-normalized REE patterns. Instead, contamination by granitoid material (Viitavaara tonalite) or Mäkisensuo Formation felsic volcanic rocks could explain the LREE enrichment and high Sr values, but only the Mäkisensuo calc-alkalic felsic volcanic rocks explain the Zn enrichment. The low Ni content in the first flow is either the result of low primary Ni

value of the magma, or it could be attributed to equilibration of the melt with sulfides. Combined with the REE patterns (Fig. 18), contamination by sulfide-bearing Mäkisensuo-type sequence seems more plausible. Accordingly, the two ages observed in the zircons of the felsic fragments of the “Small serpentinite” support the idea that the fragments were derived from Mäkisensuo-type felsic volcanic rocks. Being enclosed in hot komatiitic lava, the fragments remelted and crystallized as granodioritic inclusions. The dated zircon crystals were inherited from the original felsic volcanic rock and the cores indicate the age of felsic volcanism, but the rims got their age signature at the process of remelting, and thus indicate age of the komatiite eruption (Peltonen et al., in prep.). The amphibole rock, originally clinopyroxenite, located between the first fractionated komatiite flow and BIF/Pahakangas basalt substrate was probably crystallized from a hybrid melt that had both komatiitic and substrate materials (Fig. 18D).

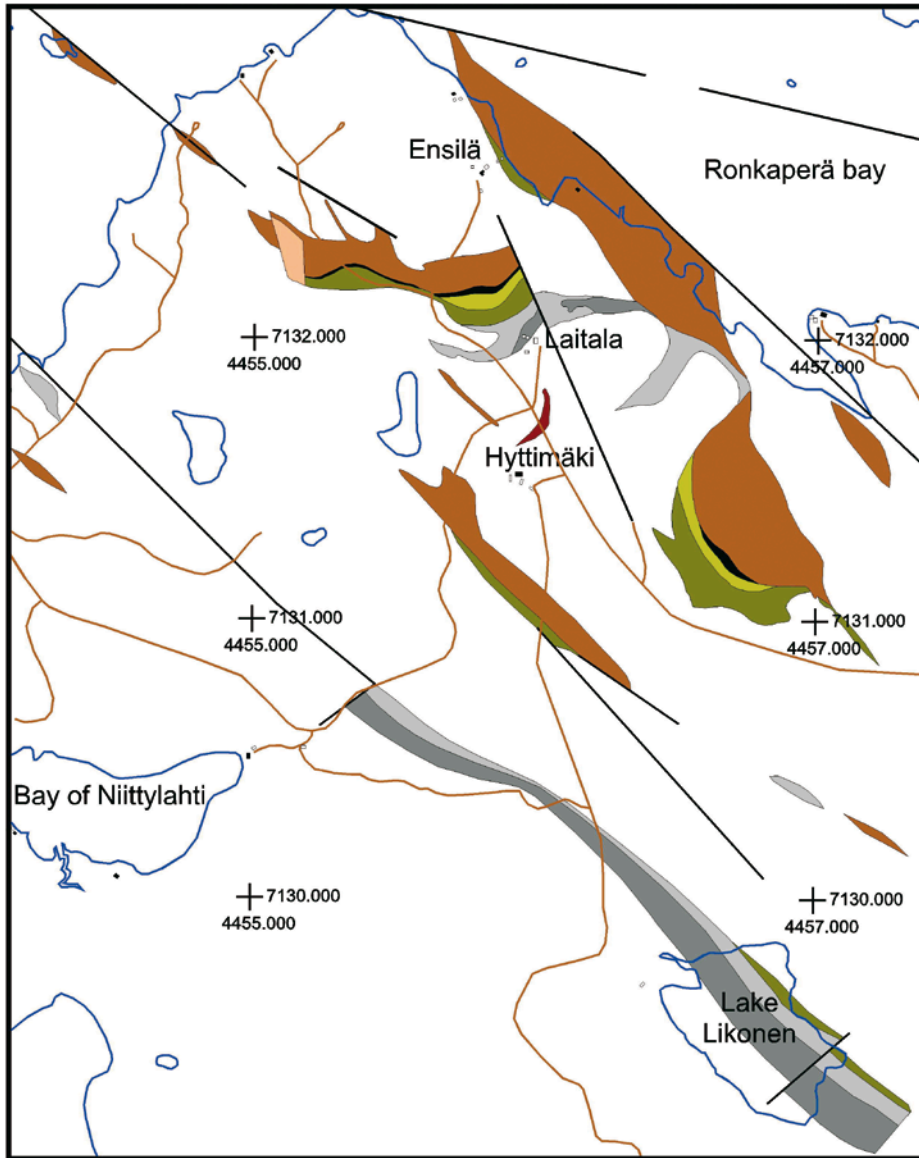
The olivine composition of komatiitic cumulates can be used to calculate the MgO content of the host magma. Olivines, especially primary magmatic olivines are rare, and cumulates are commonly totally altered to serpentine-amphibole±diopside-chlorite rocks. According to Tulenheimo (1999), the rare primary olivines fall into two compositional groups representing the  $Fo_{83}$  as analysed by Eero Hanski from the cumulate sample of Aronniemi, Näätäniemi, and  $Fo_{89}$  from Laitala in the Ensilä area (see Fig. 25 for location). Most of the analysed olivines are of metamorphic origin and display high Fo-contents,  $Fo_{94-95}$ . Serpentinized komatiitic cumulates display typical trends along the olivine control line in the volatile-free normalized MgO versus incompatible element (Al, Ti) diagrams (Fig. 23). Approximation of the fractionated, most magnesian olivine from these diagrams could yield up to 52 wt.% MgO, but the validity of this approximation can be questioned since some iron may have been remobilised from the rock during carbonate alteration and serpenti-

nization processes. Tulenheimo (1999) calculated that the melt corresponding to the primary olivine of Näätäniemi ( $Fo_{83}$ ) contained 11 wt.% MgO, and that the olivines with  $Fo_{89-92}$  crystallized from a melt with 18–23 wt.% MgO. Flow top breccias of komatiitic lavas at Pahakangas yield MgO-values between 21.7–23.3 wt.%, which is in accord to the primary olivine composition of komatiitic cumulate samples. The considerable range of primary olivine compositions could reflect variable compositions of the parental melt, and in this case the melt composition range between komatiites and komatiitic basalts.

The field relationships of clinopyroxenitic and orthopyroxenitic contact varieties of the Kellojärvi cumulate complex indicate that the clinopyroxenite was the first phase to be crystallized. The composition of clinopyroxenite resembles that of the pyroxenitic interlayer between the first komatiitic flow and the Pahakangas Formation basalts and BIF layers. The sequence from contact clinopyroxenite to orthopyroxenite and further to dunite (Fig. 11) indicates a sequential compositional change in  $(FeO+MgO)/SiO_2$  atomic ratio of the characteristic main minerals from 1:2 in clinopyroxenite to 1:1 in orthopyroxenite and further to 2:1 in dunite. The pyroxenitic contact varieties probably represent the first magmatic pulse that was contaminated by crustal material. The sharp contact features between olivine orthocumulate and pyroxenite can be interpreted as the result of (thermal) erosion, which indicates a time gap between the first pulse of contaminated magma and the magma pulses that produced olivine cumulates. The existence of large partly assimilated rafts of mafic lava in the lowermost olivine orthocumulate provides evidence that cumulates formed at or near the earth surface.

At a late stage of the greenstone belt evolution mafic melt was intruded among the ultramafic cumulates and fractionated to form a layered sequence of pyroxenite, gabbro and anorthosite, for example in the Niittylahti area (see Fig. 25 for location).





**Proterozoic Fe-tholeiitic dikes**

- Wehrlitic dike, olivine ortho-mesocumulate-olivine augite adcumulate
- Wehrlitic-pyroxenitic dike, olivine augite adcumulate-augite adcumulate
- Gabbroic dike, augite ortho-mesocumulate
- Gabbroic dike, augite ortho-mesocumulate, glomeroporphyritic
- Gabbroic dike, augite ortho-mesocumulate, Cr > 600 ppm
- Magnetite gabbro, magnetite augite orthocumulate with intercumulus plagioclase
- Gabbroic dike, plagioclase augite adcumulate

**Proterozoic Mg-tholeiitic dikes**

- Gabbroic dike
- Lake shore / small lake
- Fault
- Road
- House

Figure 25. Distribution of Paleoproterozoic dike rocks and related layered mafic intrusions in the Kellojärvi area (Tulenheimo 1999). Only dike rocks are coloured in the map.

## Post-greenstone mafic and felsic intrusive rocks

The greenstone belt is intruded by weakly foliated granodiorite and tonalite, frequently sanukitoid in composition (Käpyaho 2006, Heilimo et al. 2007), the sanukitoids are most prominent in the margins of the greenstone belts. Additionally to the west of the belt, the weakly foliated leucocratic intrusions, mainly granodiorite in composition are more prominent than to the east, probably reflecting that the leucocratic igneous rocks intruded high up in the crust since the crustal erosion level is deeper in the east (Yliniemi 1986). Luukkonen (1992) correlates the generation of these granitoids to the  $D_3$  stage of regional deformation, and that  $D_3$  faults and shear zones controlled their emplacement even a long time span after the  $D_3$  deformation. The granitoids display a calc-alkaline fractionation trend with high K, Rb and LREE and initial Sr isotope ratios (0.7044–0.7049) suggesting deep crustal derivation by partial melting of tonalite or siliceous granulite, although the melt migrated far away to the upper crustal levels (Luukkonen 1992, Martin 1987, Horneman et al. 1988). The Moisiovaara mafic sill (Luukkonen 1988) yielded an age of  $2790 \pm 18$  Ma for the mafic tholeiitic volcanism, and we argue that the age  $2771 \pm 8$  Ma obtained from the zircon rims of granitoid enclaves of the “Small serpentinite” (Peltonen 2007, pers. com., Peltonen et al., in prep.) indicates the age of komatiitic volcanism. Hence there is an interval ranging from 20 to 30 Ma between the main volcanic phase of the greenstone belt (2770 Ma) and the felsic plutonism (2750 Ma). On the other hand, the age of felsic porphyry dike intruding the Siivikkovaara mafic volcanic rocks,  $2770 \pm 30$  Ma (Tourpin 1991), the  $2774 \pm 8$  Ma age of the Kilpasuo felsic volcanic rocks at SGB and the age of the Viitavaara tonalite,  $2785 \pm 7$  Ma (Käpyaho et al. 2006) prove that also a felsic intrusive/extrusive phase was coeval with mafic volcanism. The felsic (sub)volcanic phase with associated sediments is well documented between tholeiitic and komatiitic basalts in the Kiannanniemi area (Fig. 1) close to the Hietaharju and Peura-aho Ni-Cu deposits. Vaasjoki et al. (1999) and Käpyaho et al. (2006) concluded that, in addition to the 2750–2700 Ma pulse of felsic

mainly sanukitoid igneous rocks, there was also a pulse of granitoid magmatism at 2700–2680 Ma (leucogranites and granodiorites), which caused regional metamorphism, fluid circulation and resetting of Rb-Sr and whole-rock Pb-Pb age data.

Tonalites, trondhjemites and granodiorites intersecting the greenstone belt display a calc-alkaline fractionation trend with somewhat higher K, Ba, Zr and Y concentrations and lower Sr and especially Cr and Ni concentrations than paleosomes of gray gneisses (Fig. 14). Tonalites display a more fractionated REE pattern than granodiorites, which, in turn, display higher values and more flat distributions of HREE. Tonalites also display slightly U-shaped HREE patterns.

Paleoproterozoic rapakivi-type granite batholiths (Tuliniemi granite) are present to the east of the KGB (Fig. 1). One of the plutons yields an age of  $2435 \pm 12$  Ma, and Rämö and Luukkonen (2001) consider them coeval with the Paleoproterozoic layered mafic complexes of Koillismaa (Alapieti 1982).

Linear Paleoproterozoic mafic dikes and dike swarms trending E-W, NW-SE and NE-SW transect the Late Archaean TTG granitoids and the TKS greenstone complex (Vuollo and Huhma 2005, cf. Fig. 2). Commonly within the greenstone belts, the dikes contain xenoliths of Archaean mylonitic felsic volcanic rocks or other rock types with various Archaean structural features, which testify that the major phases of deformation of the TKS complex were late Archaean in age. Chemical compositions of the dikes range from boninitic to Fe-tholeiitic and further to low-Al-tholeiitic (Kilpelä 1991). In the granitoid areas, the dikes are linear, non-fractionated and of constant thickness, whereas locally in the greenstone belt they widen to form fractionated layered gabbro-wehrlite intrusions of considerable thickness (Fig. 25). The layered dike east of Ensilä has been studied in detail (cf. Hanski 1986). At Ensilä, the ultramafic cumulates are wehrlites (Cr 1800–3000 ppm) and they are overlain by gabbroic augite orthocumulate with intercumulus plagioclase (Cr < 100 ppm), magnetite gabbro, and the uppermost plagioclase-augite cumulate. A wehrlitic-

pyroxenitic dike that extends northwestwards from the Lake Likonen (Fig. 25, see also Fig. 9C) was dated by the Sm-Nd method (isochron) at  $2125 \pm 75$  Ma (Tulenheimo 1999). The Proterozoic mafic

and ultramafic cumulates differ markedly from the Archaean komatiitic cumulates in their  $Al_2O_3/TiO_2$  values, which are close to 6 (see Table 8).

### Proterozoic overprinting

The rocks of the TKS complex were deformed and metamorphosed during successive events in Archaean time, as described by Luukkonen 1992. On the basis of trace element geochemistry and isotope systematics, Gruau et al. (1992) considered that the TKS belt experienced another phase of deformation and metamorphism in Paleoproterozoic time, during which intense fluid activity reset the whole trace element distribution. Our study proves that in terms of limited geochemical resetting and metamorphism this may be true, since the majority of the Paleoproterozoic mafic dikes intersecting the greenstones and granitoid areas are metamorphosed and deformed, and therefore these processes must have likewise affected the Archaean wall rocks, too (see also Kontinen et al. 1992). The overall geometry of the Paleoproterozoic intrusions including the development of thick fractionated layered complexes in the greenstone areas indicates that the greenstones and granitoid areas responded differently to the stress field accompanying dike emplacement. The greenstones thus allowed space for the preferential accumulation and fractionation of mafic melt by accommodating stress release coeval with the intru-

sion of dike swarms. The Paleoproterozoic tectonic reactivation of late Archaean zones of weakness is also consistent with localization of fluid flow in shear zones and at the contacts of Paleoproterozoic dikes, causing local alteration, recrystallization and small-scale migration of elements. This may be the case in the ultramafic-mafic rock suite analysed by Gruau et al. (1992) at the Siivikkovaara hill, where a Paleoproterozoic mafic dike intersected the komatiitic lava sequence, resulting in contact metasomatism and fluid-rock interaction that disturbed the local trace element spectra.

Metamorphic contact reactions, alteration and element transport across the contact can also be observed at the contacts of a mafic dike intersecting the Small Serpentinite (Fig. 7). The originally mafic dike was altered to chlorite-magnetite rock and the serpentinite wall rock experienced metamorphic increase of silica, Ca and fractionation of REE to form zones characterized by talc and amphiboles along both margins of the dike. Similar alteration, as seen in chlorite-magnetite rock, also characterizes mafic enclaves in ultramafic cumulates.

## EVOLUTION OF THE GREENSTONE BELT

According to Martin et al. (1984), the tonalite-trondhjemite gneisses (TTG) of the granitoid area originated by partial melting of a primitive oceanic crust that was metamorphosed to garnet amphibolite during subduction. They considered that the greenstone belt volcanism was related to a rift zone and deposited on a continental crust, but due to the density imbalance the heavy mafic volcanic rocks subsided ("sagducted") deep into the crust to a level of neutral buoyancy and formed a folded synclinorium.

Piirainen (1988) suggested that all the material of the greenstone belt fractionated from the late Archaean mantle and that the rocks had had a very short crustal residence time, and that they do not contain remelted Archaean crustal material. He also considered that the granitoids of the TTG series formed in a subduction zone related to Archaean plate tectonic processes, and that the bimodal volcanism of the greenstone belts formed within a volcanic island arc above a subduction zone. According to this model the continental crust

became thick and stable at 2700–2600 Ma, such that subduction ceased or was transferred elsewhere. The mobile felsic and mafic crustal materials were in density imbalance, so that gravitational equilibrium was restored by diapiric rise of the light felsic intrusions and subsidence of the mafic materials to synclinoriums to form the greenstone belts. The model thus follows that as proposed by Martin et al. (1984). Later on, based on mineralogical evidence, Liipo et al. (1994) suggested an ophiolite origin for the Kellojärvi ultramafic complex.

Luukkonen (1992) linked the magmatic activity of the TKS greenstone complex to a rifting caused by a mantle thermal plume (Campbell et al. 1989, Campbell & Griffiths 1990, White & McKenzie 1989). According to the structural model by

Etheridge et al. (1988), incipient rifting thins cold continental crust and the first volcanoes are felsic fissure eruptions, or local single cones, but with time the eruptions develop basaltic and ultramafic in composition, and thinning of the crust results in the formation of a rift graben. Finally, the mantle plume and related igneous events increase the temperature of the crust and cause extensive melting of the crust.

Figures 26 and 27 depict the stratigraphic scheme and the evolution of the Kuhmo greenstone belt. An intracratonic rift model and the subsequent D<sub>3</sub> deformation are appropriate for the symmetrical synclinal structures of the greenstone belts, as well as for the evolution of depositional environment from subaerial volcanism to shallow water and

**Formation / Member**

Ronkaperä Formation

Unconformity ?

Siivikko / Suo

Siivikko / Mäkinen

Siivikko / Vaara

Pahakangas Formation

Mäkisensuu Formation

Tonalitic to granodioritic intrusions 2740-2690 Ma  
 Mafic intrusion 2752-2757 Ma  
 Tonalitic intrusion (Viitavaara) 2785 Ma

**Lithology**

Intermediate to mafic volcanic rocks mainly pyroclastic 2744 Ma

Cr basalts  
 High-MgO basalt  
 Komatiitic interlayers  
 High-Cr basalts

Komatiitic basalts

Kellojärvi ultramafic cumulate complex

Preferred pathways for komatiitic melt  
 Non-fractionated flows 2770 Ma  
 Fractionated komatiitic flows (spinfex)  
 Metapyroxenite (a hybrid rock)  
 Felsic porphyry 2770 Ma

Tholeiitic basalts (pillow lavas) 2790 Ma

Oxide facies BIF interlayers

Calc-alkalic felsic to mafic volcanic rocks 2810-2790 Ma

Felsic sedimentary interlayers

TTG basement 2843 Ma

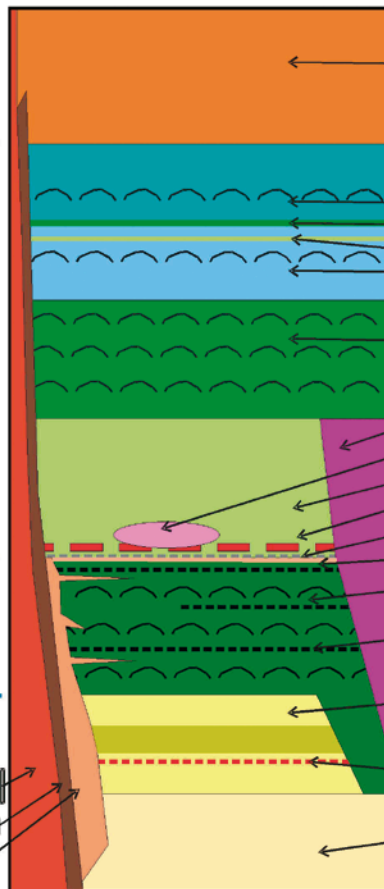


Figure 26. Stratigraphic scheme of the Kuhmo greenstone belt.

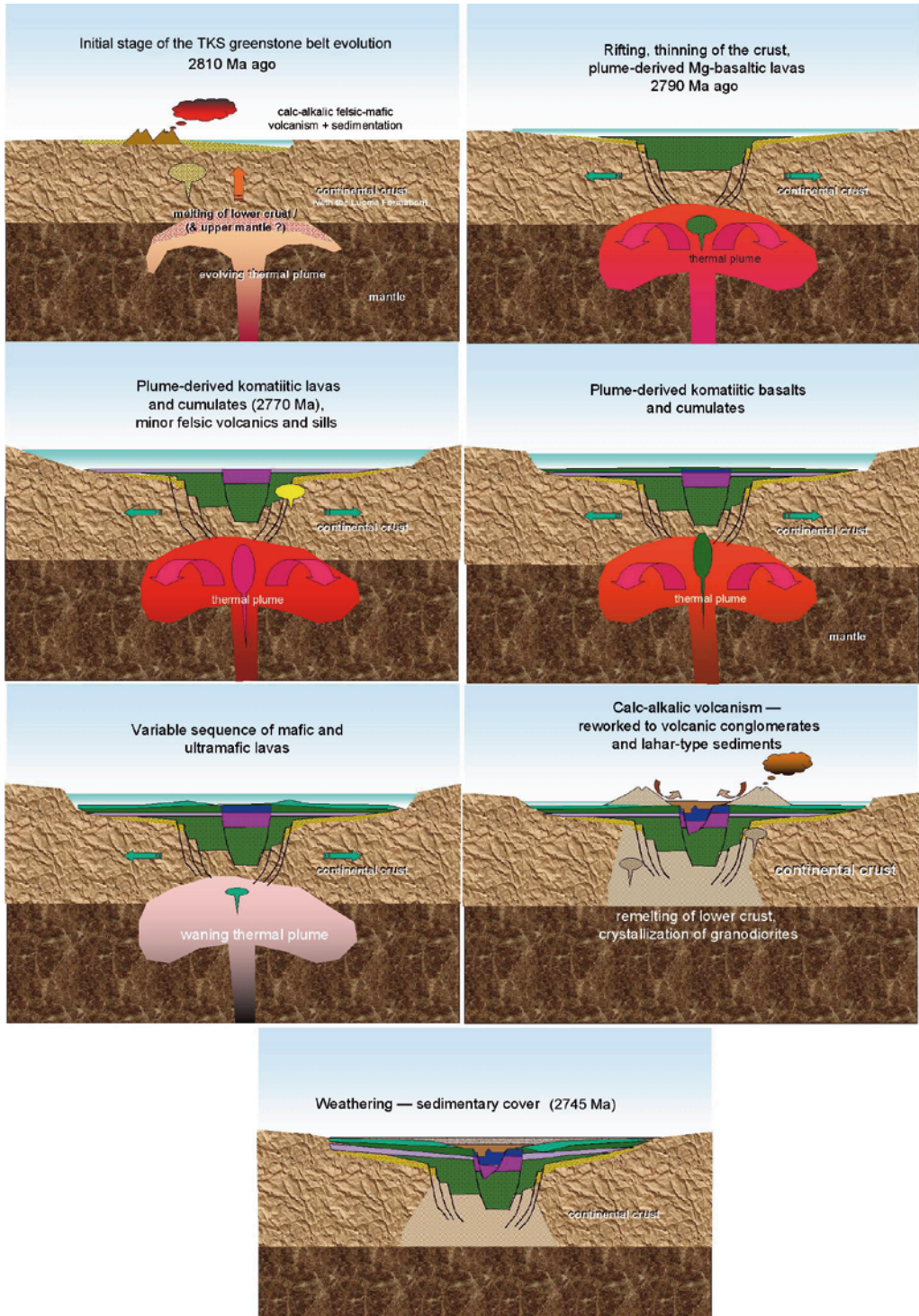


Figure 27. Schematic evolution of the TKS greenstone complex. The Luoma and Ruokojärvi Formations deposited and deformed prior to the TKS greenstone complex.

further to deep water and finally a reversion to shallow environment. The relief was probably not bold and the graben very deep since the hydrothermal activity related to the felsic volcanism evidence of boiling of fluids and the upper parts of the basaltic sequence display vesicular textures, which may reflect, although not reliable proof, of shallow water. The rafts and altered inclusions composed of intermediate to mafic volcanic rocks of the Mäkisensuo and Pahakangas Formations at the marginal parts of the Kellojärvi komatiitic olivine cumulates testify to the extrusion of komatiitic melt through the rocks of the Mäkisensuo and Pahakangas Formations. This indicates that cumulates deposited at or near the earth surface on top of the volcanic rocks or pre-greenstone granitoids. Early olivine crystals or seeds of crystals loaded the flows and then accumulated at the basal parts of the channels. Eruption through the continental crust accounts for the contamination of komatiites by felsic material, which is well documented at the margins of the Kellojärvi ultramafic complex. Felsic contamination of komatiitic volcanic rocks is also evident in the Pahakangas-Siivikkovaara stratigraphy by the pyroxenitic initial flow. The first komatiitic flows were ponded and fractionated and subsequent flows locally eroded the underlying flows indicating a time interval between the first flows. The upper flows are not fractionated since they erupted without major time intervals and did not pond or carry considerable amounts of crystallized olivine. The spinifex A-zone of the first fractionated flow is depleted in nickel, when compared to subsequent flows, indicating that the first flow interacted with sediments and became contaminated by sulfidic materials during their ascent to their present position. Felsic porphyry sills at the lower contact zone of thick komatiitic lava piles or close to cumulate contacts (Ensilä) could indicate local heating of the granitoid substrate caused by hot komatiitic eruptions.

Anorthosite is present as intensely altered xeno-

lithic inclusions in the ultramafic cumulate northwest of the Ensilä area (Fig. 11A). The xenoliths could be rafts carried by the melt from a plagioclase cumulate at the basal part of the crust. Another possibility is that they represent the depleted crustal material from which the first phase of felsic volcanic rocks was segregated and left the plagioclase residue, as was suggested above for the early evolution of the Koivumäki Formation in the Tipasjärvi greenstone belt. Accordingly, the plagioclase megacrysts of glomeroporphyritic basalts at the upper levels of the Pahakangas sequence could also be xenocrysts derived from the anorthositic depleted crustal material that the basalt met during ascent.

The available isotope age data presented in this paper indicates that the minimum time span for the evolution of the greenstone belt volcanism was 40 Ma, from 2810 to 2770. The volcanic phase was followed at about 2755 Ma by the intrusions of mafic melt, which locally fractionated to form a layered sequences of pyroxenitic, gabbroic and anorthositic cumulates, such as those met with at Niittyjoki and Niittylahti. Mafic melt experienced felsic contamination during the ascent. Granitoids intruded in several phases between 2750 and 2690 Ma. The intrusion of granitoids was combined with the main contractional deformation phase of the greenstone belt,  $D_3$ , which accompanied partial remelting of the continental crust.

In contrast with the Kostamuksha greenstone belt and some other documented greenstones in the eastern part of the Fennoscandian shield in NW Russia, which were formed at a convergent ocean-continent boundary and accreted to older crust during later collision stages (Puchtel et al. 1999), the widespread indications of contamination by felsic crustal material in the Tipasjärvi-Kuhmo-Suomussalmi greenstone belt testify that the volcanism took place in a geodynamic setting involving eruption through continental crust.

## CONCLUSIONS

The geochronological evidence indicates that the supracrustal evolution of the oldest identified greenstone belt succession started about 3007–2950 Ma ago, with the deposition of intermediate-felsic-mafic volcanic rocks and volcanoclastic sediments of the Ruokojärvi and Luoma Formations in the Suomussalmi area. Deformed primary volcanic textures prove that the rocks were deposited in shallow-water or subaerial conditions. Because of the subsequent intensive deformation and present deep erosion level, the rocks of the first greenstone belt succession occurs only sporadically as isolated remnants at the margins of the TKS greenstone complex and further away as banded amphibolites and deformed supracrustal gneisses. The deformation phase  $D_2$  is observed in the Luoma Formation and it separates Luoma from TKS, where the oldest deformation phase is  $D_3$ . Metamorphic overgrowths of zircon and deformation sequences of the rocks define an age of 2840–2810 Ma for the prominent  $D_2$  deformation event, which can be observed, in addition to the rocks of the Luoma Formation, in migmatitic gneisses outside the TKS complex (Käpyaho et al. 2007, Huhma 2007, pers. com.). In that way the evolution of the formations of the Luoma -type predates the initiation of the Tipasjärvi-Kuhmo-Suomussalmi greenstone belt volcanism.

Table 9 summarizes the stratigraphic data on the Tipasjärvi-Kuhmo-Suomussalmi greenstone complex and indicates that the greenstone belt evolution was essentially uniform throughout all parts of the greenstone complex.

In contrast to the plate tectonic accretion-collision models of the greenstones of the eastern part of the Fennoscandian Shield (Puchtel et al. 1999), the structures, stratigraphy and geochemical data support a thermal intracontinental plume model for the Kuhmo greenstone belt, as was presented earlier by Luukkonen (1992). The plume-derived volcanism started 2810–2790 Ma ago with initial felsic-intermediate volcanic rocks (Koivumäki, Mäkisensuo, Juurikkaniemi, Vuosanka and Mesaaho Formations). The most voluminous phase of volcanism consists of tholeiites, komatiites and

komatiitic basalts (Vuoriniemi, Kallio, Pahakangas, Siivikko, Tervonen and Saarikylä Formations) and erupted in the deep to shallow water rift basin. The time interval for this stage is 2790–2770 Ma.

Formation of ultramafic melt, with up to 24 wt.% MgO, requires high temperatures and melting of olivine residue in the mantle. The conditions are anomalous for accretionary plate boundaries and can be attained with extra heat flow and thermal mantle plume. Besides mantle melting, the evolving thermal plume left its marks in the whole igneous sequence with incipient crustal melting in advanced heat front resulting in felsic volcanism, and later on melting of the upwelling mantle producing tholeiitic basalts and finally the melting of mantle residue bringing about extrusion of komatiites and komatiitic basalts. We consider that zone refining process (Harris 1957, McBirney 1987) was associated with the crustal melting, and the initial melt concentrated trace incompatible and chalcophile elements, such as Zn, Pb, Ag, which are abundant in Koivumäki and Mäkisensuo Formations. High Mg-number of the Mäkisensuo felsic rocks indicate that mantle rocks participated in the initial phase of felsic melt formation.

At the end or coeval with the main volcanic period, outside the TKS proper, tonalite intrusions, such as the Viitavaara tonalite (Käpyaho et al. 2006), were emplaced into the migmatitic Archaean crust. During late-stage vanishing plume activity, felsic-intermediate subaerial or shallow-water eruption centers formed at the rift margins. Rapid erosion and steep topographic relief favoured redeposition of the tuffs and tuffites to lahar type conglomerates and volcanoclastic sediments (Kokkonniemi, Ronkaperä and Huutoniemi Formations) into structurally controlled, fault-bounded synclinal basins (sagponds or pull-apart basins). This took place after the ultramafic and mafic volcanic eruptions at about 2745 Ma ago, but the relationship of the Ronkaperä Formation to felsic intrusive phases remain to be determined.

In the time span from 2750 Ma to 2690 Ma granodiorites, diorites and gabbros of the Archaean

Table 9. Summary of the stratigraphic data on the Tipasjärvi-Kuhmo-Suomussalmi greenstone complex.

Tipasjärvi Greenstone Belt				Kuhmo Greenstone Belt				Suomussalmi Greenstone Belt				Relation to deformation					
Stratigraphic Unit	Lithology	Thickness	Age	Stratigraphic Unit	Lithology	Thickness	Age	Stratigraphic Unit	Lithology	Thickness	Age	Stratigraphic Unit	Lithology	Thickness	Age		
Formation				Formation	Member			Formation	Member			Formation	Member				
Kokkonen	Mica schist/pelite sediments; Nurmies paragneisses		2744±3 Ma (greywacke)	Ronsapää		300 m	(2744±3 Ma (greywacke from Peläjänen))	Huononemi		5 - 40 m	2774±8 Ma (zircon from the Kihvasuo felsic rocks)					Deformed in D3, but not in D2	
Kello	MgO-rich metavascs; komatites, komatiitic basalts, Cr basalts	200 m		Sivikko		1350 - 1950 m		Saarkylä								Deformed in D3 but not in D2	
					Suo	500 m			Valkainen								
					Mäkinen	300 m 300 m			Ryysälä	200 m							
					Vaara	500 m 50 m 300 m	2771±8 Ma (U-Pb age of the rim of zircon crystal from felsic enclave in komatite)		Rylys	400 m							
							2770±30 Ma (felsic sill at Sivikkovaara)										
Vuonhemi	Troilitic basalts, metaulf, BIF, black schists, mafic-felsic mixed metaulf	250 m		Panakangas		1000 m	2790±18 Ma (zircon age of mafic sill)	Tervonen		500 m						Deformed in D3 but not in D2	
Kovunmäki	Felsic Ulf and pyroclastic breccias; quartzite; Ag-Zn-Pb deposit; quartzite rock (Cap rock of a volcanic system)	500 m	2790±3 Ma (zircon from felsic volcanic rock)	Mäksensuo Juakkolahti Vuossala		300 m in W 1000 m in E	2798±15 Ma, 2810±48 Ma (zircon from Luurikkalahti and Vuossala felsic volcanic rocks)	Mesa-aho		10 - 40 m	2816±3 Ma (zircon age from felsic dike)					Deformed in D3 but not in D2	
Basement gneiss complex	Tonalite-trondhjemite-granodiorite, gray gneisses, banded amphibolites		2832±3 Ma (zircon U-Pb age from Haasiavaara tonalite)	Basement gneiss complex			2842±8 Ma (U-Pb age for zircons from D2 mesosome of Lylyvaara migmatite), 2843±18 Ma (U-Pb age of zircon from D2 metamorphic mesosome of tonalitic gneiss), > 3000 Ma (Sm-Nd model age from tonalitic palaeosome)	Basement gneiss complex								D2 deformation at 2843±18 Ma	
				Ruokojärvi		600 m	3007±7 Ma (U-Pb zircon age of felsic volcanic rock)	Luoma		50 - 1000 m	2842±3 Ma (monazite from quartz porphyry dikes), 2843±20 Ma (single zircon U-Pb age from felsic volcanic rock)					Deformed in D3, but D2 not observed	



sanukitoid suite intruded into the marginal zones of the TKS complex. According to Käpyaho et al. (2006) the tonalite suite that intruded between 2830 and 2750 Ma formed without marked input of very old crustal material (3500 Ma gneisses), but since the initial  $\epsilon_{Nd}$  decreases with decreasing age of the intrusions, the crustal recycling became an important process in the sanukitoid suite of intrusions at 2700–2680 Ma, when large amounts of leucocratic granitoids were emplaced to the west of the TKS greenstone complex.

Rock ages and structural architecture indicates that a relatively uniform kinematic framework prevailed for a long period of time between 2750 Ma and 2680 Ma denoted as  $D_3$  deformation by Luuk-

konen (1992). The structural framework reactivated several times and controlled different episodes of the igneous activity. The initial phase of the deformation caused high topographic relief, and was followed by rapid erosion resulting in ca. 2710–2690 Ma ago the deposition of greywackes, now known as the Nurmes-type paragneisses (Kontinen 1991). The late-stage  $D_3$  deformation structures initially controlled the location of the Nurmes paragneisses and their migmatization (Luukkonen 2005).

The last tectonothermal event, as seen in metamorphic growth of zircon in the plutonic rocks and paragneisses, took place at the interval 2720–2630 Ma, and initiated the cratonisation of the Archaean crust in eastern Finland (Käpyaho 2007).

## ACKNOWLEDGEMENTS

This paper is based on long lasting fieldwork conducted jointly at the Geological Survey of Finland and at the Nickel Exploration Research Group of the Turku University. We acknowledge the fruitful co-operation with Outokumpu Mining Oy and grants from the Outokumpu Oyj:n Säätiö, Ministry of Trade and Industry and the Brite EuRam GeoNickel Programme, which supported the research at the Turku University. We are grateful to Robin Hill, Sarah Dowling and Stephen Barnes at the CSIRO Research Laboratories, Perth, for fruitful and instructive discussions on komatiite volcanology. A great number of geologists and geology students participated in the work, and we here express our thanks to all of them, especially Terhi Tulenheimo, Markku Kilpelä, Jukka Jokela,

Jouko Nieminen, Jukka Välimaa, Jyrki Korteniemi and Jyrki Liimatainen deserve special thanks for meticulous work during the field mapping and resolution of specific questions in the Kellojärvi area. We thank Hannu Huhma from the Geological Survey of Finland and Petri Peltonen from the Northland Resources for the use of the isotopic age data, which is not yet published. Critical comments and suggestions by Stephen Foley, Peter Sorjonen-Ward and Kalle Taipale greatly improved the early version of the manuscript and Peter Sorjonen-Ward also corrected the English of the manuscript. We thank the editors Pasi Eilu and Pentti Hölttä for their constructive comments and criticism and also Anni Vuori and Raija Väänänen, who drew some of the figures.

## REFERENCES

- Alapieti, T. 1982.** The Koillismaa layered igneous complex, Finland: its structure, mineralogy and geochemistry, with emphasis on the distribution of chromium. Geological Survey of Finland, Bulletin 319. 116 p.
- Barnes, S. J., Hill, R. E. T., Perring, C. S. & Dowling, S. E. 2004.** Lithogeochemical exploration for komatiite-associated Ni-sulfide deposits: strategies and limitations. *Mineralogy and Petrology* 82, 259–293.
- Campbell, I. H., Griffiths, R. W. & Hill, R. I. 1989.** Melting in an Archaean mantle plume: head it's basalts, tails it's komatiites. *Nature* 339, 697–699.
- Campbell, I. H. & Griffiths, R. W. 1990.** Implications of mantle plume structure for the evolution of flood basalts. *Earth and Planetary Science Letters* 99, 79–93.
- Engel, W. W. & Diez, G.-J. 1989.** A modified stratigraphy and tectono-magmatic model for the Suomussalmi green-

- stone belt, eastern Finland, based on the re-mapping of the Ala-Luoma area. Bulletin of the Geological Society of Finland 61, 143–160.
- Etheridge, M. A., Symonds, P. A. & Powell, T. G. 1988.** Application of the detachment model for the continental extension to hydrocarbon exploration in extensional basins. The *Apea Journal*, 167–187.
- Frost, K. M. & Groves, D. I. 1989.** Ocellar units at Kam-balda: evidence for sediment assimilation by komatiite lavas. In: Prendergast, M. D. & Jones, M. J. (eds) *Magmatic Sulphides – the Zimbabwe Volume*. London: Institute of Mining and Metallurgy, 207–214.
- Gruau, G., Tourpin, S., Fourcade, S. & Blais, S. 1992.** Loss of isotopic (Nd,O) and chemical (REE) memory during metamorphism of komatiites: new evidence from eastern Finland. *Contributions to Mineralogy and Petrology* 112, 66–82.
- Green, T. H., Brunfelt, A. O. & Heier, K. S. 1972.** Rare-earth element distribution and K/Rb ratios in granulites, mangerites and anorthosites, Lofoten-Vesteraalen, Norway. *Geochimica et Cosmochimica Acta* 36, 241–257.
- Halkoaho, T., Liimatainen, J., Papunen, H. & Välimaa, J. 2000.** Exceptionally Cr-rich basalts in the komatiitic volcanic association of the Archaean Kuhmo greenstone belt, eastern Finland. *Mineralogy and Petrology* 70, 105–120.
- Halkoaho, T. & Niskanen, M. 2004.** Tutkimustyöselostus Kuhmon kaupungissa valtausalueilla Haverisensuo 1 ja 2 (kaivosrekisterinumerot 7426/1 ja 7628/1) suoritetuista nikkelimalmitutkimuksista vuosina 2002–2004. Geological Survey of Finland, unpublished report M 06/4411/2004/1/10, 16 p. (in Finnish)
- Hanski, E. J. 1980.** Komatiitic and tholeiitic metavolcanic rocks of the Kellojärvi group in the Siivikkovaara area of the Archaean Kuhmo greenstone belt, eastern Finland. Bulletin of the Geological Society of Finland 52, 67–100.
- Hanski, E. J. 1986.** The Gabbro-Wehrlite Association in the Eastern Part of the Baltic Shield. In: Friedrich, G. H., Genkin, A. D., Naldrett, A. J., Ridge, J. D., Sillitoe, R. H. & Vokes, F. M. (eds) *Geology and Metallogeny of Copper Deposits. Proceedings of the Copper Symposium 27th International Geological Congress Moscow, 1984. Special Publication No. 4 of the Society for Geology Applied to Mineral Deposits*. Berlin Heidelberg: Springer-Verlag, 151–170.
- Harris, P. G. 1957.** Zone refining and the origin of potassic basalts. *Geochimica Cosmochimica Acta* 12, 195–208.
- Heilimo, E., Mikkola, P. & Halla, J. 2007.** Age and petrology of the Kaapinsalmi sanukitoid intrusion in Suomussalmi, eastern Finland. Bulletin of the Geological Society of Finland 79, 117–125.
- Hill, R. E. T., Barnes, S. J., Gole, M. J. & Dowling, S. E. 1990.** The physical volcanology of komatiites in the Norseman – Wiluna belt, Western Australia. *Geol. Soc. Australia, Western Australia Division, Excursion Guide* 1, 100 p.
- Hölttä, P., Balagansky, V., Garde, A. A., Mertanen, S., Peltonen, P., Slabunov, A., Sorjonen-Ward, P. & Whitehouse, M. 2008.** Archaean of Greenland and Fennoscandia. Episodes 31,1, 13–19.
- Horneman, R., Hyvärinen, T. & Niskanen, P. 1988.** The granitoids surrounding and intruding the Kuhmo greenstone belt, eastern Finland. Geological Survey of Finland, Special Paper 4, 97–121.
- Huhma, H., Mänttari, I. & Vaasjoki, M. 1999.** Dating the Finnish Archaean greenstone belts – isotope geology. In: Papunen, H. & Eilu, P. (eds) *Geodynamic evolution and metallogeny of the Central Lapland, Kuhmo and Suomussalmi greenstone belts, Finland*. University of Turku, Institute of geology and mineralogy publication 42, 72–74.
- Huppert, H. E. & Sparks, R. S. J. 1985.** Komatiites I: eruption and flow. *Journal of Petrology* 26, 694–725.
- Hyppönen, V. 1973.** Hiisijärvi. Geological Map of Finland 1:100 000, Pre-Quaternary Rocks, Sheet 4412. Geological Survey of Finland.
- Hyppönen, V. 1976.** Ontojoki. Geological Map of Finland 1:100 000, Pre-Quaternary Rocks, Sheet 4411. Geological Survey of Finland.
- Hyppönen, V. 1978.** Kuhmo. Geological Map of Finland 1:100 000, Pre-Quaternary Rocks, Sheet 4413. Geological Survey of Finland.
- Hyppönen, V. 1983.** Ontojoen, Hiisijärven ja Kuhmon kartta-alueiden kallioperä. Summary: Pre-Quaternary rocks of the Ontojoki, Hiisijärvi, and Kuhmo map-sheet areas. Geological Map of Finland 1:100 000, Explanation to the Maps of Pre-Quaternary Rocks, Sheets 4411, 4412 and 4413. Geological Survey of Finland. 60 p.
- Hyvärinen, T. 1989.** Granitoids on the Puukari map sheet. In: Gaal, G. (ed.) *Archean granitoids and associated Mo, W and Au mineralization in eastern Finland*. Geological Survey of Finland, Opas – Guide 25, 29–33.
- James, R. S. & Hamilton, D. L. 1969.** Phase relations in the system  $\text{NaAlSi}_3\text{O}_8\text{-KAlSi}_3\text{O}_8\text{-CaAl}_2\text{Si}_2\text{O}_8\text{-SiO}_2$  at 1 kilobar water vapour pressure. *Contributions to Mineralogy and Petrology* 21, 111–141.
- Käpyaho, A. 2006.** Whole-rock geochemistry of some tonalite and high Mg/Fe gabbro, diorite, and granodiorite plutons (sanukitoid suites) in the Kuhmo district, eastern Finland. Bulletin of the Geological Society of Finland 78 (2), 121–141.
- Käpyaho, A. 2007.** Archaean crustal evolution in eastern Finland: new geochronological and geochemical constraints from the Kuhmo terrain and the Nurmes belt. Geological Survey of Finland. 97 p.
- Käpyaho, A., Mänttari, I. & Huhma, H. 2006.** Growth of Archaean crust in the Kuhmo district, eastern Finland: U-Pb and Sm-Nd isotope constraints on plutonic rocks. *Precambrian Research* 146 (3–4), 95–119.
- Käpyaho, A., Hölttä, P. & Whitehouse, M. J. 2007.** U-Pb zircon geochronology of selected Archaean migmatites in eastern Finland. Bulletin of the Geological Society of Finland 79 (1), 95–115.
- Kilpelä, M. 1991.** Itä-Kainuun varhaisproterotsooiset diabaasit. Unpublished MSc. Thesis, University of Turku. 113 p. (in Finnish)
- Kontinen, A. 1991.** Evidence for significant paragneiss component within the Late Archaean Nurmes gneiss complex, eastern Finland. In: Geological Survey of Finland, Cur-

- rent Research 1989–1990. Geological Survey of Finland, Special Paper 12, 17–19.
- Kontinen, A., Paavola, J. & Lukkarinen, H. 1992.** K-Ar ages of hornblende and biotite from Late Archaean rocks of eastern Finland – interpretation and discussion of tectonic implications. Geological Survey Finland, Bulletin 365, 31 p.
- Kontinen, A. & Paavola, J. 2006.** A preliminary model of the crustal structure of the eastern Finland Archaean Complex between Vartiuss and Vieremä, based on constraints from surface geology and FIRE-1 seismic survey. Geological Survey of Finland, Special Paper 43, 223–240.
- Korsman, K., Koistinen, T., Kohonen, J., Wennerström, M., Ekdahl, E., Honkamo, M., Idman, H. & Pekkala, Y. (eds) 1997.** Suomen kallioperäkarta/Bedrock map of Finland 1:1 000 000. Espoo: Geological Survey of Finland.
- Kukkonen, I. T., Heikkinen, P., Ekdahl, E., Hjelt, S.-E., Yliniemi, J., Jalkanen, E. & FIRE Working Group 2006.** Acquisition and geophysical characteristics of reflection seismic data on FIRE transects, Fennoscandian Shield. Geological Survey of Finland, Special Paper 43, 13–43.
- Kurki, J. & Papunen, H. 1985.** Geology and nickel-copper deposits of the Kianta area, Suomussalmi. In: Papunen, H. & Gorbunov, G. I. (eds) Nickel-copper deposits of the Baltic Shield and Scandinavian Caledonides. Geological Survey of Finland, Bulletin 333, 155–161.
- Lahaye, Y., Arnd, N. T., Byerly, G., Chauvel, C., Fourcade, S. & Gruau, G. 1995.** The influence of alteration on the trace-element and Nd isotopic compositions of komatiites. *Chemical Geology* 126 (1), 43–64.
- Leshner, C. M. & Keays, R. R. 2001.** Trace element lithophile and chalcophile element geochemistry, petrogenesis and metallogenesis of komatiites at Kambalda, Western Australia. In: Cassidy, K. F., Dunphy, J. M. & van-Kranendonk, M. J. (eds) Fourth international Archaean symposium, extended abstracts. Australian Geological Survey Organisation, 391–393.
- Liipo, J., Vuollo, J., Nykänen, V. & Piirainen, T. 1994.** Chromite compositions as evidence for an Archaean ophiolite in the Kuhmo greenstone belt in Finland. *Bulletin of the Geological Society of Finland* 66, 3–18.
- Luukkonen, E. J. 1988.** Moisiovaaran ja Ala-Vuokin kartta-alueen kallioperä. Summary: Pre-Quaternary rocks of the Moisiovaara and Ala-Vuoksi map-sheet areas. Geological Map of Finland 1: 100 000, Explanation to the Maps of Pre-Quaternary Rocks, Sheets 4421, 4423+4441. Geological Survey of Finland, 90 p.
- Luukkonen, E. J. 1992.** Late Archaean and early Proterozoic structural evolution in the Kuhmo-Suomussalmi terrain, eastern Finland. *Turun Yliopiston julkaisuja. Annales Universitatis Turkuensis. Sarja-Ser. A. II. Biologica-Geographica-Geologica* 78, 37 p.
- Luukkonen, E. J. 2001.** Lentiiran kartta-alueen kallioperä. Summary: Pre-Quaternary rocks of the Lentiira map-sheet area. Geological Map of Finland 1:100 000, Explanation to the Maps of Pre-Quaternary Rocks, Sheet 4414+4432. Geological Survey of Finland, 51 p.
- Luukkonen, E. J. 2005.** Nurmeksen kartta-alueen kallioperä. Summary: Pre-Quaternary rocks of the Nurmes map-sheet area. Geological Map of Finland 1:100 000, Explanation to the Maps of Pre-Quaternary Rocks, Sheet 4321. Geological Survey of Finland, 65 p.
- Luukkonen, E., Halkoaho, T., Hartikainen, A., Heino, T., Niskanen, M., Pietikäinen, K. & Tenhola, M. 2002.** Itä-Suomen Arkeaiset alueet –hankkeen (12201 ja 201 5000) toiminta vuosina 1992–2001 Suomussalmen, Hyrynsalmen, Kuhmon, Nurmeksen, Rautavaaran, Valtimon, Lieksan, Ilomantsin, Kiihtelysvaaran, Enon, Kontiolahden, Tohmajärven ja Tuupovaaran alueella. Geological Survey of Finland, unpublished report M 19/4513/2002/1. 265 p. (in Finnish)
- Martin, H. 1987.** Petrogenesis of Archaean trondhjemites, tonalites and granodiorites from eastern Finland: major and trace element geochemistry. *Journal of Petrology* 28, 921–958.
- Martin, H. 1987.** Evolution of granitic rocks controlled by time-dependent changes in petrogenetic processes: examples of the Archaean of eastern Finland. *Precambrian Research* 35, 257–276.
- Martin, H., Chauvel, C. & Jahn, B. M. 1983.** Major and trace element geochemistry and crustal evolution of Archaean granodioritic rocks from eastern Finland. *Precambrian Research* 21, 159–180.
- Martin, H., Auvray, B., Blais, S., Capdevila, R., Hameurt, J., Jahn, B. M., Piquet, D., Quérré, G. & Vidal, Ph. 1984.** Origin and geodynamic evolution of the Archaean crust of eastern Finland. *Bulletin of the Geological Society of Finland* 56, 135–160.
- Matisto, A. 1958.** Suomussalmi. General Geological Map of Finland 1:400 000, Explanation to the Map of Rocks, Sheet D5. Geological Survey of Finland, 115 p.
- McBirney, A. R. 1987.** Constitutional zone refining of layered intrusions. *NATO Advanced Science Institutes Series C*, 196, 437–452.
- Mutanen, T. & Huhma, H. 2003.** The 3.5 Ga Siurua trondhjemite gneiss in the Archaean Pudasjärvi Granulite Belt, northern Finland. *Bulletin of the Geological Society of Finland* 75 (1–2), 51–68.
- Nieminen, J. 1998.** Kuhmon Kellojärven polymiittinen vulkaaninen konglomeraatti. Unpublished MSc Thesis, University of Turku, 106 p. (in Finnish)
- O'Brien, H., Huhma, H. & Sorjonen-Ward, P. 1993.** Petrogenesis of the late Archean Hattu schist belt, Ilomantsi, eastern Finland: geochemistry and Sr-Nd isotopic composition. Geological Survey Finland, Special Paper 17, 147–184.
- Papunen, H. 1960.** Havaintoja Siivikkovaaran alueen kallioperästä Kuhmon pitäjän Vieksin kylässä. Unpublished MSc Thesis, University of Helsinki, 56 p. (in Finnish)
- Papunen, H., Kopperoinen, T. & Tuokko, I. 1989.** The Taivaljärvi Ag-Zn deposits in the Archaean greenstone belt, eastern Finland. *Economic Geology* 84, 1262–1276.
- Papunen, H., Halkoaho, T., Liimatainen, J. & Tulenheimo, T. 1998.** Komatiite geology of the Siivikkovaara and Kellojärvi areas of the Kuhmo greenstone belt. Technical Report 6.2: Mineralogy and modelling of Ni sulphide deposits in komatiitic/picritic extrusives. Task 1.2 in

- Integrated Technologies for Mineral Exploration; Pilot Project for Nickel Ore Deposits Brite-EuRam BE-1117 GeoNickel. 51 p.
- Peltonen, P., Mänttärä, I. & Halkoaho, T. (in prep.)** Precise dating of Archean komatiites using re-equilibrated country rock zircons.
- Piirainen, T. 1988.** The geology of the Archean greenstone-granitoid terrain in Kuhmo, eastern Finland. In: Marttila, E. (ed.) Archean geology of the Fennoscandian Shield. Geological Survey Finland, Special Paper 4, 39–51.
- Puchtel, I. S., Hoffmann, A. W., Jochun, K. P., Mezger, K., Shchipansky, A. A. & Samsonov, A. V. 1997.** The Kostomuksha greenstone belt, NW Baltic Shield; remnant of a late Archean oceanic plateau? *Terra Nova* 9 (2), 87–90.
- Puchtel, I. S., Hoffmann, A. W., Amelin, Yu. V., Gabre-Schönberg, C.-D., Samsonov, A. V. & Shchipansky, A. A. 1999.** Combined mantle plume-island arc model for the formation of the 2.9 Sumozero-Kenozero greenstone belt, SE Baltic Shield. *Geochimica Cosmochimica Acta* 21, 3579–3595.
- Rämö, O. T. & Luukkonen, E. J. 2001.** 2.4 Ga A-type granites of the Kainuu region, eastern Finland: Characterization and tectonic significance. EUG XI. Journal of Conference Abstracts 6.
- Slabunov, A. I., Lobach-Zhuchenko, S. B., Bibikova, E. V., Sorjonen-Ward, P., Balagansky, V. V., Volodichev, O. I., Shchipansky, A. A., Svetov, S. A., Chekulaev, V. P., Arestova, N. A. & Stepanov, V. S. 2006.** The Archean nucleus of the Baltic/Fennoscandian Shield. In: Gee, D. G. & Stephenson, R. A. (eds) *European Lithosphere Dynamics*. Geological Society of London, Memoirs 32, 627–644.
- Sorjonen-Ward, P. & Luukkonen, E. 2005.** Archean rocks. In: Lehtinen, M., Nurmi, P. A. & Rämö, O. T. (eds) *The Precambrian Geology of Finland – Key to the Evolution of the Fennoscandian Shield*. Amsterdam: Elsevier, 19–99.
- Sun, S. S. & McDonough, W. F. 1989.** Chemical composition and isotope systematics of oceanic basalts: implications for mantle composition and processes. In *Magmatism in ocean basins*. Geological Society, Special Publication 42, 313–345.
- Taylor, R. R. & McClelland, M. 1985.** The continental crust: its composition and evolution. Oxford: Blackwell. 312 p.
- Taipale, K. 1983.** The geology and geochemistry of the Archean Kuhmo greenstone – granite terrain in the Tipasjärvi area, eastern Finland. *Acta Universitatis Oulensis*. A 151. 98 p.
- Tourpin, S. 1991.** *Perte des mémoires isotopiques (Nd, Sr, O) et géochimiques (REE) primaires des komatiites au cours du métamorphisme: exemple de la Finlande orientale*. Rennes: Thèse d'Université. 181 p.
- Tulenheimo, T. 1999.** Kuhmon Kellojärven kerroksellinen ultramafinen muodostuma. Unpublished MSc Thesis, University of Turku. 199 p. (in Finnish)
- Vaasjoki, M., Taipale, K. & Tuokko, I. 1999.** Radiometric dates and other isotopic data bearing on the evolution of the Archean Crust and ores in the Kuhmo-Suomussalmi area, eastern Finland. *Bulletin of the Geological Society of Finland* 71, 155–176.
- Vuollo, J. & Huhma, H. 2005.** Paleoproterozoic mafic dikes in NE Finland. In: Lehtinen, M., Nurmi, P. & Rämö, O. T. (eds) *Precambrian geology of Finland – Key to the evolution of the Fennoscandian Shield*. Amsterdam: Elsevier B.V., 195–236.
- White, R. & McKenzie, D. 1989.** Magmatism at rift zones: the generation of volcanic continental margins and flood basalts. *Journal of Geophysical Research* 94, 7685–7729.
- Wilkman, W. W. 1921.** *Nurmes. General Geological Map of Finland 1:400 000, Explanation to the Map of Rocks, Sheet D4*. Geological Survey of Finland. 126 p.
- Yliniemi, J. 1986.** Preliminary structure of the Earth's crust on the Kostamus – Oulu and Kostamus – Viitasaari profiles. Paper presented at the 20th General Assembly of the European Seismological Commission, August 21 – 30, Kiel, Abstracts. *Terra Cognita* 6, p. 345.

## APPENDIX: DATA CD

Geochemical Analyses of the Archean Tipasjärvi-Kuhmo-Suomussalmi Greenstone Belt.

## Some notes of the analytical data

One of the main goals of this study was the classification and interpretation of volcanic rocks of the greenstone belts. For this purpose we collected a number of analyses of rock samples. The analyses were performed mainly with XRF method, but also a few trace element analyses with more specified methods were done. All the XRF analyses are here collected in the Excel spreadsheet entitled “Kuhmo XRF”, which includes the sample identification data, indication of sampling target: outcrop/drilling/excavation “P/K/M”, depth of the sample in drill hole, written description of sample location, field definitions of rock class and rock type, exact northing and easting data of the sampling site (see reference in Fig. 1), and the analytical result. Most of the XRF analyses were performed at the Geoanalytical Laboratory of VTT/Outokumpu Oy and then the samples were finely ground, ignited to volatile-free and pressed to pellets for the analyzing of all the elements. In the ignition some of the sulfide sulfur may be escaped and the indicated S percentages may hence be somewhat reduced. Another set of analyses were done at CSIRO Research laboratories at Perth, W.A., where the samples were fused with flux and the main elements were determined from fused glass discs and trace elements from pressed powder samples. In this method the S values are more realistic than in the VTT assays. The CSIRO analyses are indicated with x in specific column.

Total iron content was indicated in the analytical result either as  $\text{Fe}_2\text{O}_3$  or FeO, but in the final table the total iron was calculated in all analyses to FeO. The abundance “0” means, that the element was analyzed, but the concentration was below the detection limit of the analytical method.

Another Table indicates all the analyzed REE and trace elements. The trace element analyses were performed at Genalysis Laboratories, Perth, W.A. with ICP-MS. Main elements included in this table were determined with XRF method.

The Table “Ronkaperä” includes analytical data of the Ronkaperä Formation and the analyses were performed in the Thesis work of Jouko Nieminen (1998). The analyses were done at CSIRO laboratories with XRF.

The collection of analyses also includes the table entitled “Taivaljärvi”. It contains the analytical data of the volcanic sequence hosting the Taivaljärvi Zn-Ag-Pb deposit, and the data was first published in Papunen et al. (1989).

The terms used in the classification of rock types are included in the table entitled “Dictionary”.

*The Authors*



Table with 49 columns: ID, Name, Age, Sex, Species, Location, and various numerical data points. Rows represent individual specimens, often grouped by name and location. Includes specimen numbers like 86 TTT 96 and various geographic coordinates or identifiers.

Table with 44 columns representing various geological and geographical data points, including coordinates, elevation, and specific site identifiers. The table contains multiple rows of data, each representing a different location or sample point, with columns for identifiers like TOH, year, coordinates, and various numerical values representing different parameters.

















Table with columns for sample ID, date, location, coordinates, and various chemical analysis results. The table is organized into several vertical sections, each corresponding to a different geological sample or location. Each row contains numerical data points, likely representing concentrations of various elements or isotopes. Some rows include text labels for specific elements or isotopes.

\*K = drill hole, P = outcrop, M = trench/excavation and L = boulder









[www.gtk.fi](http://www.gtk.fi)  
[info@gtk.fi](mailto:info@gtk.fi)

The study summarizes and reviews the detailed field and geochemical data of the Tipasjärvi-Kuhmo-Suomussalmi greenstone complex collected during the regional geological mapping and ore exploration programs of the Geological Survey of Finland and the Department of Geology, University of Turku. The main emphasis of the study is on the interpretation of the data in terms of stratigraphy and reconstruction of the Archaean evolution of the greenstone belts. The authors conclude that the greenstone belts evolved in an intra-continental rift system since this geotectonic model best satisfies the overall the stratigraphic context, together with lithological, volcanological, structural, as well as major, trace element, and isotope geochemical data.

ISBN 978-952-217-074-3 (paperback)  
ISBN 978-952-217-075-0 (PDF)  
ISSN 0367-522X



9 789522 170743